Decentralized leader-follower consensus for multiple cooperative robots under temporal constraints

Pipit Anggraeni

Thèse de doctorat

Pour obtenir le grade de Docteur Sciences et Technologie

UNIVERSITE POLYTECHNIQUE HAUTS-DE-FRANCE

Discipline, specialite selon la liste des specialites pour lesquelles l'Ecole Doctorale est accreditee:

Automatique Genie Informatique

Présentée et soutenue par **Pipit ANGGRAENI**

Le 11/06/2019, à Valenciennes

Ecole doctorale:
Sciences Pour l'Ingénieur (SPI)
Equipe de recherche, Laboratoire:
Laboratoire d'Automatique, de Mécanique et d'Informatique Industrielles et Humaines (LAMIH)

Consensus Décentralisé de Type Meneur/Suiveur pour Une Flotte de Robots Coopératifs Soumis à des Contraintes Temporelles

JURY :

Président du Jury:		
M. Noureddine Manamanni	-	Professeur, Université de Reims Champagne-Ardenne Reims, Reims
Rapporteurs		
M. Faiz Ben Amar	-	Professeur, ISIR - Université Pierre-et-Marie-Curie, Paris
M. Noureddine Manamanni	-	Professeur, Université de Reims Champagne-Ardenne Reims, Reims
Examinateurs:		
Mme. Annemarie Kokosy	-	Maitre de Conférences, ISEN - Université Catholique de Lille, Lille
M. Juan Diego Sánchez Torres	-	Maitre de Conférences, ITESO - Guadalajara, Mexique
M. Abdul Muis	-	Maitre de Conférences, Université d'Indonésie, Indonésie
Directeur de Thèse:		
M. Mohamed Djemai	-	Professeur, LAMIH - UPHF, Valenciennes
Co-Directeur:		
M. Michael Defoort	-	Maitre de Conférences, LAMIH - UPHF, Valenciennes

Doctoral thesis

To obtain the degree of Doctor Science and Technology

UNIVERSITE POLYTECHNIQUE HAUTS-DE-FRANCE

Discipline, specialty according to the list of specialties for which the Doctoral School is accredited:

Automatique Genie Informatique

Presented and defended by **Pipit ANGGRAENI**

Le 11/06/2019, à Valenciennes

Doctoral School:
Sciences for the Engineer (SPI)
Research team, Laboratory:
Laboratory of Industrial and Human Automation control, Mechanical engineering and Computer Science (LAMIH)

Decentralized Leader-Follower Consensus for Multiple Cooperative Robots under Temporal Constraints

JURY :

President of Jury:		
M. Noureddine Manamanni	-	Professor, University of Reims Champagne-Ardenne Reims, Reims
Reviewers:		
M. Faiz Ben Amar	-	Professor, ISIR - Pierre and Marie Curie University, Paris
M. Noureddine Manamanni	-	Professor, University of Reims Champagne-Ardenne Reims, Reims
Examiners:		
Mme. Annemarie Kokosy	-	Associate Professor, ISEN - Catholic University of Lille, Lille
M. Juan Diego Sánchez Torres	-	Associate Professor, ITESO - Guadalajara, Mexico
M. Abdul Muis	-	Associate Professor, University of Indonesia, Indonesia
Supervisor:		
M. Mohamed Djemai	-	Professor, LAMIH - UPHF, Valenciennes
Co-Supervisor:		
M. Michael Defoort	-	Associate Professor, LAMIH - UPHF, Valenciennes

Abstract

Nowadays, robots have become increasingly important to investigate hazardous and dangerous environments. A group of collaborating robots can often deal with tasks that are difficult, or even impossible, to be accomplished by a single robot. Multiple robots working in a cooperative manner is called as a Multi-Agent System (MAS). The interaction between agents to achieve a global task is a key in cooperative control. Cooperative control of MASs poses significant theoretical and practical challenges. One of the fundamental topics in cooperative control is the consensus where the objective is to design control protocols between agents to achieve a state agreement. This thesis improves the navigation scheme for MASs, while taking into account some practical constraints (robot model and temporal constraints) in the design of cooperative controllers for each agent, in a fully decentralized way. In this thesis, two directions are investigated.

On one hand, the convergence rate is an important performance specification to design the controller for a dynamical system. As an important performance measure for the coordination control of MASs, fast convergence is always pursued to achieve better performance and robustness. Most of the existing consensus algorithms focus on asymptotic convergence, where the settling time is infinite. However, many applications require a high speed convergence generally characterized by a finite-time control strategy. Moreover, finite-time control allows some advantageous properties but the settling time depend on the initial states of agents. The objective here is to design a fixed-time leader-follower consensus protocol for MASs described in continuous-time. This problem is studied using the powerful theory of fixed-time stabilization, which guarantee that the settling time is upper bounded regardless to the initial conditions. Sliding mode controllers and sliding mode observers are designed for each agent to solve the fixed-time consensus tracking problem when the leader is dynamic.

On the other hand, compared with continuous-time systems, consensus problem in a discrete-time framework is more suitable for practical applications due to the limitation of computational resources for each agent. Model Predictive Control (MPC) has the ability to handle control and state constraints for discrete-time systems. In this thesis, this method is applied to deal with the consensus problem in discrete-time by letting each agent to solve, at each step, a constrained optimal control problem involving only the state of neighboring agents. The tracking performances are also improved in this thesis by adding new terms in the classical MPC technique. The proposed controllers will be simulated and implemented on a team of multiple Mini-Lab Enova Robots using ROS (Robotic Operating System) which is an operating system for mobile robots. ROS provides not only standard operating system services but also high-level functionalities. In this thesis, some solutions corresponding to problem of connection between multiple mobile robots in a decentralized way for a wireless robotic network, of tuning of the sampling periods and control parameters are also discussed.

KEYWORDS: Cooperative control; Multi-agent system; Leader-Follower consensus; Mobile robot; Fixed-time stability; Model predictive control; Robotic Operating System (ROS)

Résumé

Un groupe de robots collaboratifs peut gérer des tâches qui sont difficiles, voire impossibles, à accomplir par un seul. On appelle un ensemble de robots coopérant un système multi-agents (SMA). L'interaction entre agents est un facteur clé dans la commande coopérative qui pose d'importants défis théoriques et pratiques. L'une des tâches du contrôle coopératif est le consensus dont l'objectif est de concevoir des protocoles de commande afin de parvenir à un accord entre leurs états respectifs. Cette thèse améliore la navigation pour les SMA, tout en tenant compte de certaines contraintes pratiques (modèle du robot et contraintes temporelles) dans la conception de contrôleurs coopératifs pour chaque agent, de manière décentralisée. Dans cette thèse, deux directions sont étudiées.

D'une part, le taux de convergence est une spécification de performance importante pour la conception du contrôleur pour un système dynamique. La convergence rapide est toujours recherchée pour améliorer les performances et la robustesse. La plupart des algorithmes de consensus existants se concentrent sur la convergence asymptotique, où le temps d'établissement est infini. Cependant, de nombreuses applications nécessitent une convergence rapide généralement caractérisée par une stratégie de commande à temps fini. De plus, la commande à temps fini autorise certaines propriétés intéressantes, mais le temps de stabilisation dépend des conditions initiales des agents. L'objectif ici est de concevoir un protocole de consensus leader-follower à temps fixe pour les SMA décrits en temps continu. Ce problème est étudié en utilisant la théorie de la stabilisation à temps fixe, qui garantit que le temps de stabilisation est borné quelles que soient les conditions initiales. Les contrôleurs et les observateurs à modes glissants sont conçus pour que chaque agent résolve le problème du consensus à temps fixe lorsque le leader est dynamique.

D'autre part, par rapport aux systèmes à temps continu, le problème du consensus dans un cadre à temps discret convient mieux aux applications pratiques en raison de la limitation des ressources de calcul pour chaque agent. Le modèle de commande prédictive (MPC) permet de gérer les contraintes de commande et d'état des systèmes. Dans cette thèse, cette méthode est appliquée pour traiter le problème du consensus en temps discret en laissant chaque agent résoudre, à chaque étape, un problème de commande optimale contraint impliquant uniquement l'état des agents voisins. Les performances de suivi sont également améliorées dans cette thèse en ajoutant de nouveaux termes à partir du MPC classique. Les contrôleurs proposés sont simulés et implémentés sur un groupe composé de plusieurs robots réels en utilisant ROS (Robotic Operating System). Dans cette thèse, quelques solutions correspondant au problème de la connexion entre plusieurs robots mobiles de manière décentralisée, du réglage des périodes d'échantillonnage et des paramètres de contrôle sont également abordées.

MOTS-CLES: Contrôle coopératif; Système multi-agents; Consensus Meneur/Suiveur; Robot mobile; Stabilité à temps fixe; Commande prédictive; Robotic Operating System (ROS)

Contents

Acknowledgements

Firstly, I would like to express my sincere gratitude to my supervisor, Prof. Mohamed DJEMAI, for the continuous support of my Ph.D study and related research, for his patience, motivation and immense knowladge. He has been helping me come up with the thesis topic of multi-agent systems whilst allowing me the room to work in my own way.

Greatest thanks must go to my coordinating supervisor, Dr. Michael DEFOORT, for his valuable discussions, helpful suggestions, and endless support. His guidance helped me in all the time of research and writing of this thesis. I could not have imagined having a better advisor and mentor for my Ph.D study.

Beside my advisor, I would like to thank to Dr. Zongyu ZUO, from Beihang University, for his great support and excellent advice. Dr. Zuo helped me find out some promising directions in the fixed-time consensus field, which serve as the foundation of this thesis.

My sincere thanks also goes to Dr. Abdul MUIS and Dr.Aries SUBIANTORO, from Indonesia University, who provided me an opportunity to join their team as part of NUSANTARA Project and who gave research facilities. Without their precious support it would not be possible to conduct this research.

I am immensely grateful to The Directorate General of Resources for Science, Technology and Higher Education (DG-RSTHE) of the Indonesia Republic for its continuous financial support over my Ph.D period of time and its very generous donation, your contribution has dramatically helped me developed and succeed in my study.

I thank my fellow doctoral students, Ajie, Mohamed, Guillaume, Lidya, Van Anh, Hanane, Karim, Anas for their cooperation and of course friendship and all the fun we have had in the last four years. Some special words of gratitude go to my colleagues of Mechatronics Dept. who have always been a major source of support when things would get a bit discouraging: Nur Wisma, Adhitya, Siti, Nuryanti.

Last but not least, I would like to thank my family: my parents, Obay SOBARI and Lilis DJUARIAH, Lantip WIDODO, Agustina PURNANINGSIH, my beloved husband and daughters, Wahyu Adhie CANDRA, Azaria WAHYU and Elektra WAHYU, for supporting me spiritually throughout writing this thesis and my life in general.

General Introduction

This chapter illustrates some general introductory knowledge about cooperative control of multi-agent systems (MASs). The research work was done in Automation and Control Department of LAMIH UMR CNRS 8201 (Laboratory of Industrial and Human Automation control, Mechanical engineering and Computer Science) which has been structured into two complementary themes: Robustness Complexity (ROC) and Cooperating Intelligent Systems (SIC). Since we deal with MASs, this research work is in the intersection of Robustness Complexity and Cooperating Intelligent Systems themes. More precisely, it deals with decentralized cooperative control for MASs while taking into account the time constraints.

Context

Nowadays, mobile robots become more and more complex, integrate capacities of perception, communication and adaptation to diverse situations and aim at bigger and bigger requirements in terms of robustness, ergonomics and safety. Through the last century, robots have changed the structure of the society and have allowed for safer conditions for work.

For the society, robots can assist humans by taking place on the jobs that are dirty, dull or dangerous. Beyond the factory floor, robots have been instrumental in performing tasks that would be impossible for humans. In automobile industry, robots are used to assist in building cars. These high-powered machines have mechanical arms with tools, wheels and sensors that make them ideal for assembly line jobs. Not only robots save more money in manufacturing systems, but they also perform tough tasks at a pace no human could possibly do. Robots have become increasingly important for investigating hazardous and dangerous environments. These robots are capable of entering an active volcano to collect data or a burning building to search for victims. In addition, the implementation of advanced robotics in the military and NASA fields has changed the landscape of national defense and space exploration.

The introduction of multiple robots increases robustness through redundancy. A group of collabo-

rating robots can often deal with tasks that are difficult, or even impossible, to be accomplished by a single robot. The problem of cooperative control between various robots around a common objective is a stake both from the economic and the scientific point of view. Multiple robots working in a cooperative manner is called as Multi-Agent System (MAS). We denote any system with sensing, computing and communicating capabilities, such as robots, sensors with the word "agent". This set of agents interact with each other, situated in a common environment, eventually, building or participating to, an organisation.

There are many applications of MASs (see Fig. 1). It usually concerns robots in hostile environments realizing dangerous or very painful tasks for men. A classical application is the monitoring of a geographical area by measuring the temperature, pollution or humidity of a specified area. Mining robotics, certain applications of robotics in the construction field (i.e. the transport of heavy objects by means of several autonomous vehicles), or robotics in high-risk areas (i.e. mine clearance, intervention in a radioactive environment) also belong to this kind of applications.

Figure 1: Applications of MASs.

The interaction between agents to achieve a global task is a key in cooperative control. Cooperative control of MASs poses significant theoretical and practical challenges. One of the fundamental topics in cooperative control is the consensus where the objective is to design control protocols between agents to achieve a state agreement, such as position and velocity. Since the exchange of information can only occur between the agent and its neighbours, the state consensus control of MASs becomes difficult and challenging.

Objectives and Motivation

In this thesis, we will improve the navigation scheme for Multi-Agent Systems, while taking into account some practical constraints. We are mainly interested in designing cooperative controllers for each agent, in a fully decentralized way, while considering the robot model and temporal constraints. To consider the temporal constraints, two directions will be investigated:

- **The consensus problem in a fixed-time framework**. Indeed, for many practical applications (including manufacturing systems, missile guidance, spacecraft, etc.), the convergence rate is an important performance specification to design the controller for a dynamical system. As an important performance measure also for coordination control of multi-agent systems, fast convergence is always pursued to achieve better performance and robustness, such as hybrid formation flying, consensus subject to switching topology, etc. In practice, the communication bandwidth and connectivity of multiple agents are often limited and the information exchange among agents may be unreliable. In manufacturing systems, the navigation of multi-agents while taking into account the temporal constraints is very important. Hence, it is interesting to achieve consensus in a predefined-time, i.e. the settling time is uniformly bounded and independent of initial conditions. The estimation of the settling time could be very useful when switching topology or networks of clusters are considered.

  Most of the existing consensus algorithms focus on asymptotic convergence, where the settling time is infinite. However, many applications require a high speed convergence generally characterized by a finite-time control strategy. Moreover, finite-time control allows some advantageous properties such as good disturbance rejection and good robustness against uncertainties. For instance, a recursive terminal sliding mode controller has been introduced for the tracking control of unicycle-type mobile robots in finite-time. The finite-time consensus problem for multi-agent systems has been studied for single integrator, double integrator and inherent non-linear dynamics.

  Using finite time controller, an estimation of the settling time could be very useful when switching topology or networks of clusters are considered. It is worthy of noting that, for the above-mentioned works, the explicit expressions for the bound of the settling time depend on the initial states of agents. Therefore, the knowledge of these initial conditions usually prevent us from the estimation of the settling time using distributed architectures. A new approach, called fixed-time stability has been recently proposed to define algorithms which guarantee that the settling time is upper bounded regardless to the initial conditions.

Based on the above observations, the objective will be to design a fixed-time leader-follower consensus protocol for MASs described in continuous-time. This problem will be studied using the powerful theory of fixed-time stabilization. Sliding mode controllers and sliding mode observers will be designed for each follower to solve the fixed-time consensus tracking problem when the leader is dynamic.

- **The consensus problem in a discrete-time framework**. Compared with continuous-time systems, discrete-time systems are more suitable for practical applications. The limitation of computational resources of each agent becomes a significant challenge. If the communication network among agents allows continuous communication or if the communication bandwidth is sufficiently large, then the information state update of each agent can be modeled using a differential equation. On the other hand, if the communication data arrives in discrete packets, then the information state update is modeled using a difference equation.

  The dynamic behavior of discrete-time multi-agent systems with general communication topologies and the associated consensus problem have been considered by many researchers. It was proved that the states of internal agents converge to a convex combination of boundary agents in the case of communication time delays. Furthermore, Model Predictive Control (MPC) has ability to handle control and state constraints for discrete-time systems. This method can be applied for the control of a group of agents by letting each agent solve, at each step, a constrained finite-time optimal control problem involving the state of neighboring agents. MPC is a form of control in which the output of the system can be predicted from some prediction horizon. The output of the MPC controller is determined based on input and output at a previous time and the control signal along the control horizon.

  Here, the motivation of this research direction comes from the lack of decentralized discrete-time controllers which solve the consensus problem for multi-agent systems with double integrator dynamics. The proposed methodology will be based on decentralized model predictive control. Furthermore, in contrast to classical model predictive controllers, we propose to modify the classical methodology in order to improve the tracking performances.

Finally, the proposed controllers will be implemented on a team of mobile robots using multiple Mini-Lab Enova Robots and ROS (Robotic Operating System).

Previously, every robotics designer and researcher have spent a considerable amount of time to design the embedded software within a robot, as well as the hardware itself. This requires skills in mechanical engineering, electronics and embedded programming (to name a few). There was a considerable re-use of programs, as they were strongly linked to the underlying hardware. The main idea of a robotics OS is to avoid continuously reinventing and to offer standardized functionalities performing hardware abstraction, just like a conventional OS for PCs.

Robot Operating System (ROS) is an operating system for robots. In the same way as operating systems for PCs, servers or standalone devices, ROS is a full operating system for service robotics. It provides not only standard operating system services (hardware abstraction, contention management, process management), but also high-level functionalities (asynchronous and synchronous calls, centralised database, a robot configuration system, etc.).

Some of the theoretical results on the consensus problem will be experimentally implemented and validated on a mobile actuator and sensor network platform using ROS using a wireless network. This research motivation comes from the challenge of the implementation of our proposed controllers in a decentralized way using Mini-Lab mobile robots in the ROS environment. This implementation will require the resolution of some problems corresponding to the connection of multiple mobile robots in a decentralized way in wireless robotic networks, finding good sampling to implement the control algorithm, etc.

Thesis Outline

The remainder of this thesis is organized into five chapters as follows:

Chapter 1. The first chapter is a brief overview on multi-agent systems, fixed-time control strategy and model predictive control. First, the formal definition of consensus for multi-agent systems is given. After, some recalls on fixed-time stability, the concepts of stability for fixed-time control are discussed. We will present some results on fixed-time stability to establish the foundation for the understanding of our work. At the end, an overview on model predictive control for discrete-time multi-agents systems is given.

Chapter 2. In this chapter, we will propose fixed-time control strategies to solve the tracking problem for a mobile robot. Then, the fixed-time approach is applied to solve the leader-follower consensus problem for multi-agent systems in this chapter. A decentralized observer-based control protocol is proposed for each agent to solve the leader-follower consensus problem in a fixed-time. Some simulations will show the effectiveness of the proposed scheme.

Chapter 3. We analyse in this chapter the consensus for multi-agent systems using distributed

MPC. In the first part, we will deal with the consensus control problem for multi-agent systems with single-integrator dynamics. We will present, the distributed MPC scheme. The criteria function is designed using the difference between two consecutive inputs. Furthermore, multi-agent systems with double-integrator dynamics will discuss. Illustrative examples will be given.

Chapter 4. We will present in this chapter an experimental platform for the implementation of the theoretical results using mini-lab robots. Also, the architecture of multi-master ROS and the wireless robot network connectivity will be discussed in this chapter.

Chapter 5. In this chapter, we apply the consensus-based design scheme to two applications, single agent and multi-agents systems. In single agent application, we design node of path planning in ROS such that the robot can track the desired trajectory in termd of fixed-time tracking. In multiple mobile robots application, we explore issues and challenges in cooperative control with communication constraints.

General conclusion and perspectives. This chapter is a general conclusion. A contribution of the works performed in this thesis and the results given in the study of consensus under time constraints will be presented as well as perspectives on future works. Several problems and methods remain open and need to be developed.

Scientific productions

International refereed journals:

- Pipit Anggraeni, Michael Defoort, Mohamed Djemai and Zongyu Zuo (20xx) "Fixed-Time Leader-Follower Consensus Control Strategy for Multi-Agent Systems with Chained-form Dynamics", *Nonlinear Dynamics Journal Springer*, (under revision).
  (This work is presented in Chapter 2)

International conferences:

- Pipit Anggraeni, Michael Defoort, Mohamed Djemai and Zongyu Zuo (2017) "Fixed-Time Tracking Control of Chained-form Nonholonomic System with External Disturbances", *The* 5^th *International Conference on Control Engineering and Information Technology (CEIT'2017)*, December, Sousse, Tunisia.
  (This work is presented in Chapter 2)

- Pipit Anggraeni, Michael Defoort, Mohamed Djemai, Aries Subiantoro and Abdul Muis (2017) "Consensus of Double Integrator Multi-Agent Systems Using Decentralized Model Predictive Control", *The* 5^th *International Conference on Control Engineering and Information Technology*

(CEIT'2017), December, Sousse, Tunisia.
(This work is presented in Chapter 3)

- Pipit Anggraeni, Mariem Mrabet, Michael Defoort, Mohamed Djemai (2018) "Development of a wireless communication platform for multiple-mobile robots using ROS", *The* 6^th *International Conference on Control Engineering and Information Technology (CEIT'2018)*, October, Istanbul, Turkey.
(This work is presented in Chapter 4)

Chapter 1

State of the art

In this chapter, at first we will introduce some basic concepts of algebraic graph theory. Then, we will make a brief state of the art on the consensus control problem in cooperative control for multi-agent systems. The literature review of convergence rate analysis will be then presented. Since the study of MASs under the discrete-time framework is very convenient for a discrete-time implementation, we will recall, the concepts of consensus for multi-agent systems in continuous-time and discrete-time separately. At the end of this chapter, we will introduce some concepts on model predictive control as a solution of the multi-agent consensus problem in discrete-time.

1.1 Algebraic Graph Theory Background

Cooperative control studies the dynamics of multi-agent dynamical systems linked to each other by a communication graph. The graph represents the allowed information flow between the agents.

1.1.1 Graph Theory Basics

Here, we present some basic graph theory concepts that are essential in the study of multi-agent dynamical systems. Suppose that there are n mobile robots in the group of MAS which interact with each other through a communication or sensing network or a combination of both. The interaction pattern between agents can be modeled by describing the communication topology in the form of a graph. A graph is built from a finite set, where each set has a finite number of elements. Each element is called a vertex and denoted by $\mathcal{V}$. The set of vertices can have several vertices and are represented by $\mathcal{V}_n$.

A graph can be defined by $\mathcal{G}_n \triangleq (\mathcal{V}_n, \mathcal{E}_n)$, where $\mathcal{V}_n \triangleq \{1, \ldots, n\}$ defines the set of nodes, corresponding to the agents and $\mathcal{E}_n \subseteq \mathcal{V}_n \times \mathcal{V}_n$ defines the edge set, called edges. Figure 1.1 shows an undirected graph of 5 agents.

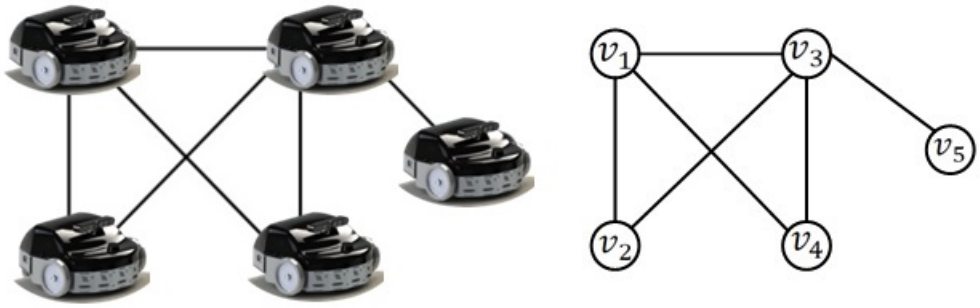

Figure 1.1: A communication graph of MAS with 5 vertices and 6 edges.

It is natural to model the interaction among agents by directed or undirected graphs. A link (i, j) in the edge set of a directed graph denotes that agent j can obtain information from agent i, but not necessarily vice versa. Self-edges (i, i) are not allowed unless otherwise indicated. For the edge (i, j), i is the parent node and j is the child node. If an edge $(i, j) \in \mathcal{E}$, then node i is a neighbor of node j. The set of neighbors of node i is denoted as $\mathcal{N}_i = \{j \neq i : (j, i) \in \mathcal{E}\}$. In contrast to a directed graph, the pairs of nodes in an undirected graph are unordered, where the edge (i, j) denotes that agents i and j can obtain information from each other. Note that an undirected graph can be viewed as a special case of a directed graph, where an edge (i, j) in the undirected graph corresponds to the edges (i, j) and (j, i) in the directed graph. A weighted graph associates a weight with every edge in the graph. The union of a collection of graphs is a graph whose node and edge sets are the unions of the node and edge sets of the graphs in the collection.

Figure 1.2 shows the communication graph among 4 agents in the directed graph. An arrow from node i to node j indicates that agent j receives information from agent i.

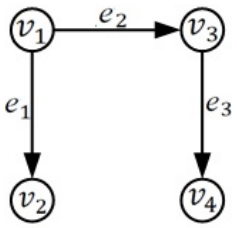

Figure 1.2: A directed graph with 4 vertices.

A directed path is a sequence of edges in a directed graph of the form (i_1, i_2), $(i_2, i_3), \ldots$. An undirected path in an undirected graph is defined analogously. In a directed graph, a cycle is a directed path that starts and ends at the same node. A directed graph is strongly connected if there is a directed path from every node to every other node. An undirected graph is connected if there is an undirected path between every pair of distinct nodes. An undirected graph is fully connected if there is an edge between every pair of distinct nodes. A directed graph is complete if there is an edge from

every node to every other node. A directed tree is a directed graph in which every node has exactly one parent except for one node, called the root, which has no parent and which has directed paths to all other nodes. Note that a directed tree has no cycle because every edge is oriented away from the root. In undirected graphs, a tree is a graph in which every pair of nodes is connected by exactly one undirected path.

A subgraph $(\mathcal{V}_1, \mathcal{E}_1)$ of $(\mathcal{V}, \mathcal{E})$ is a graph such that $\mathcal{V}_1 \subseteq \mathcal{V}$ and $\mathcal{E}_1 \subseteq \mathcal{E} \cap (\mathcal{V}_1 \times \mathcal{V}_1)$. A directed spanning tree $(\mathcal{V}_1, \mathcal{E}_1)$ of the directed graph $(\mathcal{V}, \mathcal{E})$ is a subgraph of $(\mathcal{V}, \mathcal{E})$ such that $(\mathcal{V}_1, \mathcal{E}_1)$ is a directed tree and $\mathcal{V}_1 = \mathcal{V}$. An undirected spanning tree of an undirected graph is defined analogously. The directed graph $(\mathcal{V}, \mathcal{E})$ has or contains a directed spanning tree if a directed spanning tree is a subgraph of $(\mathcal{V}, \mathcal{E})$. Note that the directed graph $(\mathcal{V}, \mathcal{E})$ has a directed spanning tree if and only if $(\mathcal{V}, \mathcal{E})$ has at least one node with directed paths to all other nodes. In undirected graphs, the existence of an undirected spanning tree is equivalent to being connected. However, in directed graphs, the existence of a directed spanning tree is a weaker condition than being strongly connected.

Graphs, can also be represented by a matrix for further analysis. For undirected graphs $\mathcal{G}_n$, the degree of vertex $d(v_i)$ is related to the neighbor set $\mathcal{N}_i$, and equals to the number of adjacent vertices with vertex v_i in graph $\mathcal{G}_n$. In Figure 1.1, the degree of vertex is:

$$d(v_1) = 3; \quad d(v_2) = 2; \quad d(v_3) = 3; \quad d(v_4) = 2; \quad d(v_5) = 1$$

The vertex degree above can be expressed with a degree matrix $\triangle(\mathcal{G})$, in the form of a diagonal matrix measuring $n \times n$ whose diagonal component is the degree of vertex in graph $\mathcal{G}$, as:

$$\triangle(\mathcal{G}) = \begin{bmatrix} d(v_1) & 0 & \cdots & 0 \\ 0 & d(v_2) & \cdots & 0 \\ \vdots & \vdots & \ddots & \vdots \\ 0 & 0 & \cdots & d(v_n) \end{bmatrix} \tag{1.1}$$

1.1.2 Adjacency Matrices

The adjacency matrix $\mathcal{A} \triangleq [a_{ij}] \in \mathbb{R}^{n \times n}$ of a directed graph $(\mathcal{V}, \mathcal{E})$ is defined such that a_{ij} is a positive weight if $(j, i) \in \mathcal{E}$ and $a_{ij} = 0$ if $(j, i) \notin \mathcal{E}$. Self-edges are not allowed (i.e., $a_{ii} = 0$) unless otherwise indicated. The adjacency matrix of an undirected graph is defined analogously except that $a_{ij} = a_{ji}$ for all $i \neq j$ because $(j, i) \in \mathcal{E}$ implies $(i, j) \in \mathcal{E}$. Note that a_{ji} denotes the weight for the edge $(j, i) \in \mathcal{E}$. If the weight is not relevant, then a_{ji} is set equal to 1 if $(j, i) \in \mathcal{E}$. The in-degree and out-degree of node i are defined as, respectively, $\sum_{j=1}^{n} a_{ij}$ and $\sum_{j=1}^{n} a_{ji}$. A node i is balanced if $\sum_{j=1}^{n} a_{ij} = \sum_{j=1}^{n} a_{ji}$. A graph is balanced if $\sum_{j=1}^{n} a_{ij} = \sum_{j=1}^{n} a_{ji}$, for all i. For an undirected graph,

$\mathcal{A}$ is symmetric, and thus every undirected graph is balanced.

Here below are the degree matrix and the adjacency matrix for the undirected graph given in Figure 1.1:

$$\triangle(\mathcal{G}) = \begin{bmatrix} 3 & 0 & 0 & 0 & 0 \\ 0 & 2 & 0 & 0 & 0 \\ 0 & 0 & 4 & 0 & 0 \\ 0 & 0 & 0 & 2 & 0 \\ 0 & 0 & 0 & 0 & 1 \end{bmatrix} \qquad \mathcal{A}(\mathcal{G}) = \begin{bmatrix} 0 & 1 & 1 & 1 & 0 \\ 1 & 0 & 1 & 0 & 0 \\ 1 & 1 & 0 & 1 & 1 \\ 1 & 0 & 1 & 0 & 0 \\ 0 & 0 & 1 & 0 & 0 \end{bmatrix}$$

For the directed graph in Figure 1.2, the degree matrix and the adjacency matrix are as follows:

$$\triangle(\mathcal{D}) = \begin{bmatrix} 2 & 0 & 0 & 0 \\ 0 & 1 & 0 & 0 \\ 0 & 0 & 1 & 0 \\ 0 & 0 & 0 & 1 \end{bmatrix} \qquad \mathcal{A}(\mathcal{D}) = \begin{bmatrix} 0 & 1 & 1 & 0 \\ 0 & 0 & 0 & 0 \\ 0 & 0 & 0 & 1 \\ 0 & 0 & 0 & 0 \end{bmatrix}$$

1.1.3 Laplacian Matrices

Many properties of a graph may be studied in terms of its Laplacian. In fact, we shall see that the Laplacian matrix is of extreme importance in the study of cooperative control of multi-agent systems.

Define the matrix $\mathcal{L} \triangleq [l_{ij}] \in \mathbb{R}^{n\times n}$ as

$$l_{ii} = \sum_{j=1, j\neq i}^{n} a_{ij}, \qquad l_{ij} = -a_{ij},\ i \neq j \tag{1.2}$$

Note that if $(j,i) \notin \mathcal{E}$ then $l_{ij} = -a_{ij} = 0$. The matrix $\mathcal{L}$ satisfies

$$l_{ij} \leq 0,\ i \neq j,\ \sum_{j=1}^{n} l_{ij} = 0, \qquad i = 1, ..., n. \tag{1.3}$$

$\mathcal{L}$ is called the Laplacian matrix. For an undirected graph, $\mathcal{L}$ is symmetric. However, for a directed graph, $\mathcal{L}$ is not necessarily symmetric and is sometimes called the nonsymmetric Laplacian matrix or directed Laplacian matrix. In both the undirected and directed cases, since $\mathcal{L}$ has zero row sums, 0 is an eigenvalue of $\mathcal{L}$ with the associated eigenvector $1 \triangleq [1, \ldots, 1]^T$, the $n \times 1$ column vector of ones. Note that $\mathcal{L}$ is diagonally dominant and has nonnegative diagonal entries. If follows from Gershgorin's disc theorem [**?**] that, for an undirected graph, all of the nonzero eigenvalues of $\mathcal{L}$ are positive ($\mathcal{L}$ is positive semidefinite), whereas, for a directed graph, all of the nonzero eigenvalues of $\mathcal{L}$ have positive real parts. Therefore, all of the nonzero eigenvalues of $-\mathcal{L}$ have negative real parts.

For example, the Laplacian matrix for the undirected graph in Figure 1.1 is:

$$\mathcal{L}(\mathcal{G}) = \triangle(\mathcal{G}) - \mathcal{A}(\mathcal{G}) = \begin{bmatrix} 3 & -1 & -1 & -1 & 0 \\ -1 & 2 & -1 & 0 & 0 \\ -1 & -1 & 4 & -1 & 0 \\ -1 & 0 & -1 & 2 & 0 \\ 0 & 0 & -1 & 0 & 1 \end{bmatrix}$$

For Figure 1.2, the Laplacian matrix is:

$$\mathcal{L}(\mathcal{D}) = \triangle(\mathcal{D}) - \mathcal{A}(\mathcal{D}) = \begin{bmatrix} 2 & -1 & -1 & 0 \\ 0 & 1 & 0 & 0 \\ 0 & 0 & 1 & -1 \\ 0 & 0 & 0 & 1 \end{bmatrix}$$

For an undirected graph, 0 is a simple eigenvalue of $\mathcal{L}$ if and only if the undirected graph is connected [**?**]. For a directed graph, 0 is a simple eigenvalue of $\mathcal{L}$ if the directed graph is strongly connected [5, Proposition 3], although the converse does not hold. For an undirected graph, let $\lambda_i(\mathcal{L})$ be the i^th smallest eigenvalue of $\mathcal{L}$ with $\lambda_1(\mathcal{L}) \leq \lambda_2(\mathcal{L}) \leq \ldots \leq \lambda_n(\mathcal{L})$ so that $\lambda_1(\mathcal{L}) = 0$. For an undirected graph, $\lambda_2(\mathcal{L})$ is the algebraic connectivity, which is positive if and only if the undirected graph is connected [**?**]. The algebraic connectivity quantifies the convergence rate of a consensus algorithm [**?**].

1.2 Consensus Control Strategy

1.2.1 Overview of Cooperative Control

A multi-agent system is a system that consists of multiple intelligent agents and their environment. The word "agent" represents any system with sensing, computing and communicating capabilities, such as a wheeled mobile robot, an unmanned air vehicle (UAV), an autonomous underwater vehicle (AUV), a manipulator or sensors. The agents interact with one-another to achieve a global task. To successfully interact, they will require the ability to cooperate, coordinate and negotiate with each other. The interaction between agents to achieve a global task is called cooperative control. Figure 1.3 shows different types of agents (Figure 1.3(a) for wheeled mobile robots, Figure 1.3(b) for unmanned air vehicles, Figure 1.3(c) for autonomous underwater vehicles).

Over the last decade, an enormous amount of researchers have drawn great interest on cooperative control of MAS) because of its variety of applications in several areas, e.g., unmanned aerial vehicle surveillance, hazardous material handling, mine-sweeping and deep sea exploration. Figure 1.4 illustrates some applications of MAS. To enable these applications, various cooperative control

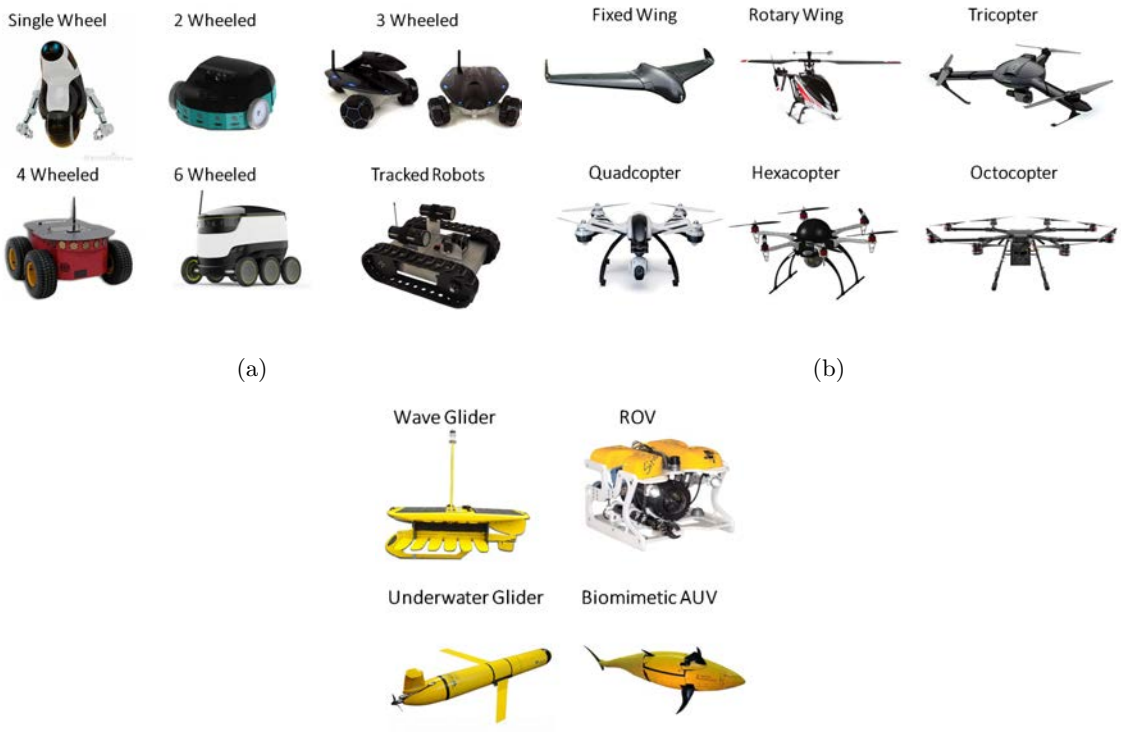

Figure 1.3: Example of different agents.

capabilities need to be developed, including target tracking [?] [?] [?] [?] [?], flocking [?] [?] [?] [?], swarming [?] [?], rendezvous [?] [?], area coverage [?] [?] [?], monitoring [?] [?], formation control [?] [?] [?] [?] [?], etc. In these works, it has been shown that the use of multi-agent cooperative systems enables to accomplish complex tasks which are difficult or impossible compared to the use of a single one.

Figure 1.4: Multi-agent system applications.

Cooperative control of multi-agent systems poses significant theoretical and practical challenges. Indeed, the objective is to develop a system of subsystems rather than a single system that has team goals and individual goals which have to be negotiated, while taking into account the limited computa-

tional resources of each individual agent, the locally sensed information, and limited inter-component communications. The consensus/agreement/synchronization/rendezvous problem is one fundamental research topic of cooperative control of MASs, which focuses on designing distributed controllers to drive agents to achieve state agreement or forcing a group of agents states to reach an agreement on a quantity of interest such as the rendezvous position, velocity and heading direction. It is crucial to design appropriate control protocols for agents with information interactions over the network.

In Figure 1.5, we show a MAS consisting of four mobile robot labeled from 1 to 4. The information transmission can be either unidirectional or bidirectional as indicated by the arrow directions. The figure shows that agent 3 receives information from agent 2, but the information of agent 3 can not be transmitted to agent 2. The bidirectional communication channel between agent 1 and 2 or agent 3 and 4 means that two agents can receive information from each other.

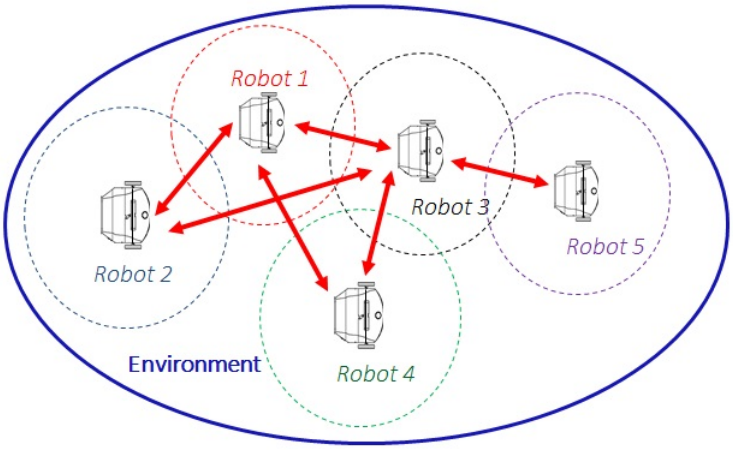

Figure 1.5: Illustration of a MAS: A group of five mobile robots.

1.2.2 Communication Graphs and Consensus

A network may be considered as a set of nodes or agents that collaborate to achieve a common objective. To capture the notion of dynamical agents, each node i of a graph endowed with a time-varying state vector $x_i(t) \in \mathbb{R}^n$. A graph with node dynamics [10] is $\mathcal{G}(x)$ with ($\mathcal{G}$ being a graph having n nodes and $x = [x_1^T, ..., x_n^T]^T$ a global state vector, where the state of each node evolves according to the following differential equation:

$$\dot{x_i}(t) = F(x_i(t), u_i(t)) \qquad \text{with} \qquad i = 1, 2, ..., n. \tag{1.4}$$

where $u_i(t) \in \mathbb{R}^m$ is the control input of agent i (resp. control input) of the multi-agent system, $F : \mathbb{R}^n \times \mathbb{R}^m \to \mathbb{R}^n$.

Definition 1 ***Decentralized Control Protocol.*** *The control given by* $u_i = k_i(x_{i1}, x_{i2}, ..., x_{im_i})$ *for some function* $k_i(.)$ *is said to be distributed if* $m_i < n$, $\forall i$, *that is, the control input of each node depends on some proper subset of all the nodes. It is said to be a protocol with topology* $\mathcal{G}$ *if* $u_i = k_i(x_i, \{x_j | j \in \mathcal{N}_i\})$, *that is, each node can obtain information about the state only of itself and its neighbors.*

Cooperative control, or control of distributed dynamical systems on graphs, refers to the situation where each node can obtain information for control design only from itself and its neighbors. The graph might represent a communication network topology that restricts the allowed communications between the nodes. This has also been referred to as multi-agent control, but is not the same as the notion of multi-agent systems used by the Computer Science community [20].

1.2.3 Consensus Algorithm

When agents reach an agreement on a certain common feature, they are said to have reached ***consensus***. Information consensus guarantees that agents sharing information over a network topology have a consistent view of information that is critical to the coordination task. To achieve consensus, there must be a shared variable of feature, called the ***information state***, as well as appropriate algorithmic methods for negotiating to reach consensus on the value of that variable, called the ***consensus algorithm***. The information state represents an instantiation of the coordination variable for the team.

The basic idea of a consensus algorithm is to impose similar dynamics on the information states of each agents. If the communication network among agents allows continuous communication or if the communication bandwidth is sufficiently large, then the information state update of each agent is modeled using a differential equation. On the other hand, if the communication data arrive in discrete packets, then the information state update is modeled using a difference equation.

A basic control design objective is the following.

Definition 2 ***Consensus Problem.*** *Find a distributed control protocol that drives several or all states to the same values* $x_i = x_j$, $\forall i, j$ *. This value is known as a consensus value.*

The most common continuous-time consensus algorithm [**?**],[**?**] [**?**] [**?**] [**?**] is given by:

$$\dot{x}_i(t) = -\sum_{j=1}^{n} a_{ij}[x_i(t) - x_j(t)], \qquad i = 1, \ldots, n. \tag{1.5}$$

where $a_{ij}(t)$ is the (i, j) entry of adjacency matrix $\mathcal{A} \in \mathbb{R}^{n \times n}$ associated with $\mathcal{G}$ and x_i is the information state of the i^{th} agent. A consequence of Equation (1.5) is that the information state $x_i(t)$ of agent i is driven toward the information state $x_j(t)$ of its neighbors j.

Average Consensus

The average consensus is discussed in [?], [?], [?], [?]. All agents in the MAS will converge to the exact average value of their initial states. When an agent moves, the average value of the states can remain constant by changing another agent's states with the same magnitude in the opposite direction [?], [?]. More complicated situations such as switching topologies, time-varying delays in the average consensus problem are discussed in [?]. Figure 1.6 illustrated the average consensus problem where the state of all agents converge to an average value.

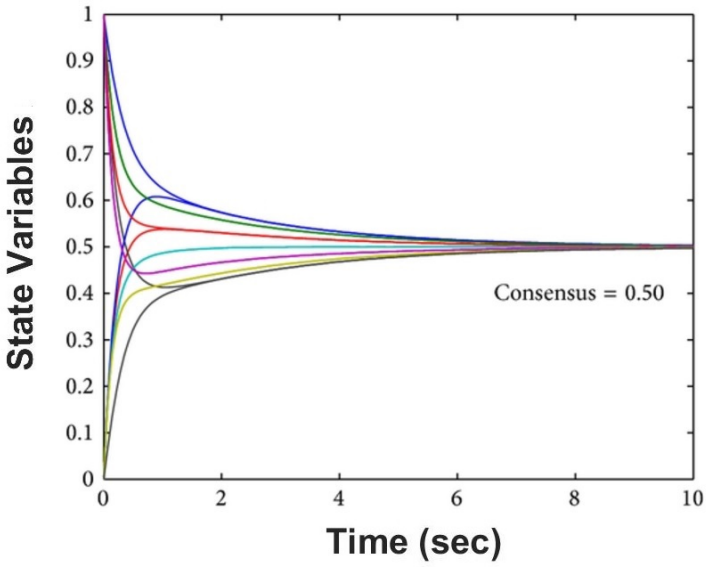

Figure 1.6: Average Consensus.

1.2.4 Leaderless and Leader-Follower Consensus

According to the number of leaders in a group of multi-agent system, current researches about the consensus problem are classified into three fields, i.e., leaderless consensus, leader-following consensus problem with a single leader, and containment control with multiple leaders.

Leaderless Consensus

In leaderless consensus, all agents have the same role. For leaderless consensus, control strategies are proposed for first-order [?] [?], second-order [?] [?], high-order [?] [?] multi-agent systems. In [?], it has been shown that for MAS represented by a simple integrator, the algebraic connectivity, that is to say, the smallest positive eigenvalue of the Laplacian graph, determines the convergence time. [?] provides an overview of consensus for first-order multi-agent systems and also some theoretical

results on information consensus-seeking under both time-invariant and time-varying communication topologies. Figure 1.7 described the leaderless consensus problem where the state of all agents converge to a consensus point.

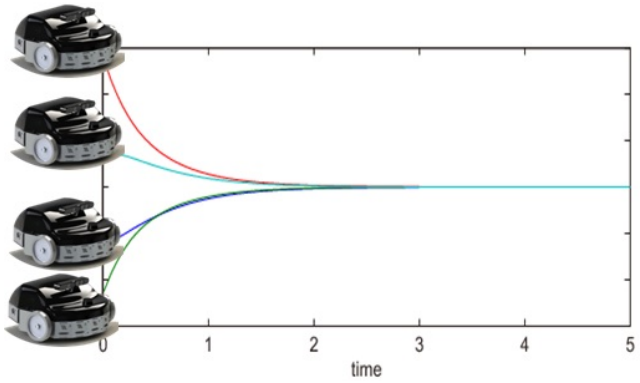

Figure 1.7: Leaderless Consensus.

Leader-Following Consensus

In leader-following consensus problem, there are consensus regulation problem with static leaders and consensus tracking problem with dynamic leaders. The leader-follower consensus problem has been firstly introduced in [**?**]. Figure 1.8 illustrated the interaction graph for five followers and one leader. Not all the followers are connected to the leader (node 0). Only followers one and two are connected to the leader in this example.

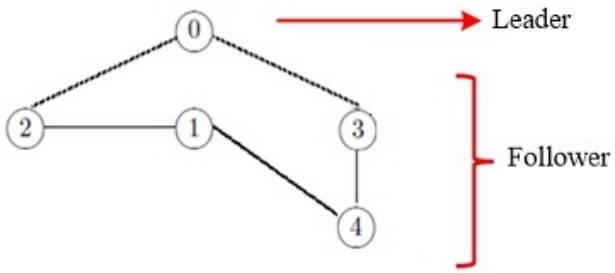

Figure 1.8: Graph of Leader Follower Model

For leader-following consensus problem with a single leader, control strategies are proposed in [**?**] [**?**] where distributed tracking control schemes have been developed for second-order MAS considering directed interconnection topology. A consensus tracking protocol has been proposed in [**?**] for second-order MAS with matched perturbations. In [**?**], the leader-follower consensus problem for linear MAS has been studied using distributed impulsive control.

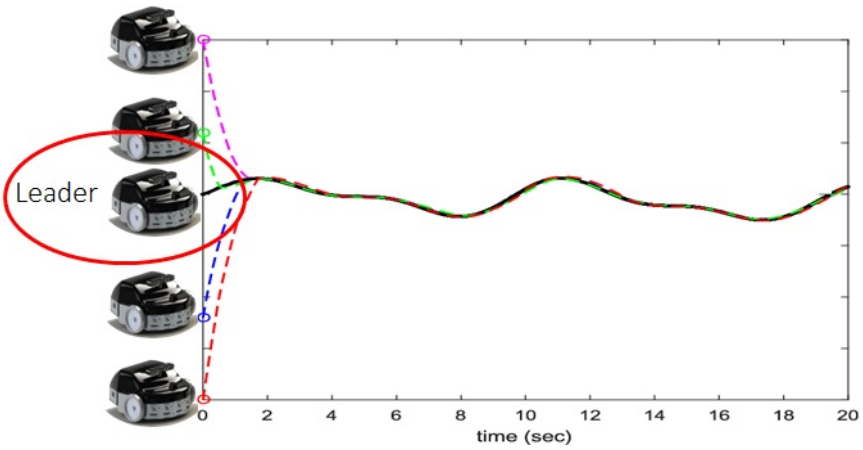

Figure 1.9: Leader Follower Consensus

Containment Control

The objective of containment control is to drive the states of followers into a convex hull spanned by those multiple leaders. In practical scenarios, it is sometimes more interesting if followers move to an area stretched by several leaders instead of tracking a specific desired path [**?**]. One possible scenario is that groups of vehicles moves from one place to a target while only a small portion of vehicles has sensing capabilities to detect dangerous obstacles. In this case, all groups have to safely reach the destination as long as followers (vehicles without sensing capabilities) remain in the safe zone formed by leaders (vehicles with sensing capabilities). Some results are reported on the containment control problem for single-integrator [**?**] or double-integrator [**?**] multi-agent systems.

1.3 Convergence Rate Analysis

The consensus problem of multi-agent systems has received much attention in recent years and many interesting results have been discussed from different directions. An important topic in the study of the consensus problem is the settling time, which characterizes the rate of convergence rate of a closed-loop system. It is well recognized as one of the performance specifications for the control system design. Fast convergence is usually pursued in practice in order to achieve better performance and robustness. It is clear that for the cooperative control of MAS, the convergence rate is one critical index to evaluate the proposed control methods.

To illustrate this important specification index, let us consider the first-order system

$$\dot{x} = u \tag{1.6}$$

where $x \in \mathbb{R}$ is the state and $u \in \mathbb{R}$ is the control input. Figure 1.10 shows the trajectory of system (1.6) under different control input ($u = -x$, $u = -sign(x)$ and $u = -(|x|^2 + 1)sign(x)$). One can see the asymptotic, finite-time and fixed-time properties of the corresponding closed-loop system.

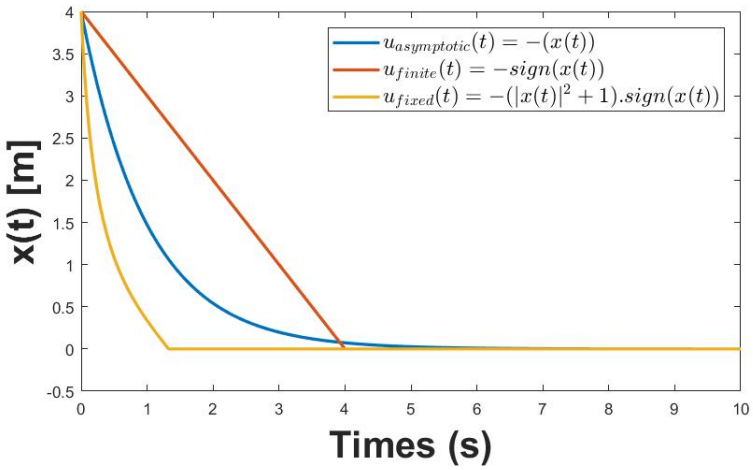

Figure 1.10: Asymptotic, finite-time and fixed-time properties of the first-order system

1.3.1 Asymptotic stability

Most of the existing consensus control algorithms for multi-agent systems are asymptotic consensus algorithms. It means that the convergence rate is at best exponential with infinite settling time. In other words, the states cannot reach a consensus in finite time. In the context of cooperative control, an initial result [**?**] shows that for MAS represented by a simple integrator, the algebraic connectivity, that is to say, the smallest eigenvalue of the Laplacian graph, determines the convergence rate. In [**?**], the authors have proposed an approach to increase this algebraic connectivity. However, linear algorithms have only focused on asymptotic convergence, where the time to reach consensus can be arbitrarily large. In [**?**], the convergence rate can be enhanced by maximizing the algebraic connectivity of the communication topology.

1.3.2 Finite-time stability

Most aforementioned consensus works can only achieve state agreement over an infinite time horizon, which fails to meet specific convergence requirements in an unknown environment. Nevertheless, in some practical cases, finite-time convergence is very interesting in terms of accuracy (which depends on the sampling period) and robustness against perturbations [**?**].

Before giving a brief state of the art on finite-time consensus, let us recall some basics on finite-time stability. The key point in finite time stability is that the power exponent should be less than one.

Generally, consider the following system

$$\begin{cases} \dot{x}(t) &= F(t, x(t)) \\ x(0) &= x_0 \end{cases} \tag{1.7}$$

where $x \in \mathbb{R}^n$ is the state, $F : \mathbb{R}^+ \times \mathbb{R}^n \to \mathbb{R}^n$ is an upper semicontinuous mapping in an open

neighborhood $F(t,0)=0$ for $t>0$. The solution of system (1.7) are understood in the Filippov sense [**?**] if $F(t,x)$ is discontinuous. Let $x(t,x_0)$ be an arbitrary solution of the Cauchy problem of system (1.7).

Definition 3 *[**?**] The origin of system (1.7) is a globally finite-time equilibrium if there is a function $T:\mathbb{R}^n\to\mathbb{R}^+$ such that for all $x_0\in\mathbb{R}^n$, the solution $x(t,x_0)$ of system (1.7) is defined and $x(t,x_0)\in\mathbb{R}^n$ for $t\in[0,T(x_0))$*

$$\begin{cases} \lim_{t\to T(x_0)} x(t,x_0)=0 \\ x(t,x_0)=0 \qquad \forall t>T(x_0) \end{cases} \tag{1.8}$$

$T(x_0)$ is called the settling time function.

Finite-time stability of the origin implies the asymptotic stability of the origin.

Lemma 1 *[**?**] Assume that there exists a continuously differentiable positive definite and radially unbounded function $V:\mathbb{R}^n\to\mathbb{R}^+$ such that*

$$\dot{V}(x)\leq -\alpha V^p(x) \tag{1.9}$$

with $\alpha>0$ and $0<p<1$. Then, the origin of system (1.7) is globally finite-time stable with settling time estimate

$$T(x_0)\leq \frac{1}{\alpha(1-p)}V^{1-p}(x_0) \tag{1.10}$$

In [**?**], the authors provide a finite-time consensus protocol for single-integrator MAS using an appropriate Lyapunov function and time-varying weighted directed graphs. In [**?**], the authors have introduced a terminal-sliding mode controller to deal with the finite-time consensus problem of second-order linear uncertain systems. In [**?**], [**?**], the finite-time tracking problem has been addressed for second-order MAS. In [**?**], a recursive terminal sliding mode controller has been introduced for the tracking control problem of uncertain chained-form systems in finite-time. Nevertheless, in these studies, the estimated bound of the settling time depends on the initial states of all the agents. Therefore, this bound cannot be a priori estimated in decentralized architectures. Hence, in some practical applications, it is required to achieve consensus in a prescribed time.

1.3.3 Fixed-time stability

Although finite-time consensus has many advantages, the estimation of convergence time depends on initial states of the networked agents. This will give limitation in practice since the knowledge of initial conditions is usually unavailable. This motivation gives rise to provide the convergence information in advance to yield more options for designers. According to this issue, a new strategy called fixed-time consensus is proposed.

Let us first recall the basics on fixed-time stability. Let us consider system

$$\begin{cases} \dot{x}(t) &= F(t, x(t)) \\ x(0) &= x_0 \end{cases} \tag{1.11}$$

where $x \in \mathbb{R}^n$ is the state, $F : \mathbb{R}^+ \times \mathbb{R}^n \to \mathbb{R}^n$ is a nonlinear function and $F(t, 0) = 0$ for $t > 0$. The solution of (1.11) are understood in the Filippov sense [**?**].

Definition 4 *[**?**] The origin of system (1.11) is a globally fixed-time equilibrium if it is globally finite-time stable and the settling time function $T(x_0)$ is bounded by a positive number $T_{max} > 0$, i.e. $T(x_0) \leq T_{max}$, $\forall x_0 \in \mathbb{R}^n$*

Lemma 2 *[**?**] Assume that there exists a continuously differentiable positive definite and radially unbounded function $V : \mathbb{R}^n \to \mathbb{R}^+$ such that*

$$\dot{V}(x) \leq -\alpha V^p(x) - \beta V^q(x) \tag{1.12}$$

with $\alpha > 0$, $\beta > 0$, $0 < p < 1$ and $q > 1$. Then, the origin of system (1.11) is globally fixed-time stable with settling time estimate

$$T(x_0) \leq T_{max} = \frac{1}{\alpha(1-p)} + \frac{1}{\beta(q-1)} \tag{1.13}$$

Remark 1 *[**?**] If $p = 1 - \frac{1}{\mu}$ and $q = 1 + \frac{1}{\mu}$ with $\mu > 1$, the settling time can be estimated by a less conservative bound:*

$$T(x_0) \leq T_{max} = \frac{\pi\mu}{2\sqrt{\alpha\beta}} \tag{1.14}$$

The concept of fixed-time stability has been introduced to design controllers such that the convergence time is upper bounded independently of the initial conditions of the system [**?**] [**?**] [**?**] [**?**]. In [**?**], a faster fixed-time nonsingular terminal sliding mode control scheme is proposed and the results are applied to suppress chaotic oscillation in power systems.

Fixed-time consensus protocols have been investigated for first-order MAS [**?**] with external perturbations in [**?**], [**?**], [**?**], for first-order switched MAS with continuous-time and discrete-time subsystems in [**?**], for second-order dynamics in [**?**], [**?**], [**?**], [**?**] and high-order integrator dynamics in [**?**]. In [**?**], for second-order multi-agent systems with directed topologies, a guaranteed settling time independent of initial conditions is obtained by using global well-defined nonlinear consensus protocols with the help of a sliding surface. An extended result is presented in [**?**] with a newly designed sliding manifold with external disturbances.

For nonlinear MAS, the fixed-time consensus is further investigated under a weighted undirected graph and uncertain disturbances in [**?**]. In [**?**] the interactions between agents are not only cooperative but also antagonistic. Under this circumstance, a distributed nonlinear protocol is proposed to

guarantee the state agreement in a fixed time as long as the interaction topologies are both structurally balanced and structurally unbalanced. Few consensus protocols consider nonlinear MAS (such as chained-form dynamics), which can model dynamics of robots. In [**?**], a class of multi-scale coordination control problem is solved by using a fixed-time controller such that the multi vehicles with disturbances are guaranteed to achieve consensus on a common quantity but of their own scales. Recently, a switching strategy has been introduced to deal with the fixed-time consensus problem for multiple nonholonomic agents [**?**]. However, in this work, the leader was static and no uncertainty was considered.

1.4 Consensus in Discrete-time

Consensus problems can be studied in different time domains: continuous-time and discrete-time. Many research studies are focused on continuous-time consensus protocols. On the other hand, it becomes more convenient and popular to study MASs under the discrete-time framework due to the development of the digital signal processing and communication technologies. Compared with the continuous-time systems, discrete-time systems are more suitable for practical applications.

Some interesting works related to the topic of first-order discrete-time consensus stability analysis were reported in [**?**] [**?**] [**?**]. The main objective of [**?**] was to theoretically study the coordination of a group of autonomous agents using the Vicsek model. In [**?**], some consensus protocols for discrete-time systems with switching topology were provided and the robustness against time delays was analyzed. These two kinds of protocols are based using the same data at two time-steps. The dynamic behavior of discrete-time multi-agent systems with general communication topologies was considered in [**?**]. For topologies that have a spanning tree, the consensus problem was studied. It was proved that the states of internal agents converge to a convex combination of boundary agents in the case of communication time delays. Much attention on discrete-time consensus can be found in [**?**] [**?**] [**?**], etc.

Despite much effort has been produced for the two types of time domain above, the solutions are not yet satisfied because MASs are usually operated using the analog measurement and embedded microcontrollers to process digital signals. In sampled-data control system, the work requires both continuous-time dynamics and discrete-time controllers. The sampling is usually assumed periodic and synchronized for all agents [**?**] [**?**].

1.4.1 Notation and Basic Definition

We use Z_+ to denote the set of all nonnegative integers. Euclidean norm is denoted simply as $|\cdot|$. For any function $\phi : Z_+ \to \mathbb{R}^n$, $\|\phi\| = sup\{|\phi(k)| : k \in Z_+\} \leq \infty$. B_r is the closed ball of radius r, i.e. $B_r = \{x \in \mathbb{R}^n || x| \leq r\}$. A continuous function $\alpha(\cdot) : \mathbb{R}_+ \to \mathbb{R}_+$ is a $\mathcal{K}$ function if $\alpha(0) = 0, \quad \alpha(s) > 0$

for all $s > 0$ and it is strictly increasing. A continuous function $\beta : \mathbb{R}_+ \times Z_+ \to \mathbb{R}_+$ is a $\mathcal{KL}$ function if $\beta(s,t)$ is a $\mathcal{K}$ function in s for any $t \geq 0$ and for each $s > 0$ $\beta(s,\cdot)$ is decreasing and $\beta(s,t) \to 0$ as $t \to \infty$. $\mathcal{M}_\Omega$ is the set of signals in some subset Ω.

Definition 5 *[?] [?] (Stability) Given the discrete-time dynamic system*

$$x(k+1) = f(x(k)) \tag{1.15}$$

where the origin $x^* = 0 \in \Omega \subset \mathbb{R}^n$ is an equilibrium point. If there exists a function $V : \mathbb{R}^n \to \mathbb{R}^+$ and functions α and β of class $\mathcal{K}$ such that

$$\alpha(||x||) \leq V(x) \leq \beta(||x||), \quad \forall x \in \Omega \subset \mathbb{R}^n \tag{1.16}$$

Then, the origin of system (1.15) *is said*

1. *Stable if*

$$\Delta V(x(k)) \leq 0, \quad \forall x \in \Omega, x \neq 0 \tag{1.17}$$

with

$$\Delta V(x(k)) = V(x(k+1)) - V(x(k)) = V(f(x(k))) - V(x(k)) \tag{1.18}$$

2. *Asymptotically stable if there exists a function φ of class $\mathcal{K}$ such that*

$$\Delta V(x(k)) \leq -\varphi(||x||), \quad x \in \Omega, x(k) \neq 0 \tag{1.19}$$

3. *Exponentially stable if there exists a constants $\alpha_1, \alpha_2, \alpha_3, p > 0$ such that the following properties are satisfied for all $x \in \Omega \subset \mathbb{R}^n$*

$$\alpha_2 ||x||^p \leq V(x) \leq \alpha_1 ||x||^p \tag{1.20}$$

and

$$\Delta V(x(k)) \leq -\alpha_3 ||x||^p \tag{1.21}$$

1.4.2 Discrete-time Consensus Algorithm

When interaction among agents occurs at discrete instants, the information state is updated using a difference equation. The most common discrete-time consensus algorithm has the following form [?] [?] [?] [?]:

$$x_i(k+1) = -\sum_{j=1}^{n} a_{ij}(x_i(k) - x_j(k)), \qquad i = 1, \ldots, n. \tag{1.22}$$

where k denotes a sampling variable, a_{ij} is the (i,j) entry of the adjacency matrix of the graph that represents the communication topology. Intuitively, the information state of each vehicle is updated as the weighted average of its current state and the current states of its neighbors. Note that a vehicle

maintains its current information state if it does not exchange information with other vehicles at that sampling time instant. The discrete-time consensus algorithm (1.22) is written in matrix form as

$$x(k+1) = -Lx(k)$$

where L is the Laplacian matrix. Similar to the continuous case, consensus is achieved if, for all $x_i(0)$ and for all $i, j = 1, \ldots, n, |x_i(k) - x_j(k)| \to 0$ as $k \to \infty$.

One interesting scheme to design the consensus algorithm for discrete-time multi-agent systems is to use a model predictive controller. This is the main topic of the next subsection.

1.5 Model Predictive Control (MPC)

A brief history of MPC techniques is shown in Figure 1.11. It depicts the evolution of the most significant MPC algorithms, illustrating their connections in a concise way. The story begins with the modern control concept of the Kalman's work, i.e. a great solution of the problem known as *Linear Quadratic Gaussian* (LQG) controller. The first description of MPC applications was presented by Richalet et al. in 1976. They described their approach as model predictive heuristic control (MPHC). The solution software was referred to as IDCOM, an acronym for Identification and Command [**?**]. Then, engineers at Shell Oil developed their own independent MPC approach in the early 1970s, with an initial application in 1973. Cutler and Ramaker presented details of an unconstrained multivariable control algorithm which they named dynamic matrix control (DMC) at the 1979 National AIChE meeting [**?**]. In the late 1980's, engineers at Shell Research in France developed the Shell Multivariable Optimizing Controller (SMOC) which they described as a bridge between state-space and MPC algorithms [**?**].

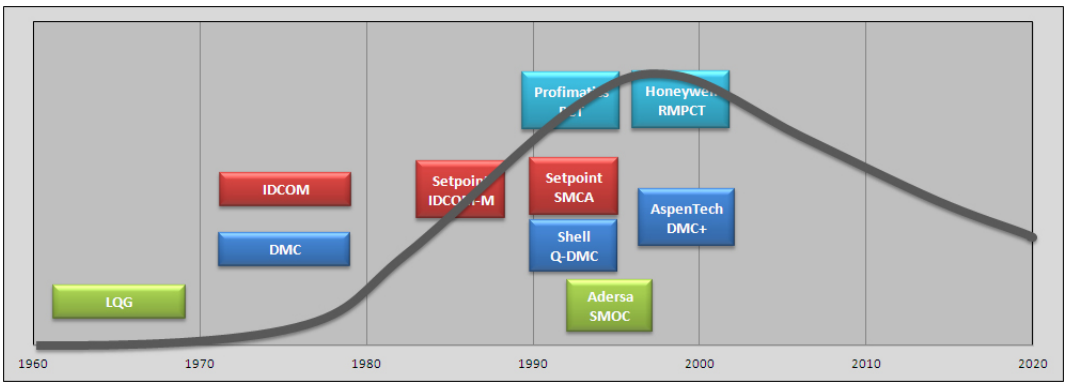

Figure 1.11: Evolution of the most significant MPC algorithms.

Model Predictive Control (MPC), also known as receding horizon control (RHC) or Generalized Predictive Control (GPC) or Dynamical Matrix Control (DMC), as solution for the consensus prob-

lem of MAS has also received great interest [1]. MPC is a form of control in which the output of the system can be predicted from some prediction horizon. The output of the MPC controller is determined based on input and output at a previous time and the control signal along the control horizon. Control algorithms of MPC are based on numerically solving an optimization problem at each step through constrained optimization. However, the control update rates use plenty of time for the necessary on-line computations [**?**].

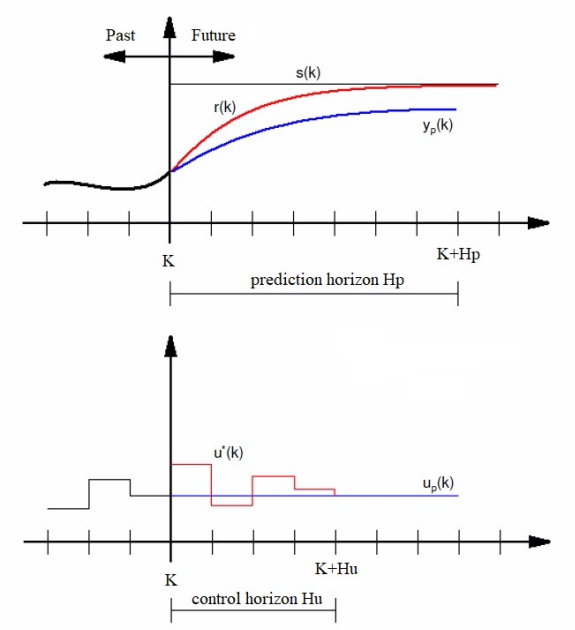

Figure 1.12: MPC concepts.

Figure 1.12 shows the general concepts of MPC algorithm for a single-input-single-output (SISO) system. At current time, say k, the system's future response (predicted output) $y_p(k)$ on a finite horizon H_p, say $[k|k+H_p]$, is predicted using the system model and the predicted control input $u_p(k)$, $[k|k+H_u]$. H_p is named as the prediction horizon and H_u is named as the control horizon ($H_u \leq H_p$).

Usually, the system's future response is expected to return to a desired set point $s(k)$ by following a reference trajectory $r(k)$ from the current states. The difference between the predicted output $y_p(k)$ and the reference trajectory $r(k)$ is called the predicted error. A finite horizon optimal control problem with a performance index that usually penalizes the predicted control input and the predicted error is solved online and an optimal control input $u^*(k)$, $[k|k+H_u]$, is obtained. Only the first element of $u^*(k)$ is implemented to the plant. All the other elements are discarded. Then, at the next time $k+1$, the whole procedure is repeated. The predicted control input $u_p(k+1)$ at time $k+1$ can be built by $u^*(k)$ with linear extrapolation. Since the prediction horizon and control horizon move one step further into future at each time interval, MPC is also named as receding horizon control (RHC).

For cooperative behavior mechanism and effective control of MAS, MPC technique has several advantages such as the acceleration of the convergence speed, the possible consideration of multi-variable constraints and the increase of the range of sampling periods. In a distributed architecture, each agent uses only local information. According to their own and neighbors's information (both actual and past), MPC may precisely reflect the autonomy of an agent. The predictive mechanism of MPC is used to predict the output state in the short-term prediction horizon. Each agent solves an optimization problem using its own and neighbor information data, to design the control input at each moment, and then realize the cooperative control.

One of the major advantages of the MPC approach is that the cooperative control will be conducted from an optimization point of view. Some physical limits such as input bounds, safety regions for the collision avoidance can be formulated as constraints in the optimization problem. MPC has the ability to handle control and state constraints for discrete-time systems [**?**]. This method can be applied for the control of a group of agents by letting each agent solve, at each step, a constrained finite-time optimal control problem involving the state of neighboring agents. For agents modeled by a discrete-time system, [**?**] proposed decentralized MPC schemes with control input constraints and showed that under the proposed decentralized schemes, multi-agent systems with single- and double-integrator dynamics asymptotically achieves consensus under mild assumptions. However, it was assumed that the control horizon equals the prediction control, which reduced the degree of freedom for the controller design. To remove the problem in degree of freedom for the controller design, [1] proposed a consensus scheme for discrete-time single-integrator MAS under switching directed interaction graphs where the control horizon can be arbitrarily picked from one to prediction horizon. Another result of MPC is [**?**] which proposed a MPC strategy to increase the consensus convergence rate in MASs under some special communication networks.

1.6 Conclusion

We have discussed in this chapter the basic concepts of algebraic graph theory for describing the communication topology among the agents. Consensus control problem in cooperative control for multi-agent systems has been also introduced. Convergence rates are discussed, which motivates us to conduct a more in-depth study to investigate how a fast controller can be designed. The concepts of consensus for multi-agent systems in continuous-time and discrete-time are separately discussed where discrete-time systems are more suitable for practical applications. Model predictive control as a solution of the multi-agent consensus problem in discrete-time has been introduced.

Chapter 2

Fixed-Time Leader-Follower Consensus Control Strategy for MAS

2.1 Introduction

This chapter is concerned with the fixed-time leader-follower consensus problem of multi-agent systems. The first part of this chapter formulates the general control objective and the considered assumptions to solve the fixed-time leader-follower consensus problem. The second and third part of this chapter deal with the consensus tracking problem for linear multi-agent systems (i.e. single-integrator and double-integrator dynamics). Here, the leader (which can be dynamic) only transmits its state to its neighbors. A decentralized controller, which uses the available local information, is designed to track the desired trajectory of the leader in a prescribed time. Using the proposed controller, an upper bound of the settling time is provided regardless of the initial conditions.

The fourth part of this chapter studies the fixed-time tracking problem for a single unicycle-type mobile robot. First, the resulting tracking error dynamics is transformed into two second-order coupled subsystems. Then, the two subsystems are studied and a step-by-step fixed-time control strategy is designed. An upper bound of the settling time, which only depends on the controller parameters is estimated regardless of the initial conditions. Finally, some simulation results are given to show the effectiveness of the proposed controller.

The fifth part is concerned with the fixed-time consensus problem of multi-agent system for unicycle-type mobile robots. For each agent, a distributed observer is designed to estimate the leader state in a fixed-time. Contrary to finite-time schemes, the estimation of the settling time does not require the knowledge of the initial state, allowing a step by step design for the controller. A decentralized observer-based control protocol is proposed for each agent to solve the leader-follower consensus

problem in a fixed-time.

The main contributions of the proposed scheme can be summarized as follows:

i) To remove the problem of the communication loop due to the dependence of the control inputs of the followers on the inputs of its neighbors in [**?**][**?**], distributed observers are designed to estimate the leader state in a prescribed time which does not depend on the initial state contrary to existing finite-time observers.

ii) A new decentralized observer-based control protocol is proposed for each follower to solve the fixed-time consensus tracking problem when the leader is dynamic.

iii) Robustness properties against matched perturbations are guaranteed.

iv) An upper bound of the settling time, which only depends on the controller parameters is estimated independently of the initial conditions, contrary to existing finite-time controllers.

The remaining parts of this chapter are organized as follows. Section 2.2 introduces some assumptions and formulates the general control objective. The main theoretical results on the consensus tracking problem are presented for single-integrator and double-integrator dynamics in Section 2.3 and 2.4. In Section 2.5, a fixed-time tracking control law for a single agent with unicycle-type dynamics is provided. In section 2.6, the main theoretical results on the consensus tracking problem are presented for unicycle-type dynamics. Section 2.7 concludes this chapter.

2.2 Problem Statement and Assumptions

Let us consider a group of $N+1$ agents with one leader (which could be virtual) labeled by 0 and N followers, labeled by $i \in \{1, \ldots, N\}$. The dynamics of the leader is given by the following general system

$$\dot{x}_0(t) = F(x_0(t), u_0(t)) \tag{2.1}$$

where $x_0 \in \mathbb{R}^n$ is the leader state and $u_0 \in \mathbb{R}^m$ is the leader control input. $F : \mathbb{R}^n \times \mathbb{R}^m \to \mathbb{R}^n$ is known. Here, it should be highlighted that solutions of (2.1) are understood in the Filippov sense [**?**].

The dynamics of the ith follower is as follows

$$\dot{x}_i(t) = F(x_i(t), u_i(t)) \qquad \text{with} \qquad i = 1, 2, \ldots, N. \tag{2.2}$$

where $x_i \in \mathbb{R}^n$ is the state and $u_i \in \mathbb{R}^m$ is the control input of the ith follower. The unknown perturbation of the ith agent is given by $d_i(t) \in \mathbb{R}^n$. Here, it should be highlighted that solutions of (2.2)

are understood in the Filippov sense [**?**].

Among the N followers, the communication topology can be represented by graph $\mathcal{G} = \{\mathcal{V}, \mathcal{E}\}$ where $\mathcal{V} = \{1, \ldots, N\}$ defines the set of nodes, corresponding to the followers, and $\mathcal{E} \subseteq \{\mathcal{V} \times \mathcal{V}\}$ defines the edge set. A link $(j, i) \in \mathcal{E}$, with $i \neq j$, exists if agent i receive information from its neighbor j. The adjacency matrix $A = (a_{ij}) \in \mathbb{R}^{N \times N}$ satisfies $a_{ij} > 0$ if $(j, i) \in \mathcal{E}$ and $a_{ij} = 0$, otherwise. The corresponding Laplacian matrix is given by $L = (l_{ij}) \in \mathbb{R}^{N \times N}$ with $l_{ii} = \sum_{j=1,\, j \neq i}^{N} a_{ij}$ and $l_{ij} = -a_{ij}$ for $i \neq j$. The links between the leader and the followers are characterized by matrix $B = diag(b_1, \ldots, b_N)$ where $b_i > 0$ if the leader state is available to follower i and where $b_i = 0$ otherwise.

Hereafter, it is assumed that the following hypotheses hold to derive the proposed fixed-time controllers.

Assumption 1 *It is assumed that the communication topology among the N followers is undirected, fixed, connected. It means that the adjacency matrix A is symmetric. It is also assumed that there is at least one strictly positive parameter b_i.*

Assumption 2 *The followers do not know the leader control input u_0. Nevertheless, its neighboring agents know its upper bounds.*

Assumption 3 *For each follower, the perturbation $d_i(t)$ is unknown but it is bounded by a known constant.*

Remark 2 *Assumption 1 is conventional to deal with the leader-follower consensus problem. Hypothesis 2-3 are not restrictive since the bounds of perturbations and leader input can be estimated a priori for any system.*

Here, the purpose is to derive a decentralized controller u_i $(i = 1, \ldots, N)$ for each follower, based on available information, such that the leader-follower consensus problem is solved in a fixed-time, in spite of matched external perturbations. It means that there exists a positive constant T, such that $\forall x_i(0)$, $\forall i = 1, \ldots, N$,

$$\begin{aligned} &\lim_{t \to T} \|x_i(t) - x_0(t)\| = 0 \\ &x_i(t) = x_0(t),\ \forall t \geq T \end{aligned} \tag{2.3}$$

Remark 3 *One can note that the settling time T does not depend on the initial states of the agents. It removes some limitations on existing finite-time consensus schemes for the application in decentralized architectures. The settling time can be prescribed according to some high-level policies (for instance in flexible manufacturing systems, when an operation should be performed before a deadline), or when cluster networks or switching communication topologies are considered [**?**].*

2.3 Consensus of MAS with Single-Integrator Dynamics

Let us first consider a holonomic mobile robot moving in a two-dimensional plane. The axes of the workspace are shown in Figure 2.1. Since we assume that motions along the x and y-axes are

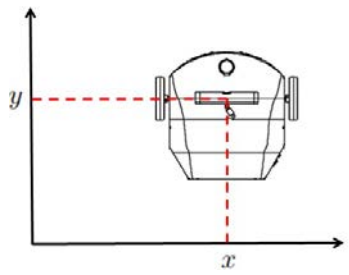

Figure 2.1: Top view of the considered mobile robot

decoupled, the system dynamics can be modeled as

$$\begin{aligned} \dot{x}_i(t) &= u_x(t) \\ \dot{y}_i(t) &= u_y(t) \end{aligned} \tag{2.4}$$

where $x_i(t) \in \mathbb{R}$ and $y_i(t) \in \mathbb{R}$ are the position, $u_x(t) \in \mathbb{R}$ and $u_y(t) \in \mathbb{R}$ are the control inputs along the x-axis and y-axis, respectively.

Remark 4 *In the following, let us only consider the dynamics along the x-direction.*

Along the x-direction, the leader dynamics is given by the following single-integrator system

$$\dot{x}_0(t) = u_0(t) \tag{2.5}$$

where $x_0 \in \mathbb{R}$ (resp. $u_0 \in \mathbb{R}$) is the leader state (resp. leader control input). Along the x-direction, the dynamics of the ith follower is as follows

$$\dot{x}_i(t) = u_i(t) + d_i(t) \tag{2.6}$$

where $x_i \in \mathbb{R}$ (resp. $u_i \in \mathbb{R}$) is the state (resp. control input) of the ith follower. The unknown perturbation of the ith agent is given by $d_i \in \mathbb{R}$.

2.3.1 Fixed-Time Observer-Based Consensus Protocol

For single-integrator dynamics MAS under matched perturbations, we propose an observer-based consensus protocol to deal with the leader-follower consensus problem.

Distributed fixed-time observer

To estimate the leader state in a prescribed time, distributed observers are designed for each follower $i \in \{1, \ldots, N\}$. Indeed, the leader state is only available to its neighboring followers. Let us introduce the following observer

$$\dot{\hat{x}}_i = \rho \,\mathrm{sign}\left(\sum_{j=1}^{N} a_{ij}(\hat{x}_j - \hat{x}_i) + b_i(x_0 - \hat{x}_i)\right) + \sigma \left[\sum_{j=1}^{N} a_{ij}(\hat{x}_j - \hat{x}_i) + b_i(x_0 - \hat{x}_i)\right]^2 \tag{2.7}$$

where $\hat{x}_i$ is the estimation of the leader state x_0 for the ith follower, ρ and σ are positive constants, which will be given hereafter.

The fixed-time stabilization of the estimation errors

$$\tilde{x}_i = \hat{x}_i - x_0 \qquad (i = \{1, \ldots, N\}) \tag{2.8}$$

is introduced in the following theorem.

Theorem 1 *Suppose that Assumptions 1-2 are satisfied. If the gains of the distributed observer* (2.7) *verify*

$$\begin{cases} \sigma &= \frac{\epsilon\sqrt{N}}{(2\lambda_{min}(L+B))^{\frac{3}{2}}} \\ \rho &= u_0^{max} + \epsilon\sqrt{\frac{\lambda_{max}(L+B)}{2\lambda_{min}(L+B)}} \end{cases} \tag{2.9}$$

with $\epsilon > 0$, then, for any initial condition, the estimation errors (2.8) *converge to zero. An upper bound of the convergence time can be given as*

$$T_o = \frac{\pi}{\epsilon} \tag{2.10}$$

Proof. Using (2.7), the dynamics of the observation error is given by

$$\dot{\tilde{x}}_i = \rho \,\mathrm{sign}\left(\sum_{j=1}^{N} a_{ij}(\tilde{x}_j - \tilde{x}_i) - b_i\tilde{x}_i\right) + \sigma \left[\sum_{j=1}^{N} a_{ij}(\tilde{x}_j - \tilde{x}_i) - b_i\tilde{x}_i\right]^2 - u_0 \tag{2.11}$$

Let us denote

$$\tilde{x} = [\tilde{x}_1, \ldots, \tilde{x}_N]^T \tag{2.12}$$

Then, for $\tilde{x}$, one can obtain

$$\dot{\tilde{x}} = -\rho \,\mathrm{sign}\left((L+B)\tilde{x}\right) - \sigma \lceil (L+B)\tilde{x} \rfloor^2 - \mathbf{1}u_0 \tag{2.13}$$

We complete the proof by consider the candidate Lyapunov function for system (2.13)

$$V_1 = \frac{1}{2}\tilde{x}^T(L+B)\tilde{x} \tag{2.14}$$

Its time derivative is given by

$$\begin{aligned}\dot{V}_1 &= \tilde{x}^T(L+B)\left(-\rho\,\mathrm{sign}\left((L+B)\tilde{x}\right)-\sigma\left\lceil(L+B)\tilde{x}\right\rfloor^2-\mathbf{1}u_0\right)\\ &\leq -(\rho-u_0^{max})\|(L+B)\tilde{x}\|_1-\sigma N^{-\frac{1}{2}}(2\lambda_{min}(L+B))^{\frac{3}{2}}V^{\frac{3}{2}}\\ &\leq -\epsilon V_1^{\frac{1}{2}}-\epsilon V_1^{\frac{3}{2}}\end{aligned}$$

Using Lemma 2, this inequality ensures that $\tilde{x}$ converges to zero in a finite-time bounded by $\frac{\pi}{\epsilon}$.

■

Remark 5 *The conditions* (2.9) *on the observer gains are relatively strong since global information like* N, $\lambda_{min}(L+B)$ *and* $\lambda_{max}(L+B)$ *is required to guarantee the fixed-time convergence. Hence, each agent must have some global knowledge about the communication topology similarly to existing works on fixed-time consensus. One should highlight that such global information is needed to provide an explicit estimate of the settling time (which is a very interesting feature of the proposed scheme). It is worthy of noting that if a prescribed convergence time* T_o *is required, one can easily tune the observer gains according to* (2.9) *to estimate the leader state. Similarly to the work of [?], parameter* ϵ *should be tuned to obtain a good compromise between robustness against measurement noises (in the presence of measurement noises, only a neighborhood of the origin of the observation error system, which depends on the size of noise and* ϵ*, could be fixed-time stable) and sufficiently fast estimation. When the observer gains are selected, through conditions* (2.9)*, the proposed scheme can be considered as a decentralized one since each neighboring agent only exchanges local information during the process.*

Decentralized fixed-time controller

From Theorem 1, one can conclude that $\hat{x}_i = x_0$ for all $t \geq T_o$. Hence, after time T_o, each follower is able to indirectly access to the state of the leader and uses the estimate $\hat{x}_i$ in the consensus protocol.

Let us denote the tracking errors as follows

$$e_i = x_i - \hat{x}_i = x_i - x_0 - \tilde{x}_i \tag{2.15}$$

From (2.5)-(2.6) and using Theorem 1, for each follower $i = \{1, \ldots, N\}$ and for all $t \geq T_o$, the tracking error dynamics becomes

$$\dot{e}_i = u_i + d_i - u_0 \tag{2.16}$$

It is clear that dynamics (2.16) is a first-order system.

In the following theorem, the control strategy is derived to solve the leader-follower consensus problem for MAS with single-integrator dynamics, in a fixed-time, in spite of the presence of matched perturbations.

Theorem 2 *Let us consider the leader-follower system* (2.5)-(2.6)*. Suppose that Assumptions 1-3 are satisfied and the gains of the distributed observer* (2.7) *verify Eq.* (2.9)*. The leader-follower consensus problem is solved in a fixed-time using the decentralized controller*

$$u_i = \begin{cases} 0 & ,\forall t < T_o \\ -(\alpha + a_i)\lfloor e_i \rceil^2 - \beta \operatorname{sign}(e_i) & ,\forall t \geq T_o \end{cases} \tag{2.17}$$

where α, β are positive constants and a_i is a positive constant given hereafter. The settling time is explicitly defined as

$$T = T_o + \frac{\pi}{\sqrt{\alpha\beta}} \tag{2.18}$$

Proof. We complete the proof by showing that the origin is fixed-time stable with the settling time estimate T under the control law (2.17). It will be also proved that in spite of the presence of matched perturbations, the fixed-time leader-follower consensus problem is solved.
Let us first consider system (2.16).

$$\dot{e}_i = u_i + d_i - u_0$$

According to Assumptions 2-3, let us denote a_i as

$$a_i \geq d_i + u_0 \tag{2.19}$$

Following [**?**], let us consider the candidate Lyapunov function $V_2 = \frac{1}{2}|e_i|^2$. Its derivative is,

$$\begin{array}{rcl} \dot{V}_2 & \leq & -\alpha|e_i|^3 + \beta|e_i| \\ & \leq & -\alpha(2V_2)^{\frac{3}{2}} + \beta(2V_2)^{\frac{1}{2}} \end{array} \tag{2.20}$$

It is clear using Lemma 2 that $e_i = 0$ when $t \geq T$.
This concludes the proof. ■

2.3.2 Simulation Results

The simulation results for all the following subsections (i.e. simple integrator, double integrator, chained-form system) are done using the same topology. A multi-agent system with $N = 6$ followers labeled by $1 - 6$ and one leader labeled by 0 is considered. Figure 2.2 shows the communication topology. One can see that it is fixed and connected. It is characterized by the following Laplacian L and the matrix B which describes links between the leader and the followers given as follows

$$L = \begin{bmatrix} 2 & -1 & 0 & 0 & 0 & -1 \\ -1 & 2 & -1 & 0 & 0 & 0 \\ 0 & -1 & 3 & -1 & 0 & -1 \\ 0 & 0 & -1 & 1 & 0 & 0 \\ 0 & 0 & 0 & 0 & 1 & -1 \\ -1 & 0 & -1 & 0 & -1 & 3 \end{bmatrix}, \qquad B = \begin{bmatrix} 0 & 0 & 0 & 0 & 0 & 0 \\ 0 & 1 & 0 & 0 & 0 & 0 \\ 0 & 0 & 0 & 0 & 0 & 0 \\ 0 & 0 & 0 & 0 & 0 & 0 \\ 0 & 0 & 0 & 0 & 1 & 0 \\ 0 & 0 & 0 & 0 & 0 & 0 \end{bmatrix}$$

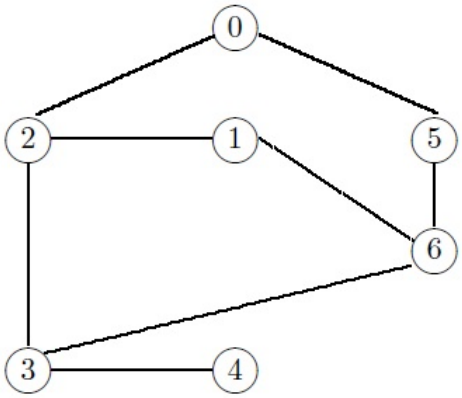

Figure 2.2: Communication topology for the considered MAS.

From matrix B, it is clear that agents 1, 3, 4 and 6 do not have direct link with agent 0. Assumption 1 is satisfied.

The performances of the proposed observer-based leader-follower consensus controller for single integrator are studied through numerical simulations. The dynamics of the leader (resp. the followers) is given by Eq. (2.5) (resp. Eq. (2.6)).

Let us set $\alpha = \beta = 0.5$ and $a_i = 0.3$ for protocol (2.17). Using Theorem 1, the distributed observer (2.7) guarantees the stabilization of the estimation errors (2.8) to the origin in a finite-time bounded by $T_o = 1s$. Figure 2.3 shows that the distributed observers accurately reconstruct the leader state for each agent before T_o. One can obtain $T = 7.28s$. Hence, the origin of the closed-loop system is globally finite-time stable contrary to existing controllers which only provide semi-global finite-time stability property. Furthermore, since T does not depend on the initial states of agents, the proposed protocol is distributed.

The tracking errors are depicted in Figure 2.4. One can see that the tracking errors between each follower and the leader converge to zero before T. One can conclude that using the proposed controller, the leader-follower consensus is achieved in a prescribed time. The control inputs for each agent are shown in Figure 2.5. One can note that the magnitude of control inputs may be large during the transients to achieve a fast convergence of the sliding surfaces given by the different steps of the consensus protocol. Hence, the control parameters should be adjusted to obtain a good compromise between magnitude of the control inputs and settling time.

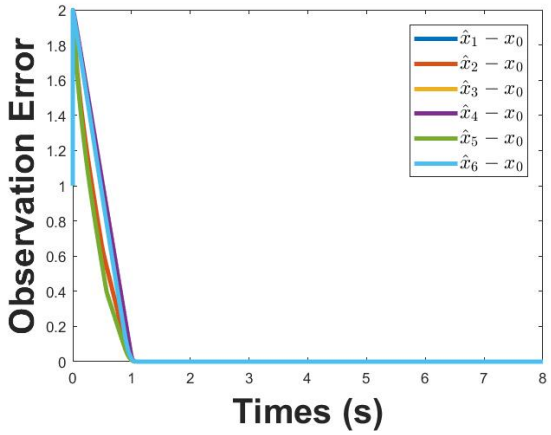

Figure 2.3: Evolution of the estimation errors (2.8) for each follower

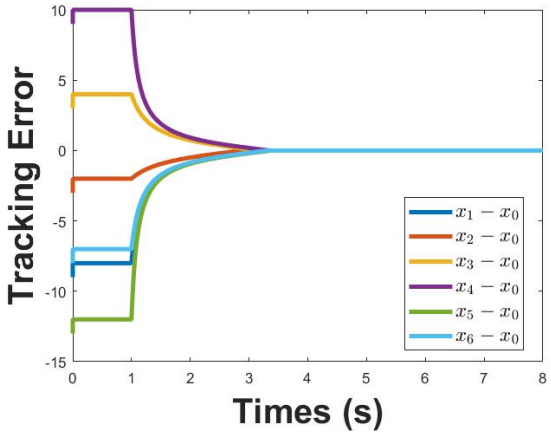

Figure 2.4: Evolution of the tracking errors between each agent and the leader.

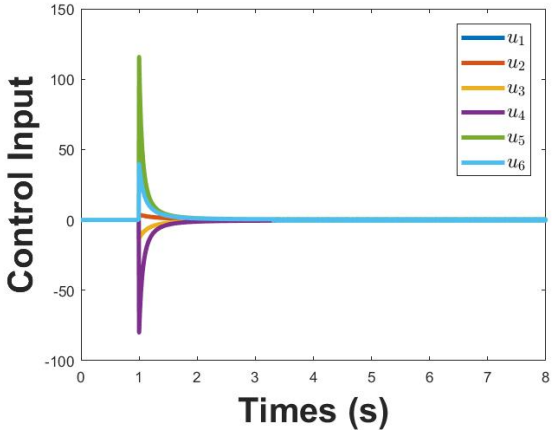

Figure 2.5: Control input for each agent

2.4 Consensus of MAS with Double-Integrator Dynamics

Consider a multi-agent system consisting of a leader (which could be virtual) labeled by 0, and N followers, labeled by $i \in \{1, \ldots, N\}$. In the following, let us only consider the dynamics along the x-direction. The leader dynamics is given by the following double-integrator system

$$\begin{cases} \dot{x}_{1,0}(t) &= x_{2,0}(t) \\ \dot{x}_{2,0}(t) &= u_0(t) \end{cases} \tag{2.21}$$

where $x_0 = [x_{1,0}, x_{2,0}]^T \in \mathbb{R}^2$ (resp. $u_0 \in \mathbb{R}$) is the leader state (resp. leader control input) along the x-axis. The dynamics of the ith follower is as follows

$$\begin{cases} \dot{x}_{1,i}(t) &= x_{2,i}(t) \\ \dot{x}_{2,i}(t) &= u_i(t) + d_i(t) \end{cases} \tag{2.22}$$

where $x_i = [x_{1,i}, x_{2,i}]^T \in \mathbb{R}^2$ (resp. $u_i \in \mathbb{R}$) is the state (resp. control input) of the ith follower. The unknown perturbation of the ith agent is given by $d_i \in \mathbb{R}$.

2.4.1 Fixed-Time Observer-Based Consensus Protocol

For double-integrator dynamics MAS under matched perturbations, we propose an observer-based consensus protocol to deal with the leader-follower consensus problem.

Distributed fixed-time observer

To estimate the leader state in a prescribed time, distributed observers are designed for each follower $i \in \{1, \ldots, N\}$. Indeed, the leader state is only available to its neighboring followers. Let us introduce the following observer as follows

$$\begin{cases} \dot{\hat{x}}_{1,i} &= \hat{x}_{2,i} + \rho_1 \operatorname{sign}\left(\sum_{j=1}^{N} a_{ij}(\hat{x}_{1,j} - \hat{x}_{1,i}) + b_i(x_{1,0} - \hat{x}_{1,i})\right) \\ & \quad +\sigma_1 \left\lceil \sum_{j=1}^{N} a_{ij}(\hat{x}_{1,j} - \hat{x}_{1,i}) + b_i(x_{1,0} - \hat{x}_{1,i}) \right\rfloor^2 \\ \dot{\hat{x}}_{2,i} &= \rho_2 \operatorname{sign}\left(\sum_{j=1}^{N} a_{ij}(\hat{x}_{2,j} - \hat{x}_{2,i}) + b_i(x_{2,0} - \hat{x}_{2,i})\right) \\ & \quad +\sigma_2 \left\lceil \sum_{j=1}^{N} a_{ij}(\hat{x}_{2,j} - \hat{x}_{2,i}) + b_i(x_{2,0} - \hat{x}_{2,i}) \right\rfloor^2 \end{cases} \tag{2.23}$$

where $\hat{x}_{k,i}$ ($k = \{1, 2\}$) is the estimation of the leader state $x_{k,0}$ for the ith follower, ρ_k and σ_k are positive constants, which will be given hereafter.

The fixed-time stabilization of the estimation errors

$$\tilde{x}_{k,i} = \hat{x}_{k,i} - x_{k,0} \qquad (i = \{1, \ldots, N\},\ k = \{1, 2\}) \tag{2.24}$$

is introduced in the following theorem.

Theorem 3 *Suppose that Assumptions 1-2 are satisfied. If the gains of the distributed observer* (2.23) *verify*

$$\begin{cases} \sigma_k &= \frac{\epsilon\sqrt{N}}{(2\lambda_{min}(L+B))^{\frac{3}{2}}}, \forall k = 1, 2 \\ \rho_1 &= \epsilon\sqrt{\frac{\lambda_{max}(L+B)}{2\lambda_{min}(L+B)}} \\ \rho_2 &= u_0^{max} + \epsilon\sqrt{\frac{\lambda_{max}(L+B)}{2\lambda_{min}(L+B)}} \end{cases} \tag{2.25}$$

with $\epsilon > 0$, then, for any initial condition, the estimation errors (2.24) *converge to zero. An upper bound of the convergence time can be given as*

$$T_o = \frac{2\pi}{\epsilon} \tag{2.26}$$

Proof. Using (2.23), the dynamics of the observation error is given by

$$\begin{aligned} \dot{\tilde{x}}_{1,i} &= \tilde{x}_{2,i} + \rho_1 \operatorname{sign}\left(\sum_{j=1}^N a_{ij}(\tilde{x}_{1,j} - \tilde{x}_{1,i}) - b_i\tilde{x}_{1,i}\right) \\ &\quad +\sigma_1 \left\lceil \sum_{j=1}^N a_{ij}(\tilde{x}_{1,j} - \tilde{x}_{1,i}) - b_i\tilde{x}_{1,i} \right\rfloor^2 \\ \dot{\tilde{x}}_{2,i} &= \rho_2 \operatorname{sign}\left(\sum_{j=1}^N a_{ij}(\tilde{x}_{2,j} - \tilde{x}_{2,i}) - b_i\tilde{x}_{2,i}\right) \\ &\quad +\sigma_2 \left\lceil \sum_{j=1}^N a_{ij}(\tilde{x}_{2,j} - \tilde{x}_{2,i}) - b_i\tilde{x}_{2,i} \right\rfloor^2 - u_0 \end{aligned} \tag{2.27}$$

Let us denote

$$\tilde{x}_k = [\tilde{x}_{k,1}, \ldots, \tilde{x}_{k,N}]^T \tag{2.28}$$

Then, for $\tilde{x}_1$ and $\tilde{x}_2$, one can obtain

$$\dot{\tilde{x}}_1 = \tilde{x}_2 - \rho_1 \operatorname{sign}\left((L+B)\tilde{x}_1\right) - \sigma_1 \left\lceil (L+B)\tilde{x}_1 \right\rfloor^2 \tag{2.29}$$

$$\dot{\tilde{x}}_2 = -\rho_2 \operatorname{sign}\left((L+B)\tilde{x}_2\right) - \sigma_2 \left\lceil (L+B)\tilde{x}_2 \right\rfloor^2 - \mathbf{1}u_0 \tag{2.30}$$

We complete the proof by two steps.

- Let us system (2.30). Consider a candidate Lyapunov function for subsystem (2.30) similar to the previous subsection. Using Lemma 2, one can prove that $\tilde{x}_2$ converges to zero in a finite-time bounded by $\frac{\pi}{\epsilon}$.

- After $\tilde{x}_2$ converges to zero (i.e. when $t \geq \frac{\pi}{\epsilon}$), the dynamics of $\tilde{x}_1$ becomes

$$\dot{\tilde{x}}_1 = -\rho_1 \operatorname{sign}\left((L+B)\tilde{x}_1\right) - \sigma_1 \left\lceil (L+B)\tilde{x}_1 \right\rfloor^2 \tag{2.31}$$

  Similarly to the previous step, the $\tilde{x}_1$ dynamics converges to zero. Indeed, consider the candidate Lyapunov function for system (2.31)

$$V_3 = \frac{1}{2}\tilde{x}_1^T(L+B)\tilde{x}_1 \tag{2.32}$$

Its time derivative along (2.31) is given by

$$\begin{aligned}\dot{V}_3 &= \tilde{x}_1^T(L+B)\left(-\rho_1 \operatorname{sign}\left((L+B)\tilde{x}_1\right) - \sigma_1 \lceil (L+B)\tilde{x}_1 \rfloor^2\right) \\ &\leq -\rho_1 \|(L+B)\tilde{x}_1\|_1 - \sigma_1 N^{-\frac{1}{2}} (2\lambda_{min}(L+B))^{\frac{3}{2}} V_2^{\frac{3}{2}} \\ &\leq -\epsilon V_3^{\frac{1}{2}} - \epsilon V_3^{\frac{3}{2}}\end{aligned}$$

Hence, one can conclude that $\tilde{x}_1$ converges to zero and after that $\tilde{x}_2$ converges to zero in a finite-time bounded by $2\frac{\pi}{\epsilon}$.

Hence, one can conclude that the estimation errors (2.24) converge to zero in a fixed-time bounded by T_o. ■

Decentralized fixed-time controller

From Theorem 3, one can conclude that $\hat{x}_i = [\hat{x}_{1,i}, \hat{x}_{2,i}]^T = x_0$ for all $t \geq T_o$. Hence, after time T_o, each follower is able to indirectly access to the state of the leader and uses the estimate $\hat{x}_i$ in the consensus protocol.

Let us denote the tracking errors as follows

$$e_{k,i} = x_{k,i} - \hat{x}_{k,i} = x_{k,i} - x_{k,0} - \tilde{x}_{k,i} \qquad (i = \{1,2\},\ k = \{1,2\}) \tag{2.33}$$

From (2.21)-(2.22) and using Theorem 3, for each follower $i = \{1, \ldots, N\}$ and for all $t \geq T_o$, the tracking error dynamics becomes

$$(\Sigma_1) \qquad \begin{aligned}\dot{e}_{1,i} &= e_{2,i} \\ \dot{e}_{2,i} &= u_i + d_i - u_0\end{aligned} \tag{2.34}$$

It is clear that dynamics (2.34) is a second-order subsystem. To deal with the observer-based consensus tracking problem, for each follower $i = \{1, \ldots, N\}$, the control objective is to design u_i such that the origin of system Σ_1 is fixed-time stable with the settling time estimate T in spite of the presence of matched perturbations.

Theorem 4 *Let us consider the leader-follower system* (2.21)-(2.22). *Suppose that Assumptions 1-3 are satisfied and the gains of the distributed observer* (2.23) *verify Eq.* (2.25). *The leader-follower consensus problem is solved in a fixed-time using the decentralized controllers*

$$u_i = \begin{cases} 0 & ,\forall t < T_o \\ -\frac{\alpha_1 + 3\beta_1 e_{1,i}^2 + 2a_i}{2} \operatorname{sign}(s_i) - \lfloor \alpha_2 s_i + \beta_2 \lfloor s_i \rceil^3 \rceil^{\frac{1}{2}} & ,\forall t \geq T_o \end{cases} \tag{2.35}$$

with the sliding surface

$$s_i = e_{2,i} + \lfloor \lfloor e_{2,i} \rceil^2 + \alpha_1 e_{1,i} + \beta_1 \lfloor e_{1,i} \rceil^3 \rceil^{\frac{1}{2}} \tag{2.36}$$

where α_1, α_2, β_1 and β_2 are positive constants, a_i is a positive constant given hereafter. The settling time is explicitly defined as

$$T = T_o + \frac{2}{\sqrt{\alpha}_2} + \frac{2}{\sqrt{\beta}_2} + \frac{2\sqrt{2}}{\sqrt{\alpha}_1} + \frac{2\sqrt{2}}{\sqrt{\beta}_1} \tag{2.37}$$

Proof. We complete the proof by two steps.

- Following [**?**], let us consider the candidate Lyapunov function $V_4 = |s_{1,i}|$. Its derivative is,

$$\dot{V}_4 = \dot{e}_{2,i}\,\mathrm{sign}\,(s_i) + \frac{|e_{2,i}|\dot{e}_{2,i}\,\mathrm{sign}\,(s_i) + \frac{\alpha_1+3\beta_1 e_{1,i}^2}{2} e_{2,i}\,\mathrm{sign}\,(s_i)}{|\lfloor e_{2,i}\rceil^2 + \alpha_1 e_{1,i} + \beta_1 \lfloor e_{1,i}\rceil^3|^{\frac{1}{2}}} \tag{2.38}$$

  Since

$$\lfloor \alpha_2 s_i + \beta_2 \lfloor s_i\rceil^3\rceil^{\frac{1}{2}}\,\mathrm{sign}\,(s_i) = (\alpha_2|s_i| + \beta_2|s_i|^3)^{\frac{1}{2}}$$

  one has

$$\begin{aligned} \dot{e}_{2,i}\,\mathrm{sign}\,(s_i) &= (u_i + d_i - u_0)\,\mathrm{sign}\,(s_i) \\ &= -\tfrac{\alpha_1+3\beta_1 e_{1,i}^2}{2} \\ &\quad -(\alpha_2|s_i| + \beta_2|s_i|^3)^{\frac{1}{2}} - (a_i - (d_i - u_0)\,\mathrm{sign}\,(s_i)) \end{aligned}$$

  Setting

$$a_i \geq d_i + u_0 \tag{2.39}$$

  one can conclude that

$$\dot{V}_4 \leq -(\alpha_2 V_4 + \beta_2 V_4^3)^{\frac{1}{2}} \tag{2.40}$$

  From Lemma 2, it is clear that $s_i = 0$ when $t \geq T_o + \frac{2}{\sqrt{\alpha}_2} + \frac{2}{\sqrt{\beta}_2}$.

- The sliding dynamics ($s_i = 0$) can be expressed as

$$\dot{e}_{1,i} = -\Big\lfloor \frac{\alpha_1 e_{1,i} + \beta_1 \lfloor e_{1,i}\rceil^3}{2} \Big\rceil^{\frac{1}{2}} \tag{2.41}$$

  Using the candidate Lyapunov function $V_5 = |e_{1,i}|$, one can obtain

$$\dot{V}_5 = -(\frac{\alpha_1}{2} V_5 + \frac{\beta_1}{2} V_5^3)^{\frac{1}{2}} \tag{2.42}$$

  It is clear using Lemma 2 that $e_{1,i} = 0$ when $t \geq T_s$. Furthermore, since $e_{1,i} = 0$ and $s_i = 0$, then $e_{2,i} = 0$.

This concludes the proof. ■

2.4.2 Simulation Results

In this subsection, some simulation results are provided to verify the theoretical analysis. We consider the leader-follower MAS with double-integrator dynamics (2.22). We use the same topology as in the previous section, where agents 1, 3, 4 and 6 do not have direct link with agent 0. Assumption 1 is satisfied.

The trajectory of the leader is generated by (2.21) with $u_0(t) = 0.1\sin(t)$. From the control input of the leader, one can see that Assumption 2 is verified. The control objective is that the followers, described by Eq. (2.22) track the leader in spite of matched perturbations ith $d_i = 0.2\sin(t)$. It is clear that Assumption 3 is also verified. The control parameter are selected as: $\alpha_1 = 20$, $\alpha_2 = 10$, $\beta_1 = 20$, $\beta_2 = 10$, $a_i = 0.3$ and $\epsilon = 4.18$. For the simulation purpose, the initial leader state $x_0(0) = [3, 2]^T$.

Using Theorem 3, the distributed observer (2.23) guarantees the stabilization of the estimation errors (2.27) to the origin in a finite-time bounded by $T_o = 1.5s$. Figure 2.6 shows that the distributed observers accurately reconstruct the leader state for each agent before T_o

Using Theorem 4, the origin of the closed-loop system is globally finite-time stable contrary to existing controllers which only provide semi-global finite-time stability property. Furthermore, the settling time $T = 4s$ does not depend on the initial states of agents. Also, the proposed protocol is distributed. The tracking errors are depicted in Figure 2.4. One can see that the tracking errors between each follower and the leader converge to zero before T_s. One can conclude that using the proposed controller, the leader-follower consensus is achieved in a prescribed time. The control inputs for each agent are shown in Figure 2.8. One can note that the magnitude of control inputs may be large during the transients to achieve a fast convergence of the sliding surfaces given by the different steps of the consensus protocol. Hence, the control parameters should be adjusted to obtain a good compromise between magnitude of the control inputs and settling time.

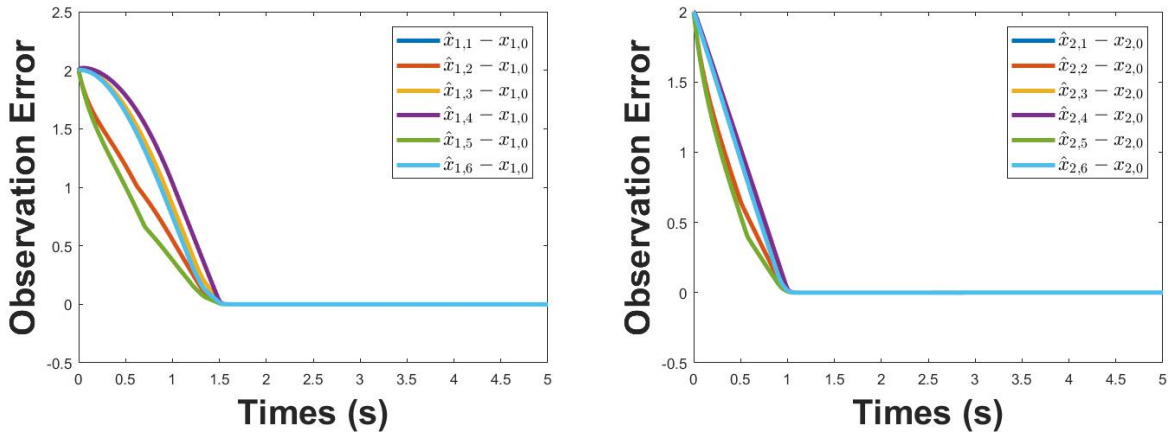

(a) (b)

Figure 2.6: Evolution of the estimation errors (2.27) for each follower.

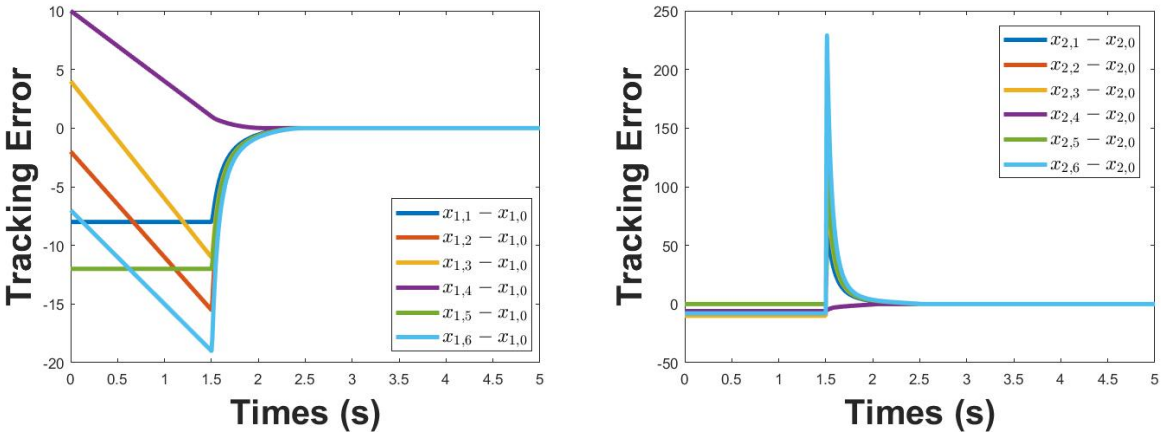

(a) (b)

Figure 2.7: Evolution of the tracking errors between each agent and the leader.

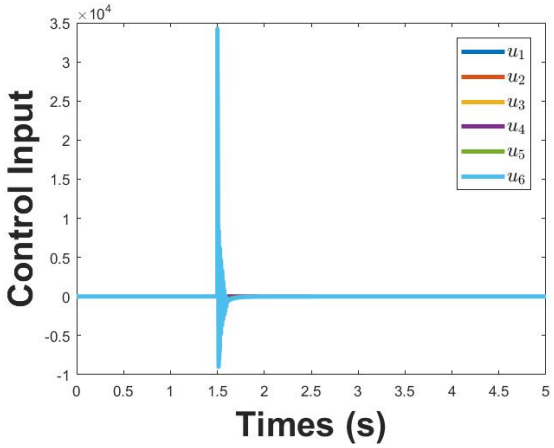

Figure 2.8: Control input for each agent.

2.5 Consensus of MAS with Unicycle-Type Dynamics

Let us now consider a nonholonomic mobile robot moving in a two-dimensional plane. The axes of the workspace are shown in Figure 2.9. The kinematics of the unicycle-type mobile robot is described under the nonholonomic constraints (contains the time derivatives of the generalized coordinates of the system and is not integrable). The configuration of the robot i can be represented by:

$$q_i(t) = (x_i(t), \;\; y_i(t), \;\; \theta_i(t))^T \tag{2.43}$$

where $x_i(t) \in \mathbb{R}$, $y_i(t) \in \mathbb{R}$ describe the robot position and $\theta_i(t)$ is its orientation in the global frame. The pure rolling and nonslipping conditions are described by:

$$G^T(q_i)\dot{q}_i = 0 \qquad \text{with} \qquad G^T(q_i) = (-\sin(\theta_i) \;\; \cos(\theta_i) \;\; 0) \tag{2.44}$$

Under the hypothesis of pure rolling and nonslipping condition, the kinematic equations can be written as follows:

$$\dot{q}_i(t) = f(q_i(t), u_i(t)) \tag{2.45}$$

where vector field $f : \mathbb{R}^3 \times \mathbb{R}^2 \to \mathbb{R}^3$ and control inputs u_i are defined as:

$$\begin{cases} f(q_i(t), u_i(t)) &= \begin{bmatrix} \cos(\theta_i) & 0 \\ \sin(\theta_i) & 0 \\ 0 & 1 \end{bmatrix} u_i(t) \\ \\ u_i(t) &= (\upsilon_i(t),\ \omega_i(t))^T \end{cases} \tag{2.46}$$

$\upsilon_i(t)$ and $\omega_i(t)$ are the linear and angular velocities, respectively.

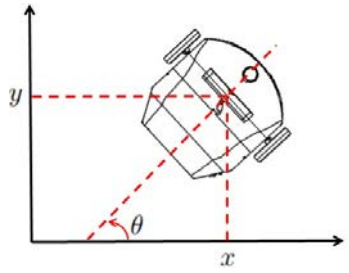

Figure 2.9: Top view of the considered mobile robot.

Before designing the consensus protocol, let us consider the classical transformation

$$\begin{cases} q_{i1}(t) &= \theta_i(t) \\ q_{i2}(t) &= x_i \sin(\theta_i(t)) - y_i \cos(\theta_i(t)) \\ q_{i3}(t) &= x_i \cos(\theta_i(t)) + y_i \sin(\theta_i(t)) \\ u_{i1}(t) &= \omega_i(t) \\ u_{i2}(t) &= \upsilon_i(t) - q_{i2}(t)\omega_i(t) \end{cases} \tag{2.47}$$

Using (2.47), system (2.45) can be written in chained-form as follows:

$$\begin{aligned} \dot{q}_{i1}(t) &= u_{i1}(t) \\ \dot{q}_{i2}(t) &= q_{i3}(t)u_{i1}(t) \\ \dot{q}_{i3}(t) &= u_{i2}(t) \end{aligned} \tag{2.48}$$

To deal with the robustness properties, some matched perturbations are added. Furthermore, for the purpose of the controller design, an additional dynamic extension is added to the chained-form dynamics. Therefore, the dynamics (2.48) becomes:

$$\begin{aligned} \dot{x}_1(t) &= x_2(t) \\ \dot{x}_2(t) &= u_1(t) + d_1(t) \\ \dot{x}_3(t) &= x_4(t)x_2(t) \\ \dot{x}_4(t) &= u_2(t) + d_2(t) \end{aligned} \tag{2.49}$$

where $x = [x_1, x_2, x_3, x_4]^T \in \mathbb{R}^4$ (resp. $u = [u_1, u_2]^T \in \mathbb{R}^2$) is the state (resp. control input) of the chained-form unicycle-type mobile robot, $d = [d_1, d_2]^T \in \mathbb{R}^2$ represents the unknown disturbances of the chained-form dynamics.

The dynamics of the desired trajectory is generated using the following system:

$$\begin{aligned} \dot{x}_{1,d}(t) &= x_{2,d}(t) \\ \dot{x}_{2,d}(t) &= u_{1,d}(t) \\ \dot{x}_{3,d}(t) &= x_{4,d}(t)x_{2,d}(t) \\ \dot{x}_{4,d}(t) &= u_{2,d}(t) \end{aligned} \tag{2.50}$$

where $x_d = [x_{1,d}, x_{2,d}, x_{3,d}, x_{4,d}]^T \in \mathbb{R}^4$ (resp. $u_d = [u_{1,d}, u_{2,d}]^T \in \mathbb{R}^2$) is the state (resp. control input) of the desired trajectory.

Before dealing with the consensus tracking problem, let us study the fixed-time trajectory tracking problem for only one single unicycle-type mobile robot. Figure 2.10 illustrates the control objective studied in the next subsection, i.e. the unicycle-type mobile robot tracks a desired trajectory in a prescribed-time.

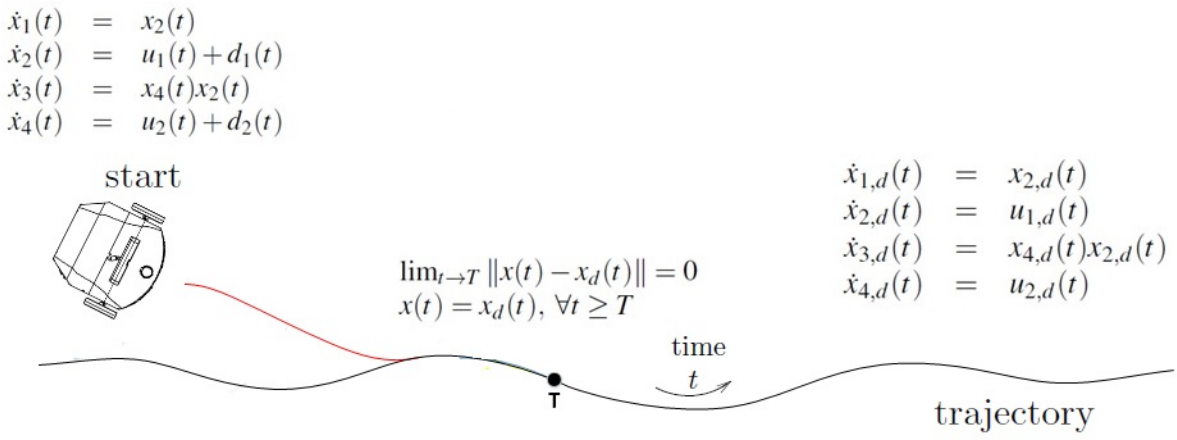

Figure 2.10: Illustration of the fixed-time trajectory tracking problem for a single agent.

2.5.1 Fixed-time trajectory tracking problem for a single unicycle-type mobile robot

In this subsection, let us first study the fixed-time trajectory tracking problem for only one single unicycle-type mobile robot. The control objective is to design a fixed-time trajectory tracking controller such that system (2.49) tracks the trajectory of system (2.50) in spite of the presence of matched perturbations.

Assumption 4 *It is assumed that the perturbations $d_1(t)$ and $d_2(t)$ are unknown but are bounded by known constants (i.e. $d_{1,max}$ and $d_{2,max}$).*

Assumption 5 *It is assumed that the desired state $x_{2,d}$ satisfies the following condition*

$$x_{2,d}(t) \neq 0 \tag{2.51}$$

Remark 6 *Hypothesis 4 is not restrictive since the bounds of perturbations can be estimated a priori for any system. Assumption 10 is relatively not restrictive since only the case $x_{2,d}(t) \neq 0$ is not considered in the proposed scheme. Therefore, the motion planner for the desired trajectory should take into account this constraint (to avoid any loss of controllability). Indeed, when $x_{2,d}(t) = 0$, we loose controllability since the state $x_{3,d}$ cannot be controlled. Since the agent track the leader, it also looses controllability in this case.*

Remark 7 *Note that there exist several tools to plan the trajectory for the leader. For instance, in [?], based on nonlinear programming and flatness properties, a constrained receding horizon planner is applied to design the state and the control input of the leader. One can easily extend this work while taking into account constraints given in Assumptions 4-10.*

Let us define the tracking errors as

$$e(t) = x(t) - x_d(t) \tag{2.52}$$

with $e = [e_1, e_2, e_3, e_4]^T \in \mathbb{R}^4$. The tracking error dynamics satisfy the following differential equations:

$$\begin{array}{lll} (\Sigma_1) & \dot{e}_1(t) = x_2(t) - x_{2,d}(t) \\ & \dot{e}_2(t) = u_1(t) + d_1(t) - u_{1,d}(t) \\ & \\ (\Sigma_2) & \dot{e}_3(t) = x_4(t)x_2(t) - x_{4,d}(t)x_{2,d}(t) \\ & \dot{e}_4(t) = u_2(t) + d_2(t) - u_{2,d}(t) \end{array} \tag{2.53}$$

To simplify the controller design, dynamics (2.53) is divided into two second-order coupled subsystems. To solve the fixed-time trajectory tracking problem, two steps are defined:

- Stabilization of subsystem Σ_1 in a fixed time T_s using control u_1,
- After $t > T_s$, stabilization of subsystem Σ_2 in a fixed time T using control u_2.

Figure 2.11 illustrated how the fixed-time trajectory tracking problem solved.

To design the fixed-time consensus tracking algorithm for a single unicycle-type mobile robot, the following theorem is derived.

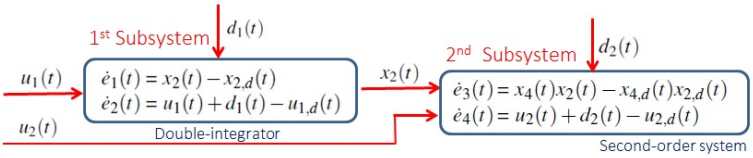

Figure 2.11: Stabilization of the two subsystems.

Theorem 5 *Assuming that Assumptions 4-10 hold. Consider system (2.53) with the trajectory tracking control law defined as:*

$$\begin{aligned} u_1 &= u_{1,d} + \varphi_1(e_1, e_2) \\ u_2 &= \begin{cases} 1 & ,\forall t < T_s \\ u_{2,d} - \frac{e_4 u_{1,d}}{x_{2,d}} + \frac{1}{x_{2,d}}\varphi_2(e_3, \zeta_4) & ,\forall t \geq T_s \end{cases} \end{aligned} \tag{2.54}$$

with $\zeta_4 = e_4 x_{2,d}$.
The sliding mode controllers are as follows:

$$\begin{aligned} \varphi_1(e_1, e_2) &= -\frac{\alpha_1 + 3\beta_1 e_1^2 + 2d_{1,max}}{2} sign\big(s_1(e_1, e_2)\big) \\ &\quad -\lfloor \alpha_2 s_1(e_1, e_2) + \beta_2 \lfloor s_1(e_1, e_2) \rceil^3 \rceil^{\frac{1}{2}} \\ \varphi_2(e_3, \zeta_4) &= -\frac{\alpha_1 + 3\beta_1 e_3^2 + 2d_{2,max}}{2} sign\big(s_2(e_3, \zeta_4)\big) \\ &\quad -\lfloor \alpha_2 s_2(e_3, \zeta_4) + \beta_2 \lfloor s_2(e_3, \zeta_4) \rceil^3 \rceil^{\frac{1}{2}} \end{aligned} \tag{2.55}$$

with sliding surfaces

$$\begin{aligned} s_1(e_1, e_2) &= e_2 + \lfloor \lfloor e_2 \rceil^2 + \alpha_1 e_1 + \beta_1 \lfloor e_1 \rceil^3 \rceil^{\frac{1}{2}} \\ s_2(e_3, \zeta_4) &= \zeta_4 + \lfloor \lfloor \zeta_4 \rceil^2 + \alpha_1 e_3 + \beta_1 \lfloor e_3 \rceil^3 \rceil^{\frac{1}{2}} \end{aligned} \tag{2.56}$$

The switching time is $T_s = \frac{2}{\sqrt{\alpha_2}} + \frac{2}{\sqrt{\beta_2}} + \frac{2\sqrt{2}}{\sqrt{\alpha_1}} + \frac{2\sqrt{2}}{\sqrt{\beta_1}}$ *and constants* α_i, β_i $(i = 1, 2)$ *are positive.*

Then, the origin of system (2.53) is globally fixed-time stable with settling time:

$$T = 2T_s \tag{2.57}$$

Hence, the fixed-time trajectory tracking problem is solved.

Proof. The proof is divided into two steps.

- Let us first consider the time interval $t \in [0, T_s]$. Using controller (2.54), it is clear that subsystem Σ_1 has been already discussed in the section double-integrator system. One can conclude that $e_1 = 0$ and $e_2 = 0$.

- Let us now consider $t > T_s$. From previously, subsystem Σ_2 can be written as:

$$\begin{aligned} \dot{e}_3 &= e_4 x_{2,d} \\ \dot{e}_4 &= u_2 + d_2 - u_{2,d} \end{aligned} \tag{2.58}$$

Setting $\zeta_4 = e_4 x_{2,d}$, system (2.58) can be expressed as:

$$\begin{aligned} \dot{e}_3 &= \zeta_4 \\ \dot{\zeta}_4 &= (u_2 + d_2 - u_{2,d}) x_{2,d} + e_4 u_{1,d} \end{aligned} \tag{2.59}$$

Using controller (2.54), system (2.59) becomes:

$$\begin{aligned} \dot{e}_3 &= \zeta_4 \\ \dot{\zeta}_4 &= \varphi_2 + d_2 x_{2,d} \end{aligned} \tag{2.60}$$

Using Assumptions 4-10 and following the same procedure as in the first step, one can conclude that the origin of system (2.59) is globally fixed-time state with settling time T given by Eq. (2.57). It is clear that the origin of system (2.53) is globally fixed-time stable with settling time T.

■

Remark 8 *It should be highlighted that since the settling time T is independent of the initial system conditions and can be estimated a priori, global finite-time stability of the closed-loop system is guaranteed (contrary to many existing works which only guarantee semi-global finite-time stability).*

2.5.2 Simulation Results

In this subsection, some simulation results are provided to verify the theoretical analysis.

We consider the unicycle-type mobile robot (2.49) where the perturbations are $d_1 = \sin(20t)$ and $d_2 = 10\cos(10t)$. The desired trajectory is generated by (2.50) with $x_d(0) = [0, 2, 0, 0]^T$, $u_{1,d}(t) = 2 + sin(t)$ and $u_{2,d}(t) = 1$. The control objective is that system (2.49) follows its derived trajectory x_d. It is clear that Assumptions 4-10 are verified. The control parameter are selected as: $\alpha_1 = 20$, $\alpha_2 = 10$, $\beta_1 = 20$, $\beta_2 = 10$ and $T_s = 2.5s$. For the simulation purpose, the initial conditions of system (2.49) are set as: $x(0) = [10, 1, 3, 1]^T$. Using Theorem 5, the robust controller (2.54) solves the fixed-time trajectory tracking problem with an estimation of the settling time $T = 4.5s$. Figure 2.12 shows that the origin of subsystem Σ_1 is globally fixed-time stable with a settling time less than $T_s = 2.5s$.

Figure 2.13 shows that the origin of subsystem Σ_2 is globally fixed-time stable with a settling time less than $T = 5s$.

Figure 2.14 displays the tracking errors. It can be seen that the trajectory tracking problem is solve in fixed-time.

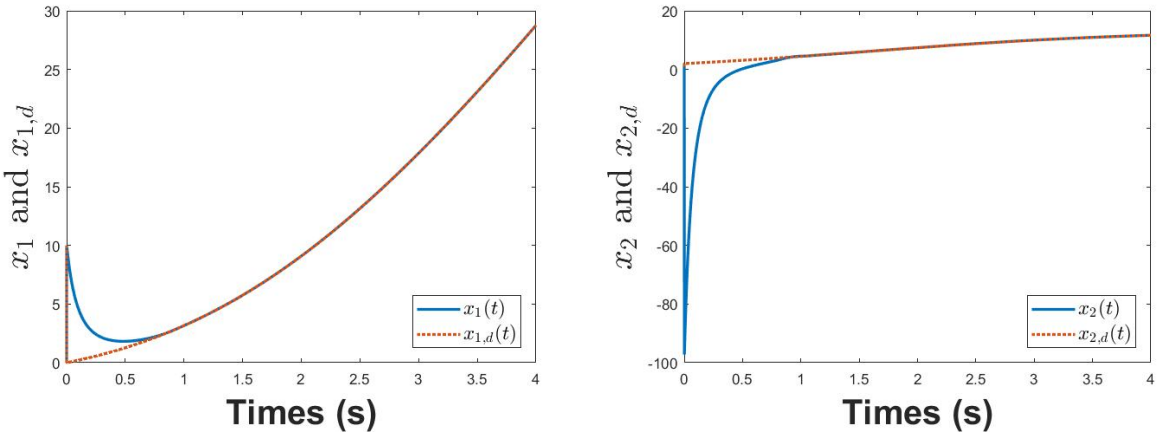

(a) (b)

Figure 2.12: Actual trajectory x_1, x_2 and desired state trajectories $x_{1,d}$, $x_{2,d}$

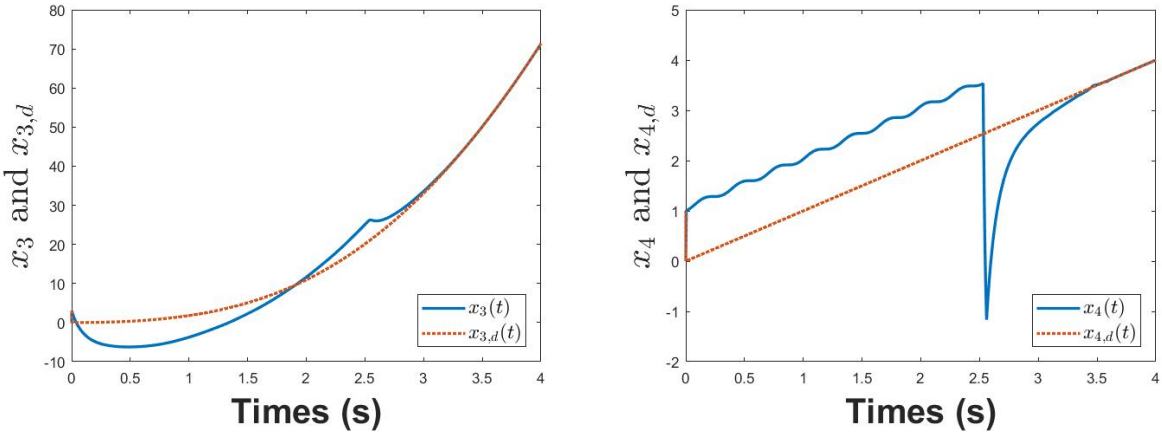

(a) (b)

Figure 2.13: Actual trajectory x_3, x_4 and desired state trajectories $x_{3,d}$, $x_{4,d}$

2.6 Consensus of MAS with Unicycle-Type Mobile Robot Dynamics

Consider a multi-agent system consisting of a leader (which could be virtual) labeled by 0, and N followers, labeled by $i \in \{1, \ldots, N\}$. The leader dynamics is given by the following chained-form unicycle-type mobile robot

$$\begin{cases} \dot{x}_{1,0}(t) &= x_{2,0}(t) \\ \dot{x}_{2,0}(t) &= u_{1,0}(t) \\ \dot{x}_{3,0}(t) &= x_{4,0}(t)x_{2,0}(t) \\ \dot{x}_{4,0}(t) &= u_{2,0}(t) \end{cases} \tag{2.61}$$

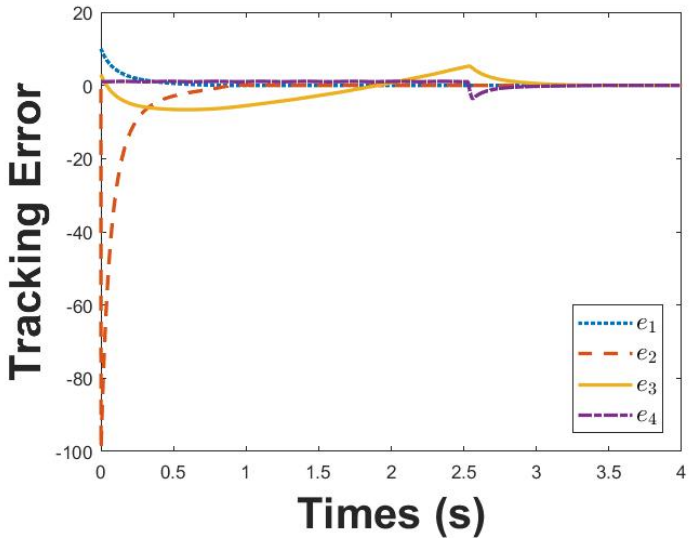

Figure 2.14: Tracking errors e

where $x_0 = [x_{1,0}, x_{2,0}, x_{3,0}, x_{4,0}]^T \in \mathbb{R}^4$ (resp. $u_0 = [u_{1,0}, u_{2,0}]^T \in \mathbb{R}^2$) is the leader state (resp. leader control input). The dynamics of the ith follower is as follows

$$\begin{cases} \dot{x}_{1,i}(t) &= x_{2,i}(t) \\ \dot{x}_{2,i}(t) &= u_{1,i}(t) + d_{1,i}(t) \\ \dot{x}_{3,i}(t) &= x_{4,i}(t)x_{2,i}(t) \\ \dot{x}_{4,i}(t) &= u_{2,i}(t) + d_{2,i}(t) \end{cases} \tag{2.62}$$

where $x_i = [x_{1,i}, x_{2,i}, x_{3,i}, x_{4,i}]^T \in \mathbb{R}^4$ (resp. $u_i = [u_{1,i}, u_{2,i}]^T \in \mathbb{R}^2$) is the state (resp. control input) of the ith follower. The unknown perturbation of the ith chained-form is given by $d_i = [d_{1,i}, d_{2,i}]^T \in \mathbb{R}^2$.

Figure 2.15 provides an illustration of fixed-time consensus tracking problem. To solve this problem, the following assumptions are considered.

Assumption 6 *It is assumed that the communication topology among the N followers is undirected, fixed, connected. It means that the adjacency matrix A is symmetric. It is also assumed that there is at least one strictly positive parameter b_i.*

Assumption 7 *The followers do not known the leader control input. Nevertheless, its neighboring agents know its upper bounds $u_{1,0}$ and $u_{2,0}$, defined as follows*

$$\begin{cases} |u_{1,0}(t)| &\leq u_{1,0}^{max} \\ |u_{2,0}(t)| &\leq u_{2,0}^{max} \end{cases} \tag{2.63}$$

with $u_{1,0}^{max}, u_{2,0}^{max} \in \mathbb{R}^+$.

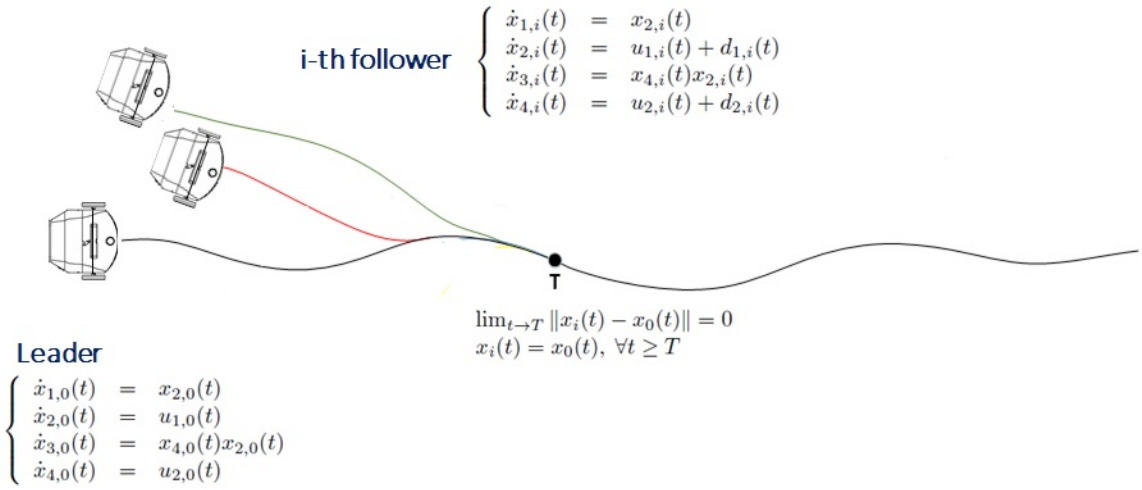

Figure 2.15: Illustration of the fixed-time consensus tracking problem.

Assumption 8 *For each follower, the perturbation $d_i(t)$ is unknown but it is bounded as follows*

$$\begin{cases} |d_{1,i}(t)| \leq d_{1,i}^{max} \\ |d_{2,i}(t)| \leq d_{2,i}^{max} \end{cases} \tag{2.64}$$

with $d_{1,i}^{max}, d_{2,i}^{max} \in \mathbb{R}^+$.

Assumption 9 *It is assumed that the leader state $x_{2,0}$ satisfies the following condition*

$$x_{2,0}(t) \neq 0 \tag{2.65}$$

2.6.1 Fixed-Time Observer-Based Consensus Protocol

For chained-form dynamics MAS under matched perturbations, we propose an observer-based consensus protocol to deal with the leader-follower consensus problem. Figure 2.16 illustrates the proposed control strategy to solve the consensus problem of MAS with chained-form dynamics.

Distributed fixed-time observer

To estimate the leader state in a prescribed time, distributed observers are designed for each follower $i \in \{1, \ldots, N\}$. Indeed, the leader state is only available to its neighboring followers. Let us introduce

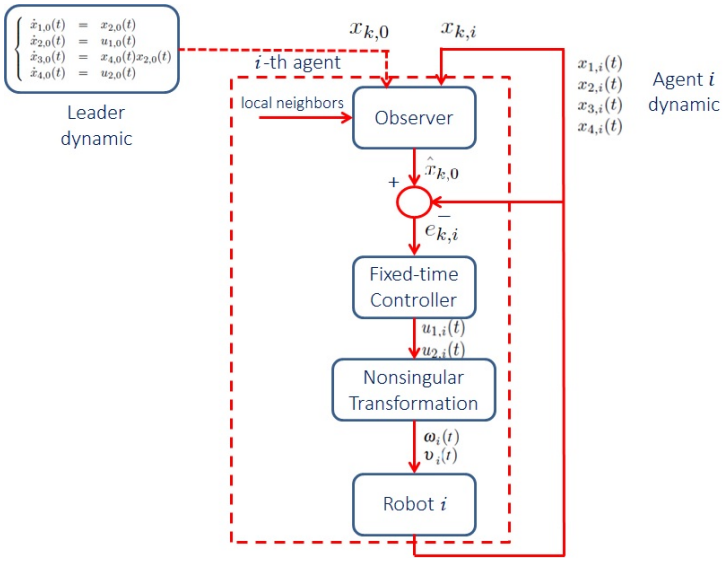

Figure 2.16: Proposed control strategy to solve the consensus problem of MAS with chained-form dynamics.

the following observer as follows

$$\begin{cases} \dot{\hat{x}}_{1,i} &= \hat{x}_{2,i} + \rho_1 \operatorname{sign}\left(\sum_{j=1}^{N} a_{ij}(\hat{x}_{1,j} - \hat{x}_{1,i}) + b_i(x_{1,0} - \hat{x}_{1,i})\right) \\ & \quad +\sigma_1 \left[\sum_{j=1}^{N} a_{ij}(\hat{x}_{1,j} - \hat{x}_{1,i}) + b_i(x_{1,0} - \hat{x}_{1,i})\right]^2 \\ \dot{\hat{x}}_{2,i} &= \rho_2 \operatorname{sign}\left(\sum_{j=1}^{N} a_{ij}(\hat{x}_{2,j} - \hat{x}_{2,i}) + b_i(x_{2,0} - \hat{x}_{2,i})\right) \\ & \quad +\sigma_2 \left[\sum_{j=1}^{N} a_{ij}(\hat{x}_{2,j} - \hat{x}_{2,i}) + b_i(x_{2,0} - \hat{x}_{2,i})\right]^2 \\ \dot{\hat{x}}_{3,i} &= \hat{x}_{4,i}\hat{x}_{2,i} + \rho_3 \operatorname{sign}\left(\sum_{j=1}^{N} a_{ij}(\hat{x}_{3,j} - \hat{x}_{3,i}) + b_i(x_{3,0} - \hat{x}_{3,i})\right) \\ & \quad +\sigma_3 \left[\sum_{j=1}^{N} a_{ij}(\hat{x}_{3,j} - \hat{x}_{3,i}) + b_i(x_{3,0} - \hat{x}_{3,i})\right]^2 \\ \dot{\hat{x}}_{4,i} &= \rho_4 \operatorname{sign}\left(\sum_{j=1}^{N} a_{ij}(\hat{x}_{4,j} - \hat{x}_{4,i}) + b_i(x_{4,0} - \hat{x}_{4,i})\right) \\ & \quad +\sigma_4 \left[\sum_{j=1}^{N} a_{ij}(\hat{x}_{4,j} - \hat{x}_{4,i}) + b_i(x_{4,0} - \hat{x}_{4,i})\right]^2 \end{cases} \tag{2.66}$$

where $\hat{x}_{k,i}$ $(k = \{1, \ldots, 4\})$ is the estimation of the leader state $x_{k,0}$ for the ith follower, ρ_k and σ_k are positive constants, which will be given hereafter.

The fixed-time stabilization of the estimation errors

$$\tilde{x}_{k,i} = \hat{x}_{k,i} - x_{k,0} \qquad (i = \{1, \ldots, N\},\ k = \{1, \ldots, 4\}) \tag{2.67}$$

is introduced in the following theorem.

Theorem 6 *Suppose that Assumptions 6-7 are satisfied. If the gains of the distributed observer* (2.66)

verify

$$\begin{cases} \sigma_k &= \frac{\epsilon\sqrt{N}}{(2\lambda_{min}(L+B))^{\frac{3}{2}}}, \forall k = 1, \ldots, 4 \\ \rho_1 &= \epsilon\sqrt{\frac{\lambda_{max}(L+B)}{2\lambda_{min}(L+B)}} \\ \rho_2 &= u_{1,0}^{max} + \epsilon\sqrt{\frac{\lambda_{max}(L+B)}{2\lambda_{min}(L+B)}} \\ \rho_3 &= \epsilon\sqrt{\frac{\lambda_{max}(L+B)}{2\lambda_{min}(L+B)}} \\ \rho_4 &= u_{2,0}^{max} + \epsilon\sqrt{\frac{\lambda_{max}(L+B)}{2\lambda_{min}(L+B)}} \end{cases} \tag{2.68}$$

with $\epsilon > 0$, then, for any initial condition, the estimation errors (2.67) *converge to zero. An upper bound of the convergence time can be given as*

$$T_o = \frac{2\pi}{\epsilon} \tag{2.69}$$

Proof. Using (2.66), the dynamics of the observation error is given by

$$\begin{aligned} \dot{\tilde{x}}_{1,i} &= \tilde{x}_{2,i} + \rho_1 \operatorname{sign}\left(\sum_{j=1}^N a_{ij}(\tilde{x}_{1,j} - \tilde{x}_{1,i}) - b_i\tilde{x}_{1,i}\right) \\ &\quad +\sigma_1 \left\lceil \sum_{j=1}^N a_{ij}(\tilde{x}_{1,j} - \tilde{x}_{1,i}) - b_i\tilde{x}_{1,i} \right\rfloor^2 \\ \dot{\tilde{x}}_{2,i} &= \rho_2 \operatorname{sign}\left(\sum_{j=1}^N a_{ij}(\tilde{x}_{2,j} - \tilde{x}_{2,i}) - b_i\tilde{x}_{2,i}\right) \\ &\quad +\sigma_2 \left\lceil \sum_{j=1}^N a_{ij}(\tilde{x}_{2,j} - \tilde{x}_{2,i}) - b_i\tilde{x}_{2,i} \right\rfloor^2 - u_{1,0} \\ \dot{\tilde{x}}_{3,i} &= \rho_3 \operatorname{sign}\left(\sum_{j=1}^N a_{ij}(\tilde{x}_{3,j} - \tilde{x}_{3,i}) - b_i\tilde{x}_{3,i}\right) \\ &\quad +\sigma_3 \left\lceil \sum_{j=1}^N a_{ij}(\tilde{x}_{3,j} - \tilde{x}_{3,i}) - b_i\tilde{x}_{3,i} \right\rfloor^2 + \hat{x}_{4,i}\hat{x}_{2,i} - x_{4,0}x_{2,0} \\ \dot{\tilde{x}}_{4,i} &= \rho_4 \operatorname{sign}\left(\sum_{j=1}^N a_{ij}(\tilde{x}_{4,j} - \tilde{x}_{4,i}) - b_i\tilde{x}_{4,i}\right) \\ &\quad +\sigma_4 \left\lceil \sum_{j=1}^N a_{ij}(\tilde{x}_{4,j} - \tilde{x}_{4,i}) - b_i\tilde{x}_{4,i} \right\rfloor^2 - u_{2,0} \end{aligned} \tag{2.70}$$

Let us denote

$$\tilde{x}_k = [\tilde{x}_{k,1}, \ldots, \tilde{x}_{k,N}]^T \tag{2.71}$$

Then, for $\tilde{x}_1$, $\tilde{x}_2$ and $\tilde{x}_4$, one can obtain

$$\dot{\tilde{x}}_1 = \tilde{x}_2 - \rho_1 \operatorname{sign}\left((L+B)\tilde{x}_1\right) - \sigma_1 \left\lceil (L+B)\tilde{x}_1 \right\rfloor^2 \tag{2.72}$$

$$\dot{\tilde{x}}_2 = -\rho_2 \operatorname{sign}\left((L+B)\tilde{x}_2\right) - \sigma_2 \left\lceil (L+B)\tilde{x}_2 \right\rfloor^2 - \mathbf{1}u_{1,0} \tag{2.73}$$

$$\dot{\tilde{x}}_4 = -\rho_4 \operatorname{sign}\left((L+B)\tilde{x}_4\right) - \sigma_4 \left\lceil (L+B)\tilde{x}_4 \right\rfloor^2 - \mathbf{1}u_{2,0} \tag{2.74}$$

We complete the proof by three steps.

- Let us first study subsystems (2.72)-(2.73). Consider the candidate Lyapunov function for subsystem (2.73):

$$V_5 = \frac{1}{2}\tilde{x}_2^T(L+B)\tilde{x}_2 \tag{2.75}$$

Its time derivative is given by

$$\begin{aligned}\dot{V}_5 &= -\rho_2\tilde{x}_2^T(L+B)\,\mathrm{sign}\left((L+B)\tilde{x}_2\right)\\ &\quad +\tilde{x}_2^T(L+B)\left(-\sigma_2\left\lceil(L+B)\tilde{x}_2\right\rfloor^2-\mathbf{1}u_{1,0}\right)\\ &\leq -(\rho_2-u_{1,0}^{max})\|(L+B)\tilde{x}_2\|_1\\ &\quad -\beta_2 N^{-\frac{1}{2}}(2\lambda_{min}(L+B))^{\frac{3}{2}}V_5^{\frac{3}{2}}\\ &\leq -\epsilon V_5^{\frac{1}{2}}-\epsilon V_5^{\frac{3}{2}}\end{aligned}$$

Using Lemma 2, this inequality guarantees that $\tilde{x}_2$ is fixed-time stable at the origin with the settling time bounded by $\frac{\pi}{\epsilon}$.

After $\tilde{x}_2$ converges to zero (i.e. when $t \geq \frac{\pi}{\epsilon}$), the dynamics of $\tilde{x}_1$ reduces to

$$\dot{\tilde{x}}_1 = -\rho_1\,\mathrm{sign}\left((L+B)\tilde{x}_1\right)-\sigma_1\left\lceil(L+B)\tilde{x}_1\right\rfloor^2 \tag{2.76}$$

Similarly to the previous step, the $\tilde{x}_1$ dynamics converges to zero. Indeed, consider the Lyapunov function:

$$V_6 = \frac{1}{2}\tilde{x}_1^T(L+B)\tilde{x}_1 \tag{2.77}$$

Its time derivative is given by

$$\begin{aligned}\dot{V}_6 &= -\rho_1\tilde{x}_1^T(L+B)\,\mathrm{sign}\left((L+B)\tilde{x}_1\right)\\ &\quad -\sigma_1\tilde{x}_1^T(L+B)\left\lceil(L+B)\tilde{x}_1\right\rfloor^2\\ &\leq -\rho_1\|(L+B)\tilde{x}_1\|_1\\ &\quad -\sigma_1 N^{-\frac{1}{2}}(2\lambda_{min}(L+B))^{\frac{3}{2}}V_6^{\frac{3}{2}}\\ &\leq -\epsilon V_6^{\frac{1}{2}}-\epsilon V_6^{\frac{3}{2}}\end{aligned}$$

Hence, one can conclude that $\tilde{x}_2$ converges to zero and after that $\tilde{x}_1$ converges to zero in a fixed-time bounded by $2\frac{\pi}{\epsilon}$.

- Let us now study subsystem (2.74).

  The time derivative of the following candidate Lyapunov function

$$V_7 = \frac{1}{2}\tilde{x}_4^T(L+B)\tilde{x}_4 \tag{2.78}$$

  is given by

$$\begin{aligned}\dot{V}_7 &= \tilde{x}_4^T(L+B)\left(-\rho_4\,\mathrm{sign}\left((L+B)\tilde{x}_4\right)-\sigma_4\left\lceil(L+B)\tilde{x}_4\right\rfloor^2-\mathbf{1}u_{2,0}\right)\\ &\leq -(\rho_4-u_{2,0}^{max})\|(L+B)\tilde{x}_4\|_1-\sigma_4 N^{-\frac{1}{2}}(2\lambda_{min}(L+B))^{\frac{3}{2}}V_7^{\frac{3}{2}}\\ &\leq -\epsilon V_7^{\frac{1}{2}}-\epsilon V_7^{\frac{3}{2}}\end{aligned}$$

  Using Lemma 2, this inequality ensures that $\tilde{x}_4$ converges to zero in a finite-time bounded by $\frac{\pi}{\epsilon}$.

- After $\tilde{x}_2$ and $\tilde{x}_4$ converge to zero (i.e. when $t \geq \frac{\pi}{\epsilon}$), the dynamics of $\tilde{x}_3$ becomes

$$\dot{\tilde{x}}_3 = -\rho_3 \operatorname{sign}\left((L+B)\tilde{x}_3\right) - \sigma_3 \lceil (L+B)\tilde{x}_3 \rfloor^2 \tag{2.79}$$

  Similarly to previously, considering the candidate Lyapunov function $V_8 = \frac{1}{2}\tilde{x}_3^T(L+B)\tilde{x}_3$ yields in the fixed-time stable at the origin of $\tilde{x}_3$ with the settling time bounded by $2\frac{\pi}{\epsilon}$.

Hence, one can conclude that the estimation errors (2.67) converge to zero in a fixed-time bounded by T_o. ■

Decentralized fixed-time controller

From Theorem 6, one can conclude that $\hat{x}_i = [\hat{x}_{1,i}, \hat{x}_{2,i}, \hat{x}_{3,i}, \hat{x}_{4,i}]^T = x_0$ for all $t \geq T_o$. Hence, after time T_o, each follower is able to indirectly access to the state of the leader and uses the estimate $\hat{x}_i$ in the consensus protocol.

Let us denote the tracking errors as follows

$$e_{k,i} = x_{k,i} - \hat{x}_{k,i} = x_{k,i} - x_{k,0} - \tilde{x}_{k,i} \qquad (i = \{1,\ldots,N\},\ k = \{1,\ldots,4\}) \tag{2.80}$$

For each follower $i = \{1,\ldots,N\}$ and for all $t \geq T_o$, the tracking error dynamics becomes

$$\begin{array}{lll} & \dot{e}_{1,i} &= e_{2,i} \\ (\Sigma_1) & \dot{e}_{2,i} &= u_{1,i} + d_{1,i} - u_{1,0} \\ & & \\ & \dot{e}_{3,i} &= e_{4,i}x_{2,0} + (e_{4,i} + x_{4,0})e_{2,i} \\ (\Sigma_2) & \dot{e}_{4,i} &= u_{2,i} + d_{2,i} - u_{2,0} \end{array} \tag{2.81}$$

It is clear that dynamics (2.81) is divided into two coupled second-order subsystems (i.e. Σ_1 and Σ_2). To deal with the observer-based consensus tracking problem, for each follower $i = \{1,\ldots,N\}$, the following two steps are introduced:

- Design $u_{1,i}$ such that the origin of subsystem Σ_1 is fixed-time stable with the settling time estimate $T_1 < T$.
- For $t \geq T_1$, design $u_{2,i}$ such that the origin of subsystem Σ_2 is fixed-time stable with the settling time estimate T. Note that for $t \geq T_1$, subsystem Σ_2 becomes

$$\begin{array}{lll} \dot{e}_{3,i} &= e_{4,i}x_{2,0} \\ \dot{e}_{4,i} &= u_{2,i} + d_{2,i} - u_{2,0} \end{array} \tag{2.82}$$

  It is clear that for $t \geq T_1$, the two subsystems are decoupled.

In the following theorem, the control strategy is derived to solve the leader-follower consensus problem for MAS with chained-form dynamics, in a fixed-time, in spite of the presence of matched perturbations.

Theorem 7 *Let us consider the leader-follower system* (2.61)-(2.62)*. Suppose that Assumptions 6-9 are satisfied and the gains of the distributed observer* (2.66) *verify Eq.* (2.68)*. The leader-follower consensus problem is solved in a fixed-time using the decentralized controllers*

$$u_{1,i} = \begin{cases} 0 & ,\forall t < T_o \\ -\frac{\alpha_1+3\beta_1 e_{1,i}^2+2a_i}{2}\,\mathrm{sign}\,(s_{1,i}) - \lfloor \alpha_2 s_{1,i} + \beta_2 \lfloor s_{1,i} \rceil^3 \rceil^{\frac{1}{2}} & ,\forall t \geq T_o \end{cases} \tag{2.83}$$

with the sliding surface

$$s_{1,i} = e_{2,i} + \lfloor \lfloor e_{2,i} \rceil^2 + \alpha_1 e_{1,i} + \beta_1 \lfloor e_{1,i} \rceil^3 \rceil^{\frac{1}{2}} \tag{2.84}$$

and

$$u_{2,i} = \begin{cases} 0 & ,\forall t < T_s \\ -\frac{1}{\hat{x}_{2,0}} \left(e_{4,i}\dot{\hat{x}}_{2,0} + \frac{\alpha_1+3\beta_1 e_{3,i}^2+2b_i}{2}\,\mathrm{sign}\,(s_{2,i}) + \lfloor \alpha_2 s_{2,i} + \beta_2 \lfloor s_{2,i} \rceil^3 \rceil^{\frac{1}{2}} \right) & ,\forall t \in [T_s, T] \\ -b_i\,\mathrm{sign}\,(e_{4,i}) & ,\forall t > T \end{cases} \tag{2.85}$$

with the sliding surface

$$s_{2,i} = e_{4,i}x_{2,0} + \lfloor \lfloor e_{4,i}x_{2,0} \rceil^2 + \gamma_1 e_{3,i} + \mu_1 \lfloor e_{3,i} \rceil^3 \rceil^{\frac{1}{2}} \tag{2.86}$$

where α_1, α_2, β_1 and β_2 are positive constants, a_i and b_i are positive constants given hereafter, and the switching time is explicitly defined as

$$T_s = T_o + \frac{2}{\sqrt{\alpha}_2} + \frac{2}{\sqrt{\beta}_2} + \frac{2\sqrt{2}}{\sqrt{\alpha}_1} + \frac{2\sqrt{2}}{\sqrt{\beta}_1} \tag{2.87}$$

Proof. We complete the proof by three steps. First, it will be shown that the origin of subsystem Σ_1 is fixed-time stable with the settling time estimate T_s under the control law (2.83)-(2.84). Then, the protocol (2.83)-(2.86) guarantees that the origin of subsystem Σ_2 is fixed-time stable with the settling time estimate T. At last, it will be proved that in spite of the presence of matched perturbations, the fixed-time leader-follower consensus problem is solved.

- Let us first consider subsystem Σ_1. Following [**?**], let us consider the candidate Lyapunov function $V_9 = |s_{1,i}|$. Its derivative is,

$$\dot{V}_9 = \dot{e}_{2,i}\,\mathrm{sign}\,(s_{1,i}) + \frac{|e_{2,i}|\dot{e}_{2,i}\,\mathrm{sign}\,(s_{1,i}) + \frac{\alpha_1+3\beta_1 e_{1,i}^2}{2} e_{2,i}\,\mathrm{sign}\,(s_{1,i})}{|\lfloor e_{2,i} \rceil^2 + \alpha_1 e_{1,i} + \beta_1 \lfloor e_{1,i} \rceil^3|^{\frac{1}{2}}} \tag{2.88}$$

  Since

$$\lfloor \alpha_2 s_{1,i} + \beta_2 \lfloor s_{1,i} \rceil^3 \rceil^{\frac{1}{2}}\,\mathrm{sign}\,(s_{1,i}) = (\alpha_2|s_{1,i}| + \beta_2|s_{1,i}|^3)^{\frac{1}{2}}$$

  one has

$$\begin{aligned} \dot{e}_{2,i}\,\mathrm{sign}\,(s_{1,i}) &= (u_{1,i} + d_{1,i} - u_{1,0})\,\mathrm{sign}\,(s_{1,i}) \\ &= -\frac{\alpha_1+3\beta_1 e_{1,i}^2}{2} \\ &\quad -(\alpha_2|s_{1,i}| + \beta_2|s_{1,i}|^3)^{\frac{1}{2}} - (a_i - (d_{1,i} - u_{1,0})\,\mathrm{sign}\,(s_{1,i})) \end{aligned}$$

Setting

$$a_i \geq d_{1,i}^{max} + u_{1,0}^{max} \tag{2.89}$$

one can conclude that

$$\dot{V}_9 \leq -(\alpha_2 V_9 + \beta_2 V_9^3)^{\frac{1}{2}} \tag{2.90}$$

From Lemma 2, it is clear that $s_{1,i} = 0$ when $t \geq T_o + \frac{2}{\sqrt{\alpha_2}} + \frac{2}{\sqrt{\beta_2}}$.

The sliding dynamics ($s_{1,i} = 0$) can be expressed as

$$\dot{e}_{1,i} = -\Big\lfloor \frac{\alpha_1 e_{1,i} + \beta_1 \lfloor e_{1,i} \rceil^3}{2} \Big\rceil^{\frac{1}{2}} \tag{2.91}$$

Using the candidate Lyapunov function $V_{10} = |e_{1,i}|$, one can obtain

$$\dot{V}_{10} = -(\frac{\alpha_1}{2} V_{10} + \frac{\beta_1}{2} V_{10}^3)^{\frac{1}{2}} \tag{2.92}$$

It is clear using Lemma 2 that $e_{1,i} = 0$ when $t \geq T_s$. Furthermore, since $e_{1,i} = 0$ and $s_{1,i} = 0$, then $e_{2,i} = 0$.

- Let us now consider subsystem Σ_2 for $t \in [T_s, T]$. In this case, since $e_{1,i} = e_{2,i} = 0$, subsystem Σ_2 becomes (2.82). Note that Assumption 4 is introduced to avoid singularity problem in the controller design. Hence, let us set $\zeta_i = e_{4,i} x_{2,0}$. Dynamics (2.82) can be written as follows,

$$\begin{array}{rcl} \dot{e}_{3,i} & = & \zeta_i \\ \dot{\zeta}_i & = & e_{4,i} \dot{x}_{2,0} + x_{2,0}(u_{2,i} + d_{2,i} - u_{2,0}) \end{array} \tag{2.93}$$

Setting

$$b_i \geq d_{2,i}^{max} + u_{2,0}^{max} \tag{2.94}$$

and using the controller (2.85)-(2.86), similarly to the previous step, one can easily deduce that $e_{3,i} = 0$ for all $t \geq T = T_s + \frac{2}{\sqrt{\alpha_2}} + \frac{2}{\sqrt{\beta_2}} + \frac{2\sqrt{2}}{\sqrt{\alpha_1}} + \frac{2\sqrt{2}}{\sqrt{\beta_1}}$. Furthermore, since $e_{3,i} = 0$ and $s_{2,i} = 0$, then $e_{4,i} = 0$.

- The last step is to study subsystem Σ_2 for $t > T$. From subsystem Σ_2, one can obtain

$$\dot{e}_{4,i} = -b_i \operatorname{sign}(e_{4,i}) + d_{2,i} - u_{2,0} \tag{2.95}$$

The controller $u_{2,i}$ is used to reject the effect of uncertain terms $d_{2,i}$ and $u_{2,0}$. Let us consider the candidate Lyapunov function $V_{11} = \frac{1}{2} e_{4,i}^2$. Its derivative is given by

$$\begin{array}{rcl} \dot{V}_{11} & = & -b_i |e_{4,i}| + e_{4,i}(d_{2,i} - u_{2,0}) \\ & \leq & -(b_i + d_{2,i}^{max} + u_{2,0}^{max}) |e_{4,i}| \\ & \leq & 0 \end{array} \tag{2.96}$$

For the previous step, one has $e_{3,i}(T) = e_{4,i}(T) = 0$. Hence, one can conclude that for any initial condition, the tracking errors converge to zero in a finite-time bounded by T and remains there in spite of the presence of matched perturbations.

This concludes the proof. ■

Remark 9 *When the settling time T is prescribed, the switching time T_s should be appropriately tuned using α_1, α_2, β_1 and β_2 through Eq.* (2.87).

Remark 10 *In the presence of measurement noise or unmatched perturbations, only practical consensus (i.e. uniformly ultimate boundedness of the tracking errors) can be achieved.*

Remark 11 *The design guidelines for our fixed-time controller are as follows:*

- *Select the parameter ϵ. Parameter ϵ should be tuned to obtain a good compromise between robustness against measurement noises and sufficiently fast estimation (T_o can be computed according to Eq.* (2.69)*).*
- *Design the observer gain parameters using Eq.* (2.68).
- *Select the settling time T. This parameter T should be tuned to obtain a good compromise between the control magnitudes and sufficiently fast convergence for the tracking errors.*
- *Select the switching time T_s as follows:*

  $$T_s = \frac{T - T_o}{2}$$

  It enables to divide the time interval $[T_o, T_s]$ into two equal parts. This is useful for our two steps procedure described previously (i.e. fixed-time stabilization of system Σ_1 and system Σ_2 described in Eq. (2.81)*).*
- *Knowing T_o and T_s, select the parameters γ_1, γ_2, μ_1 and μ_2 according to* (2.87). *A possible choice for these parameters is the following:*

  $$(\mu_1/2) = \mu_2 = (\gamma_1/2) = \gamma_2 = \frac{64}{(T_s - T_o)^2} \tag{2.97}$$

- *Select the control parameters a_i and b_i which satisfy inequalities* (2.89) *and* (2.94).

2.6.2 Simulation Results

Here, the performances of the proposed observer-based leader-follower consensus controller are studied through numerical simulations. Suppose that the MAS is composed of $N = 6$ followers labeled by $1-6$ and one leader labeled by 0. The nonlinear dynamics of the leader (resp. the followers) is given by Eq. (2.61) (resp. Eq. (2.62)). Hereafter, the leader control input is set as $u_0 = [0.1\sin(t), -0.5\cos(0.5t)]$. Each follower is affected by the unknown perturbation $d_i = \left[0.2\sin(x_{1,i}), 0.3e^{-t}\right)]$. Therefore, one can easily verify that Assumptions 7-8 are fulfilled with $u_{1,max} = 0.1$, $u_{2,max} = 0.5$, $d_{1,max} = 0.2$ and $d_{2,max} = 0.3$.

Using the same topology as previous section, from matrix B, it is clear that agents 1, 3, 4 and 6 do not have direct link with agent 0. Assumption 6 is satisfied. The initial leader state is set as $x_0(0) = [3, 2, 2, 0.5]^T$. From the control input of the leader, one can see that Assumption 9 is verified.

The parameters of the distributed observer are selected as $\rho_1 = \rho_3 = 10$, $\rho_2 = 10.1$, $\rho_4 = 10.5$ and $\sigma_k = 24$, $\forall k = 1, \ldots, 4$. The parameters of the decentralized controller are chosen as follows: $\alpha_1 = 5.12$, $\beta_1 = 5.12$, $\alpha_2 = 2.56$, $\beta_2 = 2.56$, $a_i = 0.3$ and $b_i = 0.8$.

Using Theorem 6, the distributed observer (2.66) guarantees the stabilization of the estimation errors (2.67) to the origin in a finite-time bounded by $T_o = 1s$. Figure 2.17 shows that the distributed observers accurately reconstruct the leader state for each agent before T_o. Contrary to [**?**, **?**], the proposed fixed-time observer removes the problem of the communication loop due to the dependence of the control inputs of the followers on the inputs of its neighbors. The switching time can be calculated using Eq. (2.69). One can obtain $T_s = 4.5s$. Hence, the origin of the closed-loop system is globally finite-time stable contrary to existing controllers which only provide semi-global finite-time stability property. Furthermore, since T_s does not depend on the initial states of agents, the proposed protocol is distributed.

Here, an upper bound of the settling time, independently of the initial conditions, can be estimated using Eq. (2.87), i.e. $T = 9s$ from Theorem 7. The tracking errors are depicted in Fig. 2.18. One can see that the tracking errors between each follower and the leader converge to zero before T. From Fig. 2.18, one can conclude that using the proposed controller, the leader-follower consensus is achieved in a prescribed time. The control inputs for each agent are shown in Fig. 2.19. One can note that the magnitude of control inputs may be large during the transients to achieve a fast convergence of the sliding surfaces given by the different steps of the consensus protocol. Hence, the control parameters should be adjusted to obtain a good compromise between magnitude of the control inputs and settling time.

Based on the simulation results, one can see that the proposed observer-based controller achieves the fixed-time leader-follower consensus for MAS with chained-form dynamics in spite of the presence of matched perturbations.

2.7 Conclusion

For the second and third section, the fixed-time consensus problem of linear multi-agent systems (i.e. single-integrator and double-integrator dynamics) has been considered. The proposed distributed observers has been used to estimate the leader state in a fixed-time. A decentralized controller has been designed for each agent to solve the leader-follower consensus problem in a prescribed-time.

For the fourth section, the fixed-time trajectory tracking problem for unicycle-type mobile robots has been considered. A switching controller has been proposed to solve this problem. An upper bound

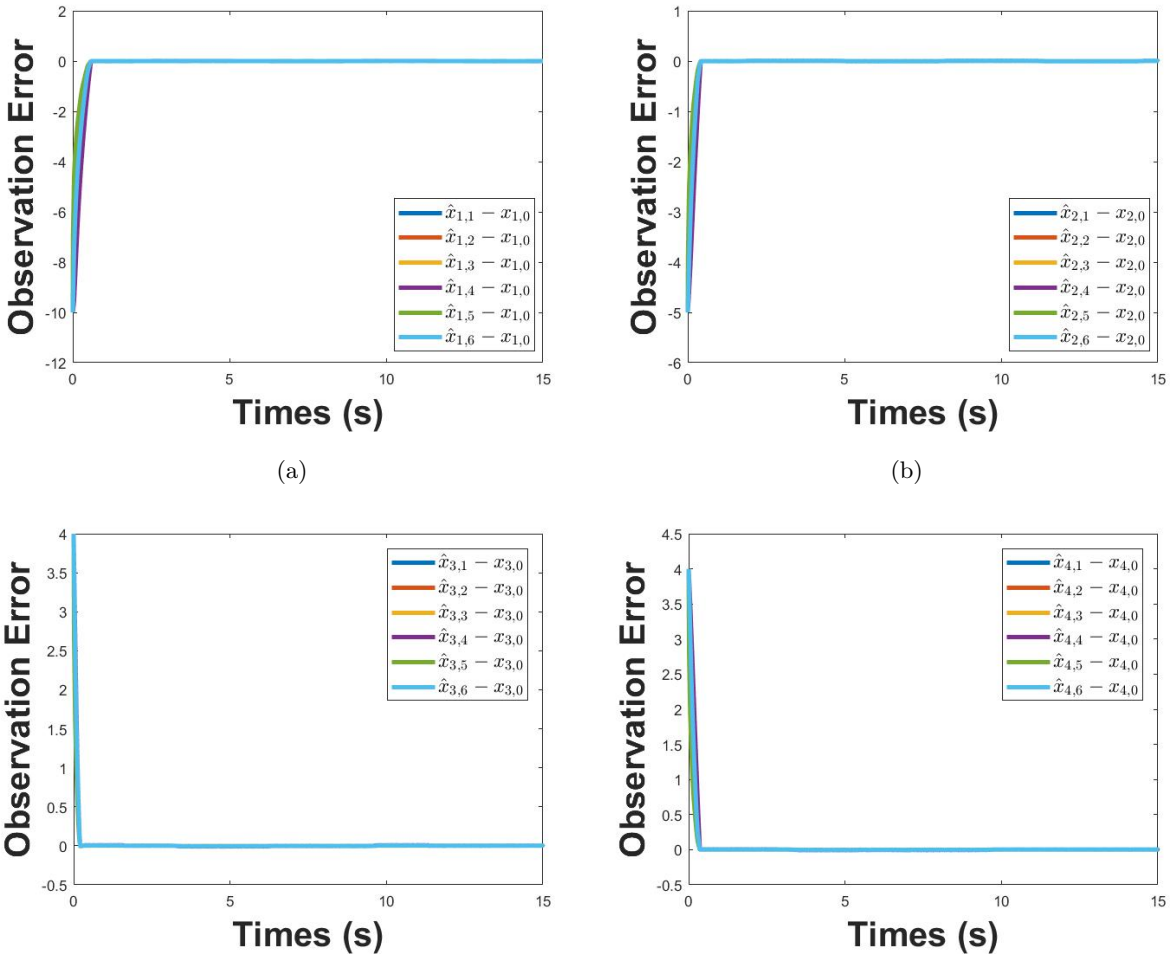

Figure 2.17: Evolution of the estimation errors (2.67) for each follower

of the settling time, which only depends on the controller parameters has been estimated regardless of the initial conditions. Some simulation results have been given to show the effectiveness of the proposed controller.

In the fifth section, the fixed-time consensus problem of multiple unicycle-type mobile robots under matched perturbations has been considered. Thanks to the proposed distributed observers, the leader state has been estimated in a fixed-time. A decentralized observer-based control protocol has been proposed for each agent to solve the leader-follower consensus problem in a fixed-time.

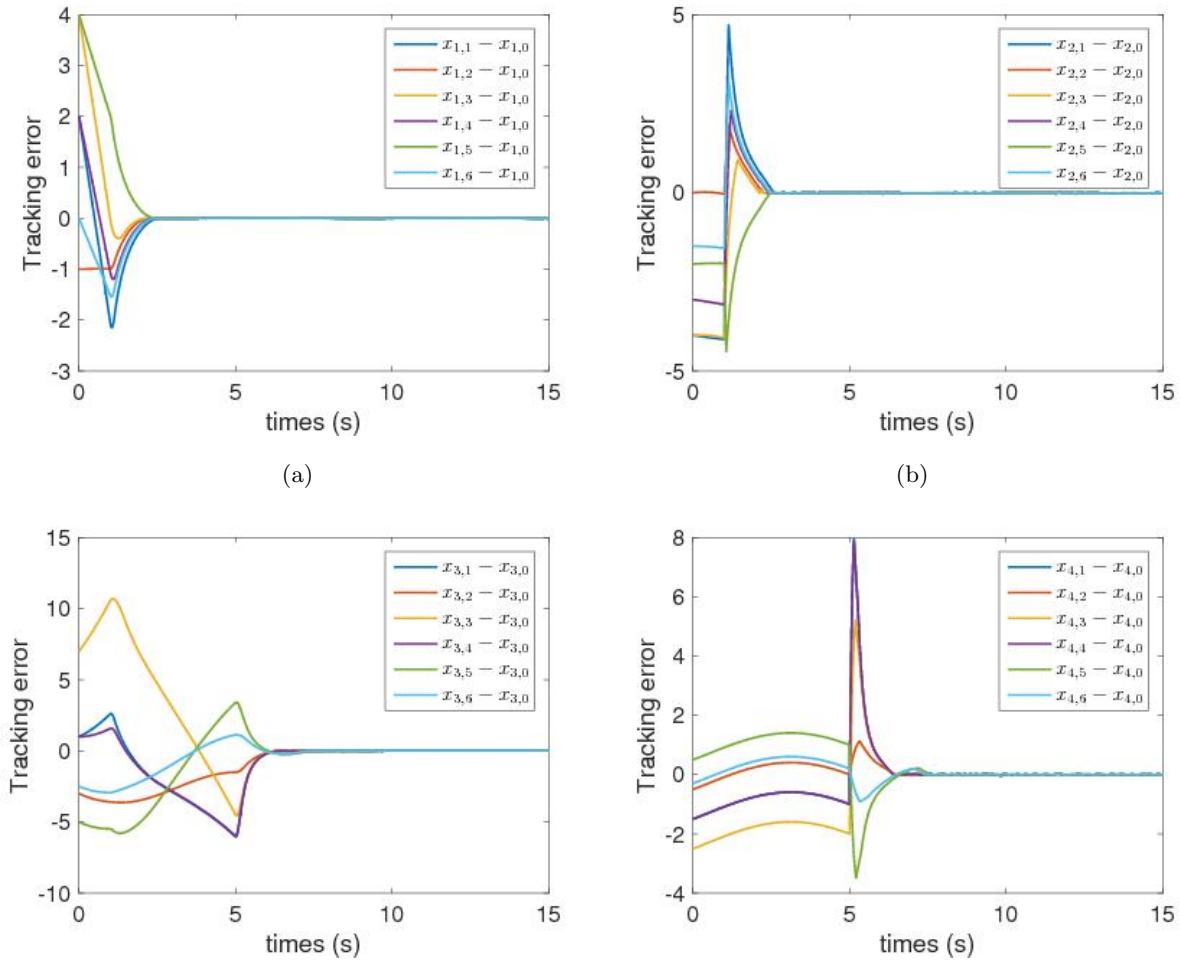

Figure 2.18: Evolution of the tracking errors between each agent and the leader.

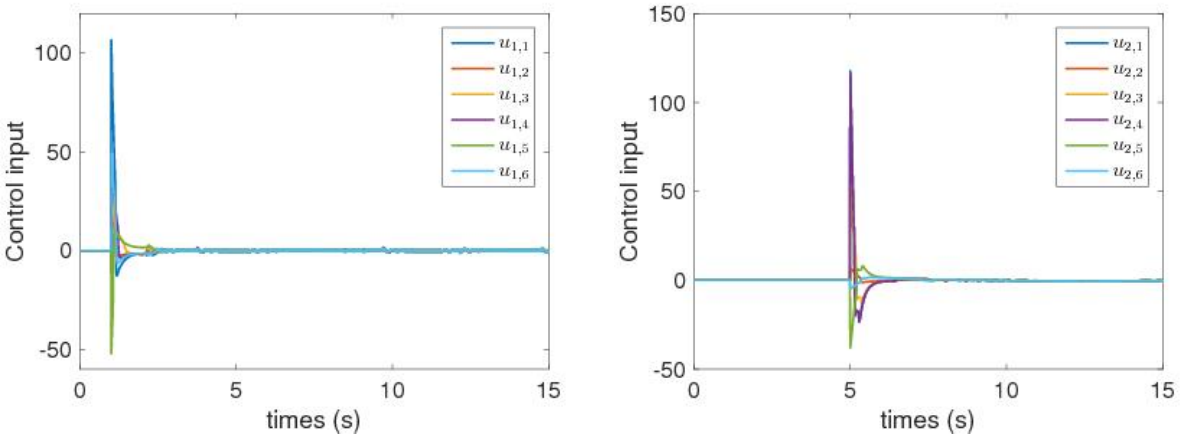

Figure 2.19: Control input for each agent

Chapter 3

Consensus for Multi-Agent Systems Using Distributed Model Predictive Control

3.1 Introduction

This chapter is concerned with the consensus problem for a group of mobile agents which have a discrete-time dynamics using distributed model predictive control (DMPC). The first part of this chapter formulates the general control objective and the considered assumptions to solve the consensus problem under switching topologies. The second and third part of this chapter deal with the consensus problem for linear multi-agent systems (i.e. single-integrator and double-integrator dynamics). The proposed consensus control protocol is distributed and is designed by combining graph theory with a predictive control algorithm to take into account the switches on the communication topology. The predictive strategy is used to estimate input and output of agent through a receding horizon. Contrary to many existing works, the cost function is designed using the difference between two consecutive inputs. The controller has integrator properties to eliminate steady-state errors.

The objective is to develop a DMPC protocol such that the states of all agents reach an agreement eventually. The main features of the proposed scheme can be summarized as follows:

i) The control horizon can be arbitrarily picked from one to less than the prediction horizon, which increases the degree of freedom in controller design.

ii) The communication topolgy is assumed to be directed and dynamically switching.

iii) The sampling period can be arbitrarily large provided that each communication topology has a directed spanning tree.

The remaining parts of this chapter are organized as follows. Section 3.2 introduces some assumptions and formulates the general control objective. The distributed model predictive controller based consensus strategy is introduced in Section 3.3. Some simulation results are given in Section 3.4 to illustrate the effectiveness and advantages of the proposed scheme for single and double integrator dynamic. Section 3.5 concludes this chapter.

3.2 Problem statement and considered assumptions

Let us consider a group of N agents labeled by $i \in \{1, \ldots, N\}$. The dynamics of each agent is expressed by the following discrete-time equation

$$x_i(k+1) = F(x_i(k), u_i(k)) \tag{3.1}$$

where $x_i(k) \in \mathbb{R}^n$ is the state of agent i and $u_i(k) \in \mathbb{R}^m$ is the control input of agent i. $F : \mathbb{R}^n \times \mathbb{R}^m \to \mathbb{R}^n$ is known. $T \in \mathbb{R}^+$ is the sampling period.

Among the N agents, at time $t = kT$, the communication topology can be represented by the time-varying digraph $\mathcal{G}(k) = \{\mathcal{V}, \mathcal{E}(k)\}$ where $\mathcal{V} = \{1, \ldots, N\}$ defines the set of nodes, corresponding to the agents, and $\mathcal{E}(k) \subseteq \{\mathcal{V} \times \mathcal{V}\}$ defines the edge set at time kT. An edge $(j, i) \in \mathcal{E}(k)$, with $i \neq j$, exists if at time kT agent i receive information from its neighbor j. At time k, the set of neighbors to the node $i \in \mathcal{V}$ is $\mathcal{N}_i(k) = \{j \in \mathcal{V} : (j, i) \in \mathcal{E}(k)\}$ and $|\mathcal{N}_i(k)|, i \in \mathcal{V}$, is the valency or degree of i-th node at time k. The adjacency matrix $A(k) = (a_{ij}(k)) \in \mathbb{R}^{N \times N}$ satisfies $a_{ij}(k) > 0$ if $(j, i) \in \mathcal{E}$ at time kT and $a_{ij}(k) = 0$, otherwise. The corresponding Laplacian matrix is given by $L(k) = (l_{ij}(k)) \in \mathbb{R}^{N \times N}$ with $l_{ii}(k) = \sum_{j=1,\, j \neq i}^{N} a_{ij}(k)$ and $l_{ij}(k) = -a_{ij}(k)$ for $i \neq j$.

Hereafter, it is assumed that the following hypothesis holds to derive the proposed DMPC scheme.

Assumption 10 *It is assumed that the communication topology among the N agents is directed and dynamical switching and at each time kT it contains a directed spanning tree.*

Such time-varying graphs can be found in many engineering applications due to the creation or failure of communication links, reconfiguration of formations, presence of obstacles and so on.

Here, the purpose is to derive a decentralized controller u_i $(i = 1, \ldots, N)$ for each agent, based on available information, such that the consensus problem is solved. It means that

$$\lim_{k \to \infty} \|x_i(k) - x_j(k)\| = 0 \qquad \forall i, j \in \mathcal{V}, i \neq j \tag{3.2}$$

3.3 Distributed model predictive controller based consensus

3.3.1 Generalities on model predictive controller

MPC (Model Predictive Control) is a kind of finite horizon optimal control. It solves a finite horizon optimal control and applies the first part of the resulting optimal control sequence to the plant at

every sampling instant.

In this subsection, the general structure of MPC is briefly introduced. Let us consider a discrete-time linear system described by

$$x(k+1) = Ax(k) + Bu(k) \tag{3.3}$$

where $x(k) \in \mathbb{R}^n$ and $u(k) \in \mathbb{R}^m$ are the state and control input, respectively. $A \in \mathbb{R}^{n\times n}$ and $B \in \mathbb{R}^{n\times m}$ are the state and input matrices, respectively.

The MPC implementation can be formulated by introducing the following optimization problem at every time instant kT:

$$min_{u(.)}\, J_{(H_p,H_u)}(k) \tag{3.4}$$

subject to

$$\begin{aligned} &x(k+l|k) = Ax(k+l-1|k) + Bu(k+l-1|k), \qquad l = 1,2,\ldots,H_p \\ &x_{min} \le x(k+l|k) \le x_{max}, \qquad l = 1,2,\ldots,H_p \\ &u_{min} \le u(k+l|k) \le u_{max}, \qquad l = 0,1,2,\ldots,H_u-1 \end{aligned} \tag{3.5}$$

The performance index is defined as

$$J_{(H_p,H_u)}(k) = \sum_{l=1}^{H_p} x^T(k+l|k)Qx(k+l|k) + \sum_{l=0}^{H_u-1} u^T(k+l|k)Ru(k+l|k) \tag{3.6}$$

where $Q \in \mathbb{R}^{n\times n}$ and $R \in \mathbb{R}^{m\times m}$ are the weighting matrices, with $Q = Q^T > 0$, $R = R^T > 0$. H_p and H_u denote the length of the prediction horizon and the length of the control horizon, respectively. Usually, $H_p \ge H_u$. The first term is called the state penalty while the second one is called the control penalty.

Equations (3.3)-(3.8) define a quadratic optimization problem and many algorithms and software packages are available to solve it. When the optimal control sequence $u(k+l|k)$, $l = 0,\ldots,H_u-1$ is obtained, only the first control input $uk|k)(0|x(k)$ is applied to the system at time kT according to the so-called receding horizon principle. The rest of the control sequence is discarded. Then, at the next time $(k+1)T$ a new quadratic optimization problem (Equation (3.4)) begins and the process is repeated.

The generic MPC algorithm can be described as follows,

1. At current time kT, measure the current state $x(k)$.

2. Solve the optimization control problem (3.4) with the initial condition $x(k)$. It yields the optimal control sequence $u(k+l|k)$ over the control horizon.

3. Apply the first element in control sequence $u(k+l|k)$ to the system. The remaining elements of the control sequence is discarded.

4. At time $(k+1)T$, repeat from step 1.

3.3.2 Further improvements on MPC

In classical MPC, the control objective is to minimize the cost function (3.4). In the following, in order to improve the performances in terms of steady state error, we introduce in the cost function the difference Δu between two consecutive inputs.

Therefore, let us define the following optimization problem at every time instant kT:

$$min_{u(.)}\, J_{(H_p,H_u)}(k) \tag{3.7}$$

subject to

$$\begin{aligned} &x(k+l|k) = Ax(k+l-1|k) + B(\Delta u(k+l-1|k) + u(k+l-1|k)), \qquad l = 1,2,\ldots,H_p \\ &x_{min} \leq x(k+l|k) \leq x_{max}, \qquad l = 1,2,\ldots,H_p \\ &u_{min} \leq u(k+l|k) \leq u_{max}, \qquad l = 0,1,2,\ldots,H_u-1 \end{aligned} \tag{3.8}$$

The performance index is defined as

$$J_{(H_p,H_u)}(k) = \sum_{l=1}^{H_p} x^T(k+l|k)Qx(k+l|k) + \sum_{l=0}^{H_u-1} \Delta u^T(k+l|k)R\Delta u(k+l|k) \tag{3.9}$$

The difference Δu between two consecutive inputs is as follows

$$\Delta u(k+l|k) = \begin{cases} u(k+l|k) - u(k+l-1|k) & 0 \leq l \leq H_u - 1 \\ 0 & H_u \leq l \leq H_p \end{cases} \tag{3.10}$$

3.3.3 Distributed MPC for linear MAS

Next, we will introduce the common method to design MPC input $u_i(k)$ for agent i at instant k.

Let us consider a group of N agents. The dynamics of each agent is expressed by the following discrete-time linear equation as:

$$x_i(k+1) = Ax_i(k) + Bu_i(k) \qquad \forall i \in \{1,\ldots,N\} \tag{3.11}$$

where $x_i(k) \in \mathbb{R}^n$ and $u_i(k) \in \mathbb{R}^m$ are the state and the control input of agent i, respectively.

Basically, the distributed model predictive control (DMPC) strategy is a model predictive control (MPC) strategy in the form of a distributed optimization problem for each agent. The proposed DMPC controller is designed by optimizing a quadratic optimization function which depends on the difference between the state of the agent and the reference value of the agent state along the prediction horizon H_p. H_u denotes the control horizon. Using the proposed scheme, each agent in the fleet design its own control protocol for each DMPC iteration, by only taking into account the state of the neighbor agents. The proposed method solves the consensus problem even in the presence of switched communication topologies. Indeed, the proposed DMPC strategy is able to adapt to the changes in

the MAS parameters (for instance the topology) and to predict the state of the agent up to a few steps along the prediction horizon H_p.

Define the quadratic cost function as below:

$$\begin{aligned} J_i(k) &= \sum_{l=1}^{H_p} (x_i^T(k+l|k) - r_i^T(k)) Q (x_i(k+l|k) - r_i(k)) + \sum_{l=0}^{H_u-1} u_i^T(k+l|k) R u_i(k+l|k) \\ &= \sum_{l=1}^{H_p} \|x_i(k+l|k) - r_i(k)\|_Q^2 + \sum_{l=0}^{H_u-1} \|u(k+l|k)\|_R^2 \end{aligned} \tag{3.12}$$

subject to

$$\begin{aligned} & x_i(k+l|k) = A x_i(k+l-1|k) + B u_i(k+l-1|k), \qquad l = 1, 2, \ldots, H_p \\ & x_{i\,min} \leq x_i(k+l|k) \leq x_{i\,max}, \qquad l = 1, 2, \ldots, H_p \\ & u_{i\,min} \leq u_i(k+l|k) \leq u_{i\,max}, \qquad l = 0, 1, 2, \ldots, H_u - 1 \end{aligned} \tag{3.13}$$

The reference state is chosen as

$$r_i(k) = \frac{1}{|\mathcal{N}_i(k)| + 1} \sum_{j \in \mathcal{N}_i(k) \bigcup i} x_j(k) \tag{3.14}$$

It is important to note that this reference only depends on the states of the ith agent and its neighbors. This implies that the cost function is distributed. Furthermore, it evolves during time according to the communication topology through the set $\mathcal{N}_i(k)$.

Similarly to the previous subsection, let us introduce the difference Δu_i between two consecutive inputs proposed. The control input for each agent is then defined as

$$\Delta u_i(k+l|k) = \begin{cases} u_i(k+l|k) - u_i(k+l-1|k) & 0 \leq l \leq H_u - 1 \\ 0 & H_u \leq l \leq H_p \end{cases} \tag{3.15}$$

Hence, the first equation of (3.13) can be rewritten as

$$x_i(k+l|k) = A x_i(k+l-1|k) + B(\Delta u_i(k+l-1|k) + u_i(k+l-1|k)), \qquad l = 1, 2, \ldots, H_p \tag{3.16}$$

Therefore, the prediction states $x_i(k+l|k)$, $(l = 1, 2, ..., H_p)$ at time k can be derived as follows:

$$\begin{aligned}
x_i(k+1|k) &= Ax_i(k) + B(\Delta u_i(k) + u_i(k)) \\
\\
x_i(k+2|k) &= Ax_i(k+1|k) + Bu_i(k+1) \\
&= A\big(Ax_i(k) + B(\Delta u_i(k) + u_i(k))\big) + B(\Delta u_i(k+1) + \Delta u_i(k) + u_i(k)) \\
&= A^2x_i(k) + AB + B)\Delta u_i(k) + B\Delta u_i(k+1) + (AB + B)u_i(k) \\
\\
x_i(k+3|k) &= Ax_i(k+2|k) + Bu_i(k+2) \\
&= A^3x_i(k) + (A^2B + AB + B)\Delta u_i(k) + (AB + B)\Delta u_i(k+1) + B\Delta u_i(k+2) \\
&\quad +(A^2B + AB + B)u_i(k) \\
\\
x_i(k+H_p|k) &= A^{H_p}x_i(k) + \Big(\sum_{l=0}^{H_p-1} A^lB\Big)\Delta u_i(k) + \Big(\sum_{l=0}^{H_p-2} A^lB\Big)\Delta u_i(k+1) + \dots \\
&\quad B\Delta u_i(k+H_p-1) + \Big(\sum_{l=0}^{H_p-1} A^lB\Big)u_i(k)
\end{aligned}$$

Hence, one can write the previous equalities as follows:

$$\begin{bmatrix} x_i(k+1|k) \\ x_i(k+2|k) \\ x_i(k+3|k) \\ \vdots \\ x_i(k+H_p|k) \end{bmatrix} = \begin{bmatrix} A \\ A^2 \\ A^3 \\ \vdots \\ A^{H_p} \end{bmatrix} x_i(k) + \begin{bmatrix} B \\ AB + B \\ A^2B + AB + B \\ \vdots \\ \sum_{l=0}^{H_p-1} A^lB \end{bmatrix} u_i(k) +$$

$$\begin{bmatrix} B & 0 & 0 & 0 \\ AB + B & B & 0 & 0 \\ A^2B + AB + B & AB + B & B & \vdots \\ \vdots & \vdots & \ddots & \vdots \\ \sum_{l=0}^{H_p-1} A^lB & \sum_{l=0}^{H_p-2} A^lB & \dots & B \end{bmatrix} \begin{bmatrix} \Delta u_i(k) \\ \Delta u_i(k+1) \\ \Delta u_i(k+2) \\ \vdots \\ \Delta u_i(k+H_p-1) \end{bmatrix}$$

In a compact form, the dynamic system becomes as follows:

$$X_i(k) = P_x x_i(k) + P_u u_i(k) + P_\triangle \Delta U_i(k) \tag{3.17}$$

with $\mathbf{X_i}(k) = \begin{bmatrix} x_i(k+1|k) \\ x_i(k+2|k) \\ x_i(k+3|k) \\ \vdots \\ x_i(k+H_p|k) \end{bmatrix}$, $\Delta U_i(k) = \begin{bmatrix} \Delta u_i(k) \\ \Delta u_i(k+1) \\ \Delta u_i(k+2) \\ \vdots \\ \Delta u_i(k+H_p-1) \end{bmatrix}$,

$$P_x = \begin{bmatrix} A \\ A^2 \\ A^3 \\ \vdots \\ A^{H_p} \end{bmatrix}, \; P_u = \begin{bmatrix} B \\ AB+B \\ A^2B+AB+B \\ \vdots \\ \sum_{l=0}^{H_p-1} A^l B \end{bmatrix} \text{ and}$$

$$P_\triangle = \begin{bmatrix} B & 0 & 0 & 0 \\ AB+B & B & 0 & 0 \\ A^2B+AB+B & AB+B & B & \vdots \\ \vdots & \vdots & \ddots & \vdots \\ \sum_{l=0}^{H_p-1} A^l B & \sum_{l=0}^{H_p-2} A^l B & \dots & B \end{bmatrix}.$$

Then, we select the MPC cost function for agent i as follows:

$$J_i(k) = \|P_x x_i(k) + P_u U_i(k) - r_i(k)\|_Q^2 + \|P_\triangle \Delta U_i(k)\|_R^2 \tag{3.18}$$

where Q and R represent the associated state-weighted matrix and control-weighted matrix with appropriate dimensions, respectively. $r_i(k)$ denotes the reference state for agent i over the future H_p prediction steps.

Furthermore, equation (3.18) is described as follows:

$$\begin{aligned} J_i(k) &= (P_x x_i(k) + P_u U_i(k) - r_i(k))^T Q(P_x x_i(k) + P_u U_i(k) - r_i(k)) + (P_\triangle \Delta U_i(k))^T R(P_\triangle \Delta U_i(k)) \\ &= (P_x^T x_i^T(k) + P_u^T U_i^T(k) - r_i^T(k))(QP_x x_i(k) + QP_u U_i(k) - Qr_i(k)) + (P_\triangle^T \Delta U_i^T(k) R P_\triangle \Delta U_i(k)) \\ &= P_x^T x_i^T(k) Q P_x x_i(k) + P_x^T x_i^T(k) Q P_u U_i(k) - P_x^T x_i^T(k) Q r_i(k) + P_u^T U_i^T(k) Q P_x x_i(k) \\ &\quad + P_u^T U_i^T(k) Q P_u U_i(k) - P_u^T U_i^T(k) Q r_i(k) - r_i^T(k) Q P_x x_i(k) - r_i^T(k) Q P_u U_i(k) + r_i^T(k) Q r_i(k) \\ &\quad + (P_\triangle^T \Delta U_i^T(k) R P_\triangle \Delta U_i(k)) \end{aligned}$$

By letting $\partial J_i(k)/\partial U_i = 0$, one can obtain the optimal control vector

$$\begin{aligned} \partial J_i(k)/\partial U_i(k) &= 0 \\ 0 &= P_u Q P_x x_i(k) + P_u^T Q P_x x_i(k) + P_u^T Q P_u U_i(k) + P_u^T Q^T P_u U_i(k) - P_u^T Q r_i(k) - P_u^T Q^T r_i(k) \\ 0 &= 2[P_u^T Q P_x x_i(k) + P_u^T Q P_u U_i(k) - P_u^T Q r_i(k)] \end{aligned} \tag{3.19}$$

Then, Equation (3.19) yields

$$\begin{aligned} P_u^T Q P_u U_i(k) &= -P_u^T Q P_x x_i(k) + P_u^T Q r_i(k) \\ U_i(k) &= [P_u^T Q P_u]^{-1}(-P_u^T Q P_x x_i(k) + P_u^T Q r_i(k)) \\ &= [P_u^T Q P_u]^{-1}(-P_u^T Q[P_x x_i(k) - r_i(k)]) \end{aligned}$$

Remark 12 *It should be notified that the proposed cost function* (3.18) *is distributed since the reference state* $\mathbf{r_i(k)}$ *only depends on the neighboring agents of agent* i *at time* k.

After the design of the control protocol, one must guarantee that the consensus problem is solved (i.e. Eq. (3.2)). Equation (3.2) illustrates that a MAS has reached a consensus if for time goes to infinity, the difference in the state between two agents is zero. It is clear the minimization of the cost function (3.18) implies that

$$x_i(k+1) = \frac{1}{|\mathcal{N}_i(k)|+1} \sum_{j \in \mathcal{N}_i(k) \bigcup i} x_j(k) \tag{3.20}$$

In a compact form, Eq. (3.21) is equivalent to

$$x(k+1) = D(k)x(k) \tag{3.21}$$

Due to properties of matrix D, the consensus is achieved.

3.4 Simulation results

The simulation results for all the following subsections (i.e. simple integrator, double integrator) are done using the switching topology. A multi-agent system with $N = 4$ followers labeled by $1-4$ is considered. Figure 3.1 shows the switching communication topology. One can see that it is switched and connected. In the following, $\mathcal{G}(k)$ periodically switches from $\mathcal{G}_1$ to $\mathcal{G}_2$ and then to $\mathcal{G}_3$ every $\delta = 0.1$

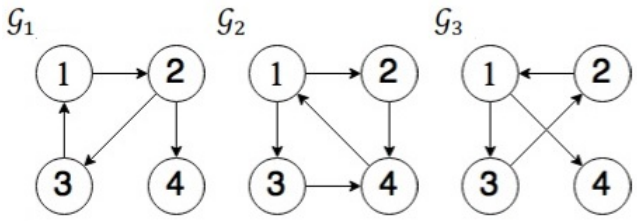

Figure 3.1: Switching communication topologies between agents

seconds. The process then repeats. Note that each graph of the collection $\{\mathcal{G}_1, \mathcal{G}_2, \mathcal{G}_3\}$ has a directed spanning tree.

3.4.1 First-order integrator MAS

Consider a multi-agent system consisting of N agents with discrete-time single-integrator model

$$x_i(k+1) = x_i(k) + Tu_i(k) \tag{3.22}$$

where $T \in \mathbb{R}^+$ is the sampling period, $x_i(k) \in \mathbb{R}^m$ and $u_i(k) \in \mathbb{R}^m$ are the state and the control input to be designed for agent i, respectively.

Let us define the quadratic optimization problem as (3.18) subject to (3.16). It is clear that Assumption 10 is satisfied. The initial states of the agents are given as $x_1(0) = 50$, $x_2(0) = -35$, $x_3(0) = 60$, $x_4(0) = -200$. The parameters are set as $H_u = 2$ and different values of H_p (i.e. $H_p = 3, 6, 9$.

As shown in Figure 3.2, the consensus problem for MAS with dynamics (3.22) is achieve using the control protocol (3.15). We can see that the state of all agents converge to a consensus point. Figure 3.2.a. shows that the state x converges toward the consensus point.

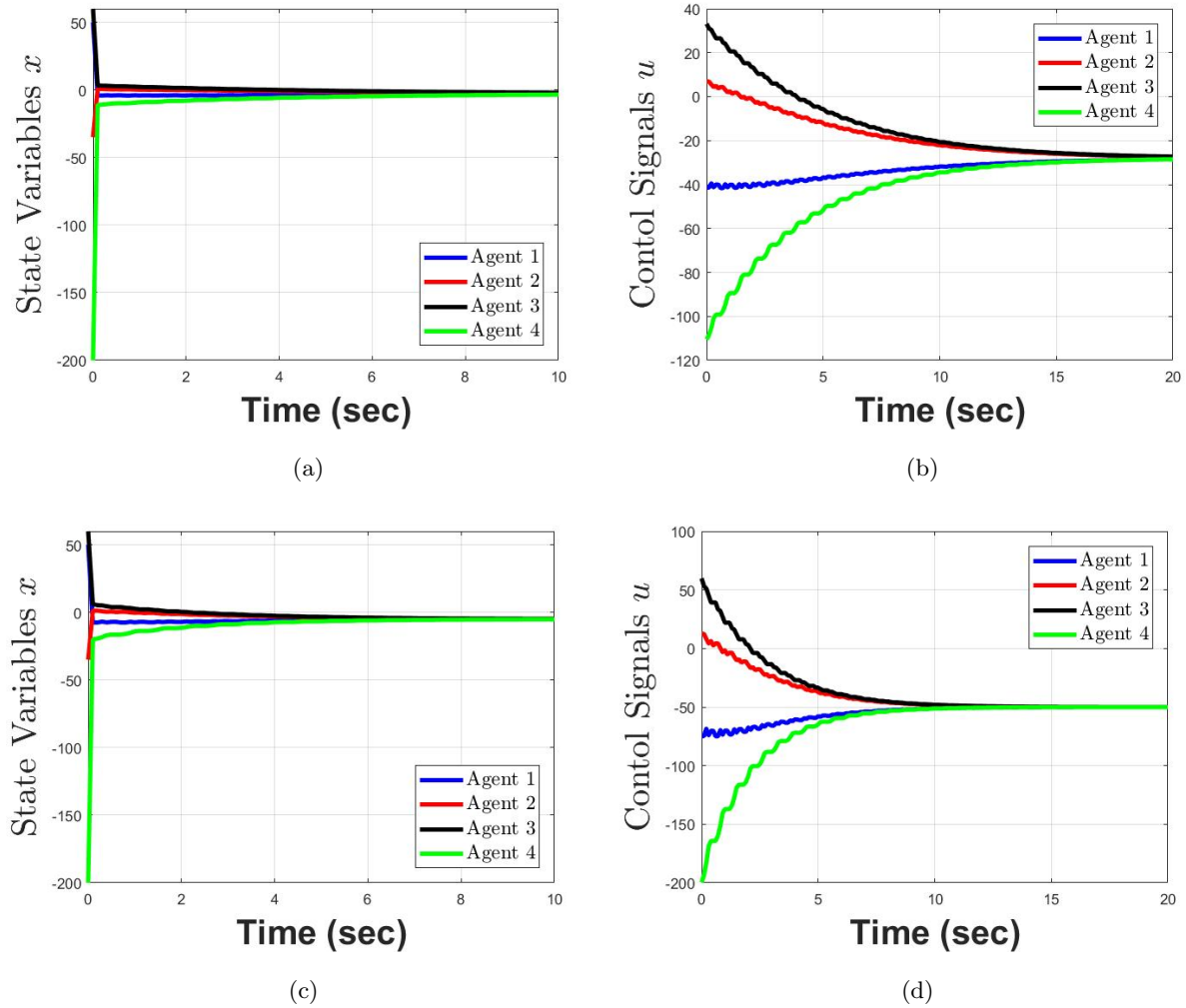

Figure 3.2 illustates the influence of the prediction horizon H_p especially in terms of convergence time. The higher H_p is, the fast convergence rate for to achieve consensus is. When $H_p = 3$, the consensus is achieved at $t = 10s$ and when $H_p = 9$, the consensus point achieved at $t = 6s$

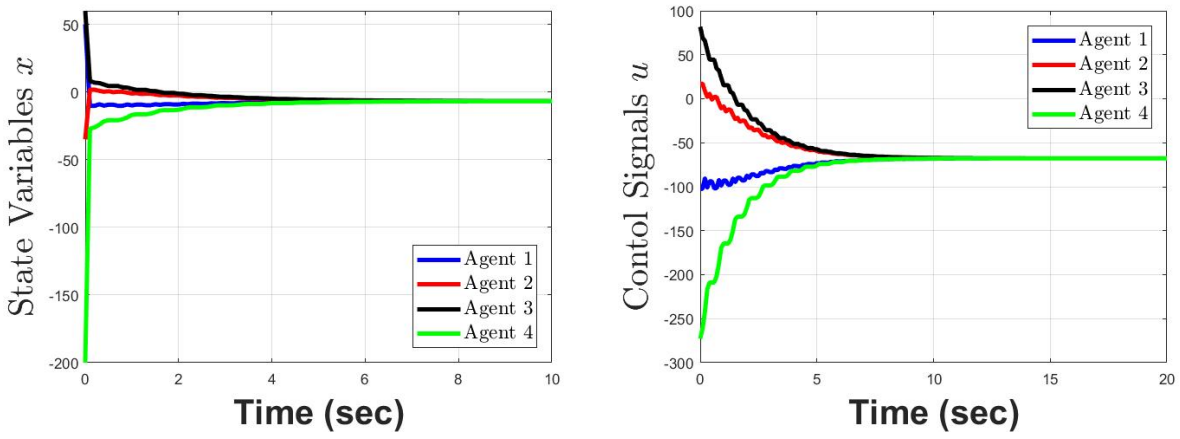

(e) (f)

Figure 3.2: Evolution of agent state x and control input u for a. $H_p = 3$, b. $H_p = 6$ and c. $H_p = 9$

Comparison Results

Hereafter, we give a comparison between the consensus protocol proposed in this chapter and the one proposed in [1] (without the use of difference between input, i.e. Δu_i). Using the same switching topology, let us set the same parameters $H_p = 10$, $H_u = 6$, sampling time $\delta = 0.1s$ and initial state of agents between the two schemes. The comparison between our proposed controller with [1] is shown in the following figures.

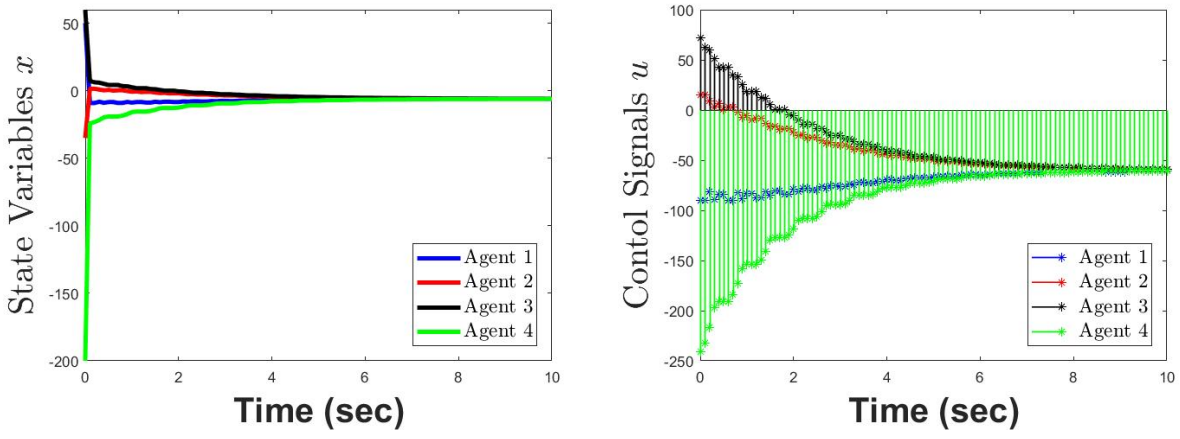

(a) (b)

Figure 3.3: Evolution of agent state x and control input u using our proposed DMPC

As seen in Figures 3.3 and 3.4, we can see the influence of the controller parameters. Our proposed controller is designed using the difference between two consecutive inputs. The controller has integrator properties to eliminate the steady-state errors. In Figure 3.3, the state of all agents converge to a

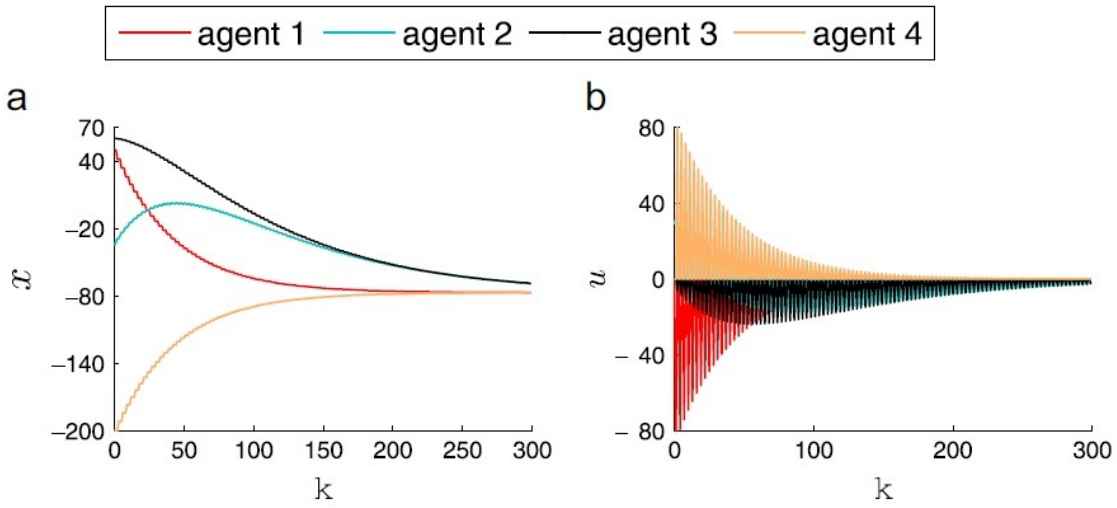

Figure 3.4: Evolution of the agent states x and the control input u using [1]

consensus point less then $t = 10s$ while in Figure 3.4, the state of all agents converge to a consensus point more then $t = 30s$. Hence, our results shows a faster convergence rate.

3.4.2 Second-order integrator MAS

Consider a multi-agent system consisting of N agents with double-integrator model:

$$\begin{aligned} \dot{x}_{1,i}(t) &= x_{2,i}(t) \\ \dot{x}_{2,i}(t) &= u_i(t) \qquad i = 1, 2, ..., N \end{aligned} \tag{3.23}$$

where $x_{1,i}(t) \in \mathbb{R}^n$ and $x_{2,i}(t) \in \mathbb{R}^n$ denote the position and the velocity of the ith agent at time t, respectively. $u_i(t) \in \mathbb{R}^n$ is the corresponding control input. Let us discretize (3.23) using the forward-difference approximation:

$$\begin{aligned} x_{1,i}(k+1) &= x_{1,i}(k) + Tx_{2,i}(k) \\ x_{2,i}(k+1) &= x_{2,i}(k) + Tu_i(k) \end{aligned} \tag{3.24}$$

where T indicates the sampling period and k indicates the discrete-time index. $x_{1,i}(k) \in \mathbb{R}^n$, $x_{2,i}(k) \in \mathbb{R}^n$ and $u_i(k) \in \mathbb{R}^n$ denote, respectively, the position, velocity and the control input of agent i at $t = kT$. Following (3.2), the consensus is reached if

$$\begin{aligned} &\lim_{k\to\infty} \|x_{1,i}(k) - x_{1,j}(k)\| = 0 \\ &\lim_{k\to\infty} \|x_{2,i}(k) - x_{2,j}(k)\| = 0 \qquad \forall i, j \in \mathcal{V}, i \neq j \end{aligned} \tag{3.25}$$

In a compact form, Eq. (3.24) can be written as, $\forall i = 1, \ldots, 4$,

$$p_i(k+1) = \begin{pmatrix} 1 & 0.1 \\ 0 & 1 \end{pmatrix} p_i(k) + \begin{pmatrix} 0.005 \\ 0.1 \end{pmatrix} u_i(k) \tag{3.26}$$

The control parameter are selected as $H_p = 3$, $H_p = 6$, $H_p = 9$ and $H_u = 2$. The initial states of each agent are given by: $x_1(0) = \begin{bmatrix} 10 \\ 0 \end{bmatrix}$, $x_2(0) = \begin{bmatrix} 0 \\ 0 \end{bmatrix}$, $x_3(0) = \begin{bmatrix} -2 \\ 0 \end{bmatrix}$, $x_4(0) = \begin{bmatrix} 6 \\ 0 \end{bmatrix}$

The consensus problem described in Equation 3.25 is achieved using the proposed distributed model predictive control. We can see that the state of all agents converge to a consensus point. Figure 3.5.a (resp Figure 3.5.b) shows the state $x_{1,i}$ (resp. the state $x_{2,i}$) . it can be seen that the consensus is achieved with a convergence time which depends on the value of the prediction horizon H_p. When $H_p = 3$, the consensus point of agent position $x_{1,i}$ is achieved at $t = 40s$. When $H_p = 6$ and $H_p = 9$, the consensus point is achieved at $t = 25s$ and $t = 15s$. The consensus point for agent velocity $x_{2,i}$, with $H_p = 3$, $H_p = 6$, $H_p = 9$ is $t = 40s$, $t = 25s$ and $t = 20s$.

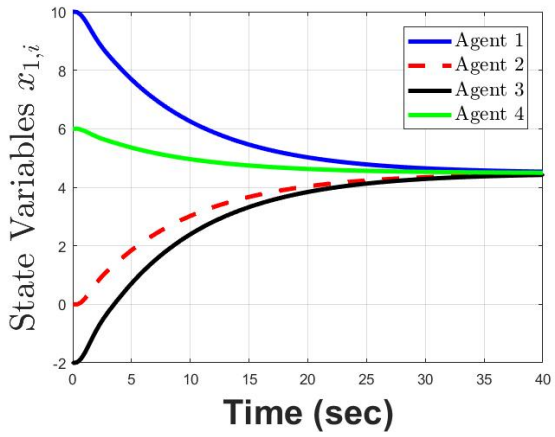

(a)

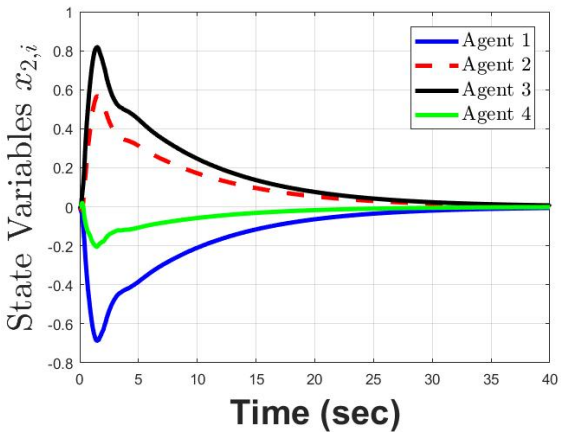

(b)

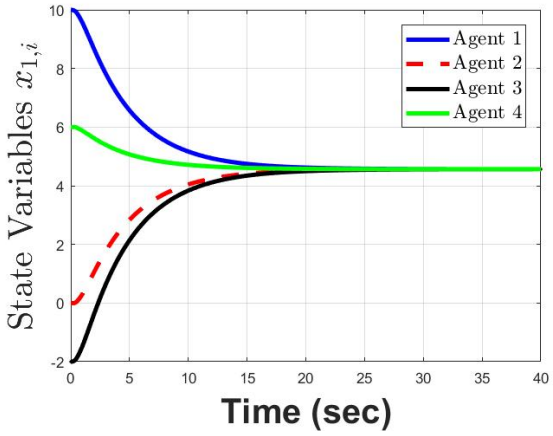

(c)

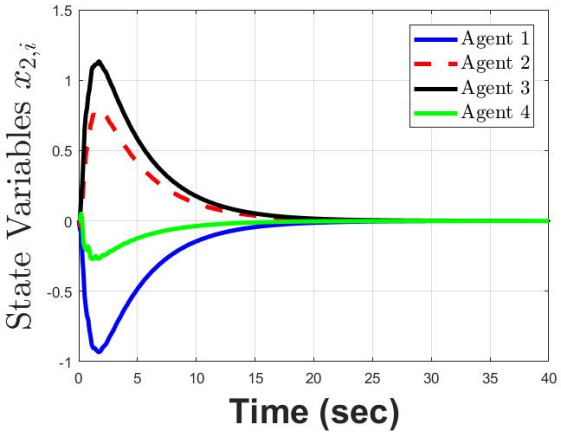

(d)

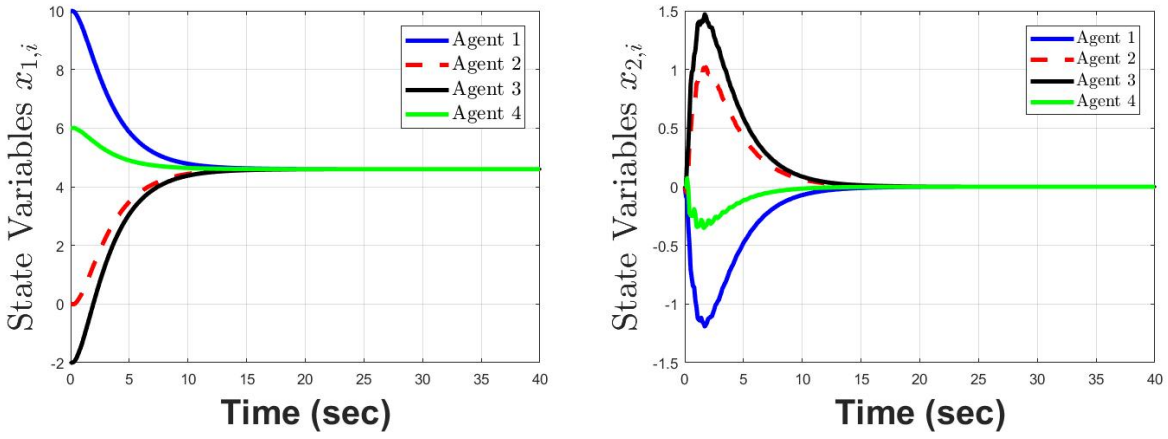

(e) (f)

Figure 3.5: Evolution of agent state $x_{1,i}$ and $x_{2,i}$ with a.$H_p = 3$, b.$H_p = 6$, c.$H_p = 9$

The corresponding control input is given in Figure 3.6.

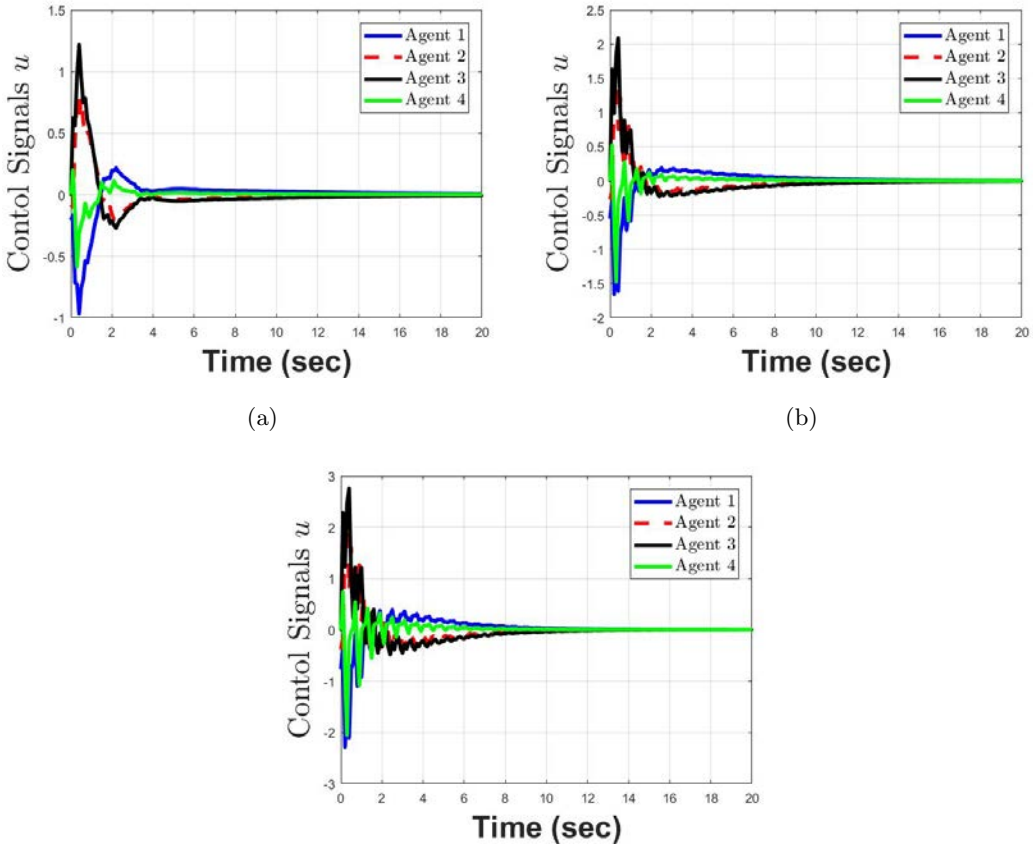

(a) (b)

(c)

Figure 3.6: Evolution of the control input u_i

3.5 Conclusion

In this chapter, a model predictive control protocol is developed for consensus of MASs with discrete-time linear dynamics under time-varying directed interaction topologies. The control protocol is distributed and is designed by combining graph theory with a predictive control algorithm to take into account the switches on the communication topology. The cost function is design using the difference between two consecutive inputs. The controller has integrator properties to reduce the steady-state errors. The convergence time of consensus depends on the prediction horizon parameter. Some simulation results have been given to show the effectiveness of the proposed controller.

Chapter 4

Experimental Setup

4.1 Introduction

For the reader convenience, this chapter briefly introduces the experimental platform Minilab Robot, available at the Department of Automation and Control, LAMIH (Laboratory of Industrial and Human Automation Control, Mechanical Engineering and Computer Science), Université Polytechnique Hauts-de-France. The platform was used to test and validate the effectiveness of the theoretical results given in the previous chapters. Figure 4.1 shows the architecture of the experimental platform. In this process, control algorithms are programmed using ROS (Robotic Operating System) with Gazebo-ROS as a reality virtual simulation.

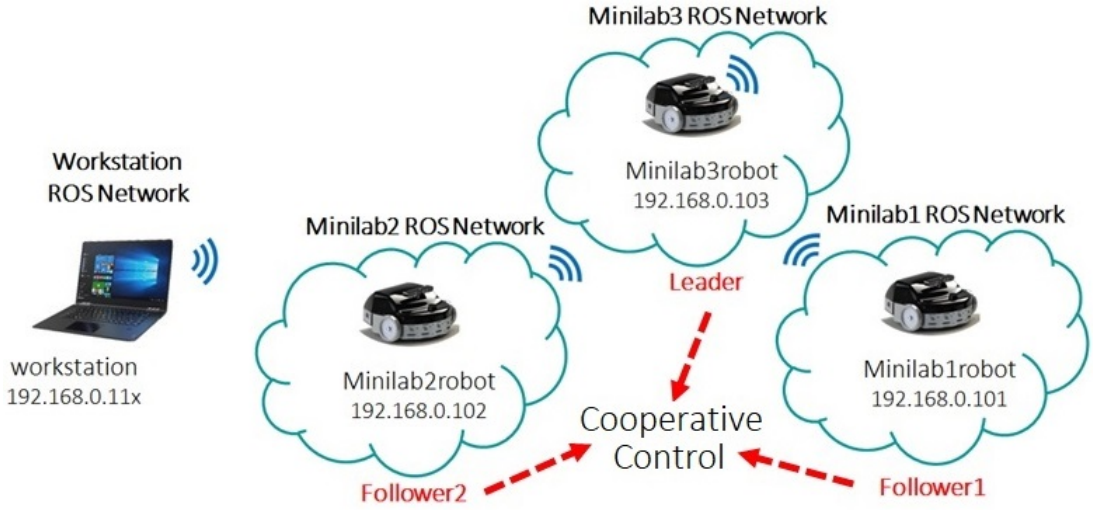

Figure 4.1: Multiple Minilab robots with wireless communication architecture.

Experiments were performed on a group of three mobile robots supplied by Enova Robotics to verify the feasibility and effectiveness of the proposed consensus control strategies. The three robots consist of one robot which was designated as the leader, and two robots were designated as the

followers. Figure 4.2 illustrates the experiments which were carried out in an indoor environment.

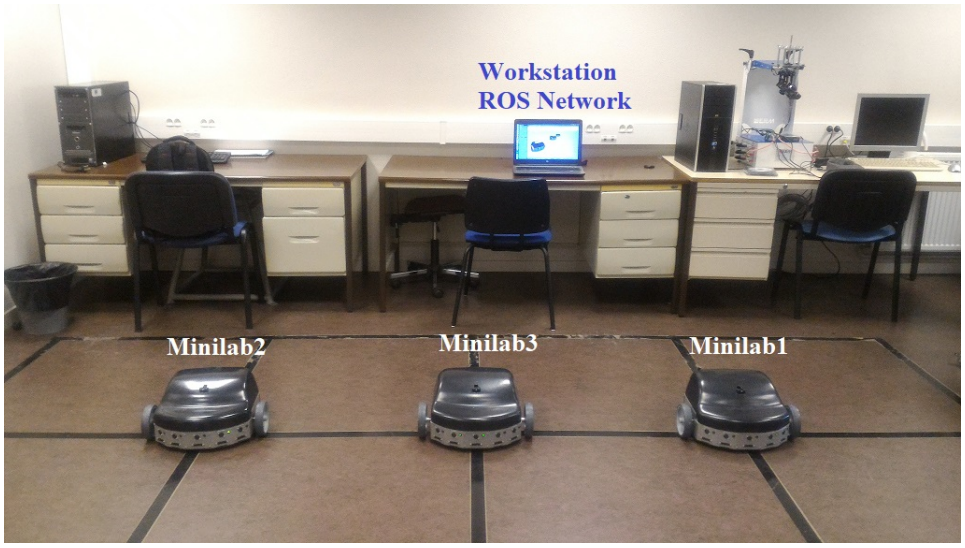

Figure 4.2: Illustration of the experimental setup.

Generally, in ROS environment, we can control one robot by one or several machines/ workstations. Except in the case of using Gazebo simulator, we can perform simulation for several robots by only one workstation. Instead of using multiple machines/ workstation, in this chapter we demonstrate the idea of gazebo simulator into real robots to reduce cost and utilisation of several workstations. Since we are working on consensus problem for multi-agent systems and we are using only one workstation, we need to appropriately select the wifi configuration and design multiple master ROS in a decentralized architecture for multiple robots. Furthermore, since there are some difficulties to create the leader-follower topology in this ROS multi-agent system network, we have to propose an algorithm to solve this problem.

The remainder of this chapter is organized as follows. Section 4.2 describes the Minilab Enova robot platform. Section 4.3 introduces the robotic operating system (ROS). In Section 4.4, reality virtual simulation using Gazebo-ROS examples are provided. MiniLab robots as platform for cooperative control of multi-agent systems are given in Section 4.5. Section 4.6 concludes this chapter.

4.2 Minilab Enova Robot

The Minilab robot, as shown in Figure 4.3, is a medium-sized two wheels mobile robot designed by Enova Robotics. The left and right wheels, are controlled independently using two DC motors to design the linear and angular speed such that robot can move in its environment. The robot can navigate autonomously or be teleoperated using its camera, which transmits video in real time. Each MiniLab robot is equipped with an intel X86 main board, an hard drive and also a wide variety of parts and sensors that are useful for navigation tasks, such as 5 ultrasonic sensors, 5 infra-red (IR) distance

sensors which provide the distance from obstacles to the robot, orbbec depth camera, encoders with a resolution of 16 bits, LED indicators, buttons and arduino microcontroller.

Figure 4.3: Minilab Enova Robot.

MiniLab is optimized for indoor applications, with dimensions of 0.409m x 0.364m x 0.231m in width x length x height and weight 11.5kg. It also has a load capacity of 3kg. Figure 4.4 shows the dimensions of Minilab robot.

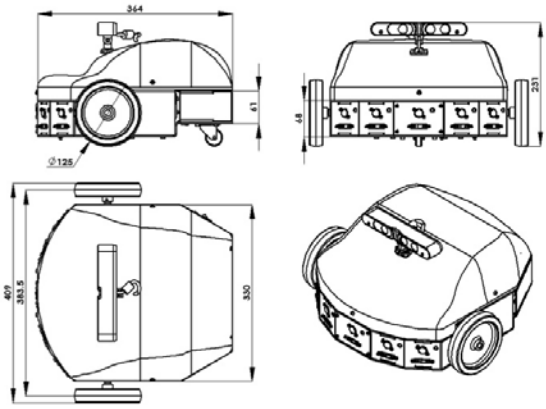

Figure 4.4: Minilab physical dimensions.

The control architecture of the Minilab robot is an open-source based on the Robot Operating System (ROS). ROS is a flexible framework for writing robotic software. It includes several contributed libraries and packages as localization, mapping, planning, perception, etc. Figure 4.5 shows the hardware features of Minilab robot.
Table 4.1 illustrates some hardware configurations of the Minilab. Some hardware descriptions of the Minilab Enova robot will be explained in the following subsection.

4.2.1 MiTAC Board Intel X86

The processing on the Minilab is performed by an Intel X86. Intel Atom is the brand name for a line of ultra-low-voltage x86-64 microprocessors by Intel Corporation. Atom is mainly used in netbooks, nettops, embedded applications ranging from health care to advanced robotics, and mobile Internet devices (MIDs). The line was originally designed in 45 nm complementary metal–oxide–semiconductor (CMOS) technology and subsequent models, codenamed Cedar, used a 32 nm process. Figure 4.6

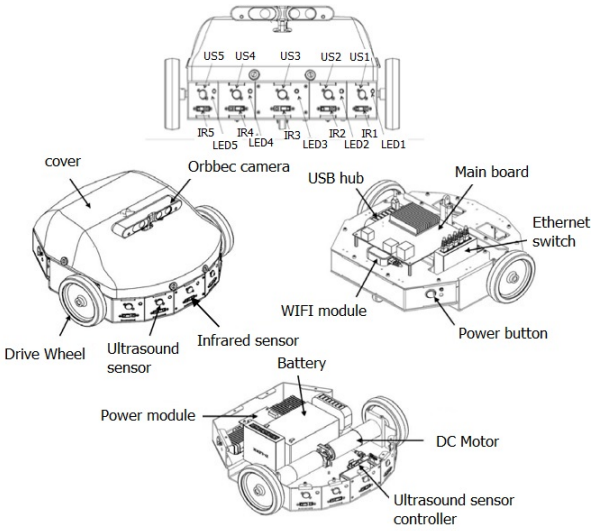

Figure 4.5: Minilab hardware features.

Table 4.1: Parts of the Minilab components

Component	Description
Main board	Intel X86
Wifi module	TL-WR802N 300Mbps Wireless N Nano Router
USB HUB	D-Link DGS-105 Gigabit Ethernet Switches
Motors	Max speed of the robot is 1.5m/s
Wheels controller	Roboteq SDC2130 Controller
Encoders	16 bits resolution
Sensor board	Arduino Micro Board
Infrared array	5 SHARP 2Y0A21 F 46 sensors, range from 10 cm to 80 cm
Ultrasound	5 MaxSonar-EZ0 sensors, range from 0 m to 6.45 m, resolution 2.54 cm
ORBBEC depth camera	ORBBEC Asrtra pro camera
Batteries	12 Volts/ 10 Ampere-hour, sealed lead/acid battery

depicts the processor board of Intel Atom N2800 1.86GHz Dual-Core 4Gb DDR3-1066MHz Mini ITX Motherboard.

4.2.2 TL-WR802N 300Mbps Wireless N Nano Router

Each robot equipped with one TL-WR802N wireless router as shown in Figure 4.7 to connect the Minilab to the network. It allows to design a communication network for multiple robots. This device performs the functions of a router and also includes functions of wireless access point. It is used to

Figure 4.6: Intel Atom N2800.

provide access to Internet or a private computer network. This router has 300Mbps wireless data rate with several operation modes such as router, repeater, client, access point and hotspot. Powered through a micro USB port by an external power adapter or USB connection to a computer it provides flexibility for any situation.

Figure 4.7: TL-WR802N Wireless routers.

4.2.3 D-Link USB HUB

The DUB-H7 as shown in Figure 4.8 is fully compliant to USB 2.0 specifications with data transfer rates of up to 480 Mbps. It is an ideal solution for transferring data between intel x86 and USB devices (Orbbec Camera and Roboteq controller). The DUB-H7 features 7 USB fast charging ports which are designed to feed high currents up to 2.4A when the DUB-H7 is powered by the included power adapter in fast charging mode or of up to 1.5A via battery charging. Power input for this USB hub is 5 V / 3A DC.

4.2.4 DC Motor

The maximum speed of the robot is 1.5 m/s in both forward and backward movement but for safety reason maximum allowed speed is 0.8 m/s. The maximum slope angle is 10^o. Each wheel has a driving DC motor mounted on his axis. The wheels have been chosen to provide more accurate odometry

Figure 4.8: DUB-H7 7-Port USB 2.0 HUB.

localization. The DC motor, shown in Figure 4.9, is brushed moter with permanent magnet. Input voltage for the motor is 12 V and torque 0.07 Nm. Rotational speed of motor is 3,000 rpm.

Figure 4.9: Buhler Motor DC.

4.2.5 Roboteq Controller

Fitting into a very compact 73x73mm enclosure, Roboteq's SDC2130 controller is designed to convert commands received from an RC radio, Analog Joystick, wireless modem, PC (via RS232 or USB) or microcomputer into high voltage and high current output for driving one or two DC motors. A CAN bus interface allows up to 127 controllers to communicate at up to 1Mbit/s on a single twisted pair. Figure 4.10 illustrates the Roboteq controller.

Figure 4.10: Roboteq SDC2130 controller.

The controller features a high-performance 32-bit microcomputer and quadrature encoder inputs to perform advanced motion control algorithms in open loop or closed loop (speed or position). The SDC21xx features several analog, pulse and digital I/Os which can be remapped as command or feedback inputs, limit switches, or many other functions. For mobile robotic applications, the controller two motor channels can either be operated independently or mixed to set the direction and rotation of a vehicle by coordinating the motion of each motor.

4.2.6 Arduino Micro Board

The Arduino Micro board, illustrated in Figure 4.11, is a microcontroller board based on the ATmega32u4, developed in conjunction with Adafruit. It has 20 digital input/output pins (of which 7 can be used as PWM outputs and 12 as analog inputs), a 16 MHz crystal oscillator, a micro USB connection, an ICSP header, and a reset button. It contains everything needed to support the microcontroller. Micro USB cable is used to connect Arduino board with computer. It has a form factor that enables it to be easily placed on a breadboard.

The Micro has built-in USB communication, eliminating the need for a secondary processor. This allows the Micro to appear to a connected computer as a mouse and keyboard, in addition to a virtual (CDC) serial / COM port. It also has other implications for the behavior of the board.

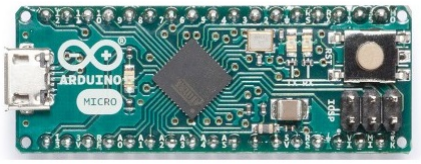

Figure 4.11: Arduino Micro Board.

4.2.7 Infrared SHARP 2Y0A21

Infrared SHARP as shown in Figure 4.12 is a distance measuring sensor unit, composed of an integrated combination of PSD (position densitive detector), IRED (infrared emitting diode) and signal processing circuit. This device outputs the voltage corresponding to the detection distance between 10 to 80 cm. So this sensor can also be used as a proximity sensor.

Figure 4.12: Infrared sensor SHARP.

4.2.8 Orbbec Astra Pro Camera

Orbbec Astra Pro is optimized for applications that require high RGB stream quality. Astra Pro is world first 3D sensor that can stream 30 FPS HD RGB stream and VGA depth at the same time through USB 2.0. Astra Pro now comes in a bundle with the powerful gestural Interaction SDK by Gestoos. Gestoos interact using C++, Java and Processing to develop and enhance applications. Figure 4.13 illustrates the camera.

Figure 4.13: Orbbec Astra Pro Camera.

4.2.9 Power-Sonic Battery

The Minilab use 12V rechargeable batteries for all its system, as shown in Figure 4.14, with 4 hours of autonomy. Power-Sonic battery are lead-lead dioxide systems. The dilute sulphuric acid electrolyte is suspended and thus immobilised. Otherwise, the battery is completely sealed and is, therefore, maintenance-free and leak proof.

Figure 4.14: Power-Sonic Battery

4.3 Robotic Operating System

Robot Operating System (ROS) is an open-source platform, meta-operating system that is widely used in robotics. The philosophy is to make a piece of software that could work in other robots by making little changes in the code. What we get with this idea is to create functionalities that can be shared and used in other robots without much effort so that we do not reinvent the wheel. It provides libraries and tools to help software developers create robot applications. Primary goal of ROS is to support code reuse in robotics research and development. ROS framework is easy to implement in any modern programming language such as Python, C++, and Lisp (experimental libraries in Java and Lua).

ROS was originally developed in 2007 by the Stanford Artificial Intelligence Laboratory (SAIL) with the support of the Stanford AI Robot project. As of 2008, development continues primarily at Willow Garage, a robotics research institute, with more than 20 institutions collaborating within a federated development model. A lot of research institutions have started to develop projects in ROS by adding hardware and sharing their code samples. Also, the companies have started to adapt their

products to be used in ROS.

The sensors and actuators used in robotics have also been adapted to be used with ROS. Every day an increasing number of devices are supported by this framework. ROS provides standard operating system facilities such as hardware abstraction, low-level device control, implementation of commonly used functionalities, message passing between processes, and package management. It is based on graph architecture with a centralized topology where processing takes place in nodes that may receive or post, such as multiplex sensor, control, state, planning, actuator, and so on. ROS currently only runs on Unix-based platforms. Software for ROS is primarily tested on Ubuntu and Mac OS X systems. While a port to Microsoft Windows for ROS is possible, it has not yet been fully explored.

The ROS architecture has been designed and divided into three sections or levels of concepts:

- File system level
- Computation Graph level
- Community level

More detailed for ROS architecture explanations will be given in the following subsection.

4.3.1 ROS File System Level

The first level is the **Filesystem level**. In this level, a group of concepts are used to explain how ROS is internally formed, the folder structure, and the minimum number of files that it needs to work. Figure 4.15 illustrated level in ROS Filesystem.

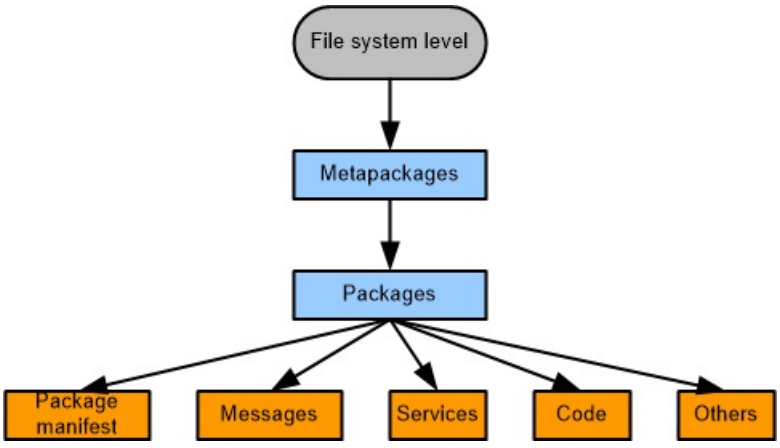

Figure 4.15: ROS File System Level.

Package

Packages are the software organization unit of ROS code. Each package can contain ROS runtime processes (nodes), a ROS-dependent library, datasets, configuration files, or anything else that is usefully organized together. ROS uses packages to organize its programs. A package can be describe as all the files that a specific ROS program contains; all its cpp files, python files, configuration files, compilation files, launch files, and parameters files.

Catkin is the official build system of ROS and the successor to the original ROS build system, rosbuild. Catkin combines CMake macros and Python scripts to provide some functionality on top of CMake's normal workflow. Catkin was designed to be more conventional than rosbuild, allowing for better distribution of packages, better cross-compiling support, and better portability. Catkin's workflow is very similar to CMake's but adds support for automatic 'find package' infrastructure and building multiple, dependent projects at the same time.

All those files in the package are organized with the following structure:

launch folder	Contain launch files
src folder	Source files (cpp, phyton)
CMakelist.txt file	List of cmake rules for compilation
package.xml file	Package information and dependencies

Meta-Package

This is a collection of packages forming a higher level library (previously called stacks). The concept of stacks was removed with catkin command to simplify the growing code base and to support better distribution of packages.

Manifests

Manifests (manifest.xml) provide metadata about a package, including its license information and dependencies, as well as language-specific information such as compiler flags.

Stacks

Stacks are collections of packages that provide aggregate functionality, such as a "navigation stack". Stacks are also how ROS software is released and have associated version numbers.

Stack Manifests

Stack manifests (stack.xml) provide data about a stack, including its license information and its dependencies on other stacks.

Message (msg) types

Message descriptions are stored in a package msg MyMessageType.msg. It defines the data structures for messages sent in ROS.

Service (srv) types

Service descriptions are stored in a package srv MyServiceType.srv. It defines the request and response data structures for services in ROS.

4.3.2 ROS Computation Graph Level

The second level is the **Computation Graph level** where communication between processes and systems happens. In this subsection, we will see all the concepts and mechanisms that ROS has to set up systems, handle all the processes, and communicate with more than a single computer, and so on.

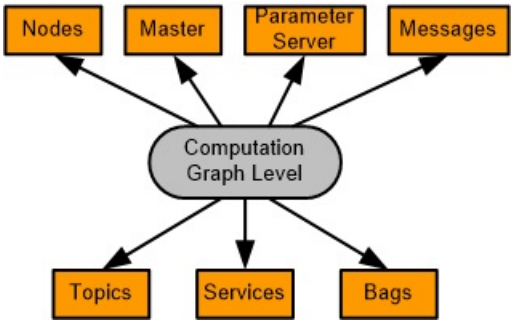

Figure 4.16: ROS Computation Graph Level.

Figure 4.16 show contents of computation graph level. The illustration on how computation graph work can be shown in Figure 4.17. More detail information about computation graph will be given in the following explanations.

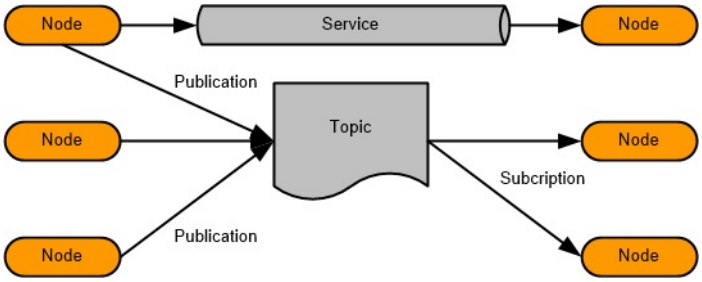

Figure 4.17: ROS Computation Graph Level.

Node

A node is a participant in the ROS graph. ROS nodes use a ROS client library to communicate with other nodes. Nodes can publish or subscribe to a topic using typed messages. Nodes can also provide or use a Service. Services means request / response paradigm (think of method or operation) via typed messages. There are configurable parameters associated with a node. Connections between nodes are established through a distributed discovery process. Nodes may be located in the same process, in different processes, or in different machines. Nodes are processes which perform specific computations, for example: control robot wheel motors, acquire data from laser scanner, acquire images from camera, perform localisation, perform path planning, provide graphical visualisation of the system

Master

The ROS Master provides name registration and lookup to the rest of the Computation Graph. Without the Master, nodes would not be able to find each other, exchange messages, or invoke services. Master is the core node of ROS, called roscore. Roscore is a collection of nodes and programs that are pre-requisites of a ROS-based system. We must have a roscore running in order for ROS nodes to communicate. It is launched using the roscore command in the terminal.

Messages

Nodes communicate with each other by passing messages. A message is simply a data structure, comprising typed fields. Standard primitive types (integer, floating point, boolean, etc.) are supported, and arrays of primitive types. Messages can include arbitrarily nested structures and arrays (much like C structs).

Topic

Messages are routed via a transport system with publish / subscribe semantics. A node sends out a message by publishing it to a given topic. The topic is a name that is used to identify the content of the message. A node that is interested in a certain kind of data will subscribe to the appropriate topic. There may be multiple concurrent publishers and subscribers for a single topic, and a single node may publish and/or subscribe to multiple topics. In general, publishers and subscribers are not aware of each others' existence. The idea is to decouple the production of information from its consumption. Logically, one can think of a topic as a strongly typed message bus. Each bus has a name, and anyone can connect to the bus to send or receive messages as long as they are the right type.

Services

The publish / subscribe model is a very flexible communication paradigm, but its many-to-many, one-way transport is not appropriate for request / reply interactions, which are often required in a distributed system. Request / reply is done via services, which are defined by a pair of message structures: one for the request and one for the reply. A providing node offers a service under a name and a client uses the service by sending the request message and awaiting the reply. ROS client libraries generally present this interaction to the programmer as if it were a remote procedure call.

Bags

Bags are a format for saving and playing back ROS message data. Bags are an important mechanism for storing data, such as sensor data, that can be difficult to collect but is necessary for developing and testing algorithms.

Computation graph example

Figure 4.18 illustrates all explanation for a simple computation graph level. Wheel odometer node sends out a message of x, y, z robot position by publishing it to /odom topic. The topic type is defined by the message type publishing on it. Path planner subscribe /odom topic to receive messages as well as publish messages of linear velocity x, y and angular velocity z to a /cmd_vel topic. Then motor controller subscribe /cmd_vel topic to make motor movement.

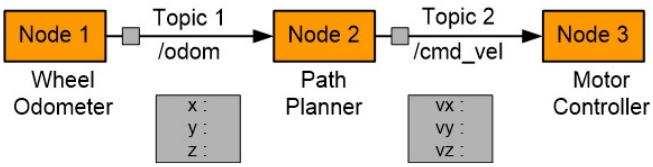

Figure 4.18: Computation graph for control wheel motor.

To verify computation graph, we can use rqt_graph. rqt_graph which provides a GUI plugin for visualizing the ROS computation graph. rqt_graph shows the ROS nodes that are currently running, as well as the ROS topics that connect them. Its components are made generic so that other packages can depend upon this package. Figure 4.19 shows rqt_graph for control wheel motor of minilab3 robot in the real platform.

Figure 4.19 shows that by using rqt_graph, we can perform diagnostic and localize where the problem occurred. It depicts a chained topic from one node to another. By determining any broken chain in the graph, we could detect and locate any occurred problem.

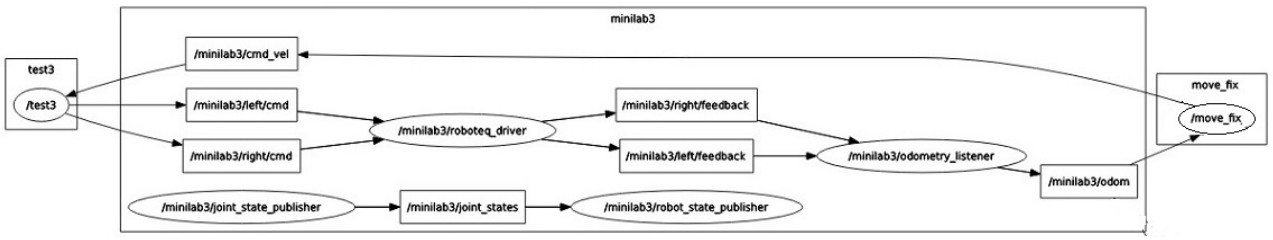

Figure 4.19: rqt_graph for control wheel motors.

4.3.3 Community level

The third level is the **Community level**, which comprises a set of tools and concepts to share knowledge, algorithms, and code between developers. This level is of great importance. As with most open source software projects, having a strong community not only improves the ability of newcomers to understand the intricacies of the software as well as solve the most common issues, it is also the main force driving its growth.

4.3.4 ROS General Communication

In general, Minilab robot has its own ROS network (either wired, wireless or a combination of both), where a single roscore manages all the communications between all the ROS nodes, either in a single computer or multiple computers in the same network (depending on the complexity and computational needs of the system). Figure 4.20 shows a generic hardware setup/ configuration as explained above.

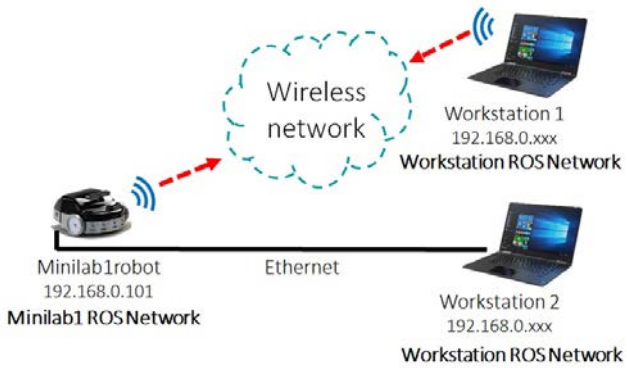

Figure 4.20: MiniLab robot setup for a single ROS system.

Communication among the mobile robots plays an important role in the successful coordination of a multi-agent system. Minilab provides the ad-hoc peer-to-peer wireless TCP/IP protocol for multi-vehicle information interactions. Each robots is configured with a predefined unique IP address. When the power of the Minilab is turned on, the Host PC can detect a network called ML201704001-3

(robot1, 2, 3), as shown in Figure 4.21(a) for Minilab1. The IP address of the Host PC is set as shown in Figure 4.21(b).

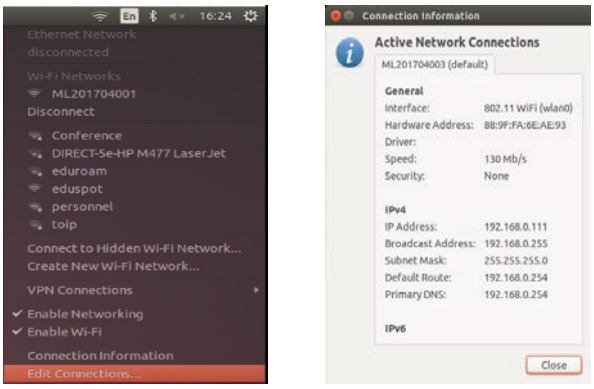

(a) (b)

Figure 4.21: Wireless network setup on the host PC.

The connection between robots and the host PC can be checked by the command address of the Minilab in the terminal run box. Figure 4.22 shows an example of successful connection.

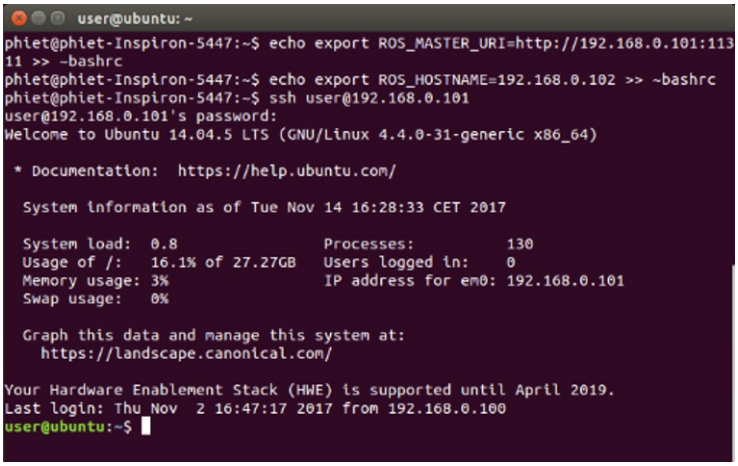

Figure 4.22: Communication checking results.

To download the compiled file into the Minilab, IP addresses of the targets are specified as linux-verdex targets and the default model URI is replaced by the IP address of the target vehicles, i.e., tcpip://182.168.0.101 for Minilab1.

4.4 Gazebo-ROS Simulation

Gazebo-ROS is a robot simulator that allows to accurately design, simulate and test robots in various environments. It uses the URDF file format, which is an XML format used to describe objects and

environments in robot simulators and was originally developed specifically for Gazebo. Below we quickly go through some of the XML tags that are important to understand and show what kind of environments we use.

With Gazebo we are able to create a 3D scenario on our computer with robots, obstacles and many other objects. Gazebo also uses a physical engine for illumination, gravity, inertia, etc. We can evaluate and test our robot in difficult or dangerous scenarios without any harm to our robot. Most of the time it is faster to run a simulator instead of starting the whole scenario on our real robot.

Originally Gazebo was designed to evaluate algorithms for robots. For many applications it is essential to do some tests, like error handling, battery life, localization, navigation and grasping. Gazebo was developed and improved as well as significant requirement on multi-robot simulation.

Gazebo provides a set of ROS APIs that allows users to modify and get information about various aspects of the simulated world. The complete list of ROS messages and services for gazebo can be found here also.

The simulation world and minilab objects can be created for only one robot and multiple ones. Figure 4.23(a) shows visualisation of Gazebo-ROS simulation for one minilab robot and Figure 4.3 (b) shows visualisation of Gazebo-ROS simulation for multiple-minilab robots.

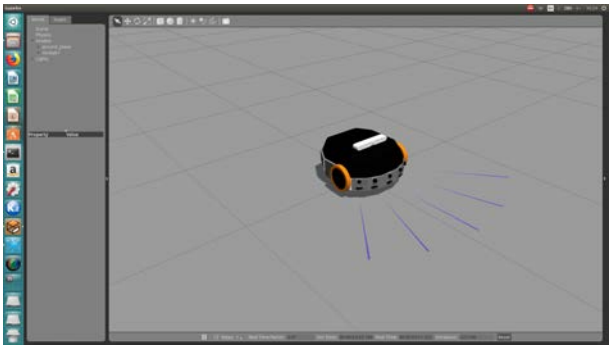

(a)

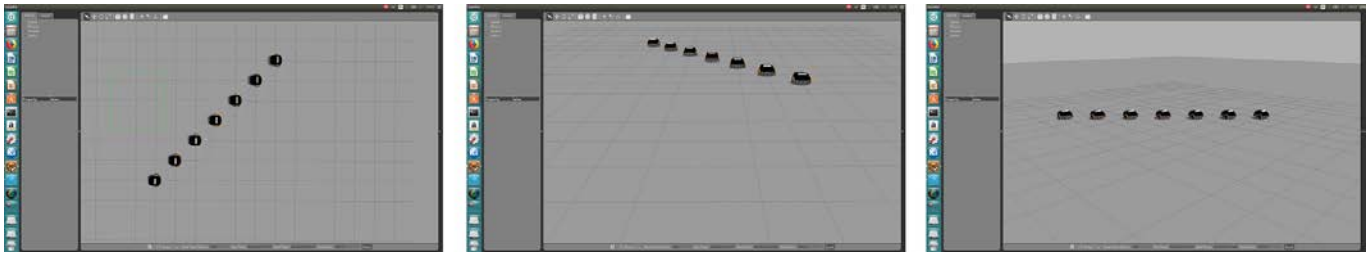

(b)

Figure 4.23: Gazebo-ROS simulation for minilab robot.

We verify the computation graph for Gazebo-ROS using rqt_graph. Figure 4.24 shows the rqt_graph for controlling minilab3 robot in the Gazebo-ROS simulation. From Figure 4.24, we can verify that all nodes are connected in the network as required. For example, this figure shows that node minilab3

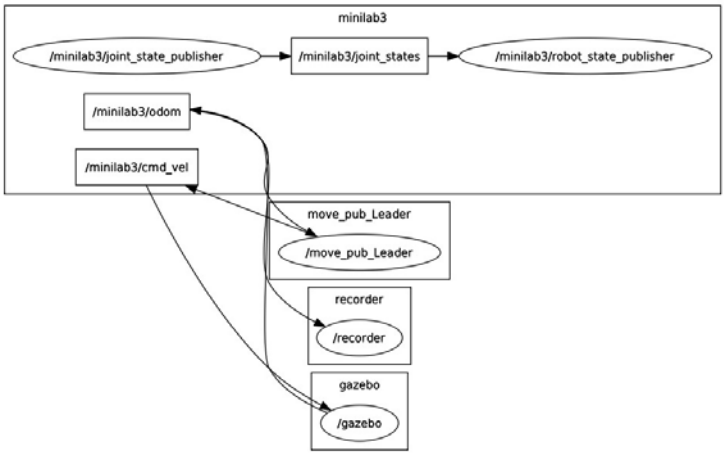

Figure 4.24: rqt_graph for minilab in Gazebo-ROS

with topic odom and cmd_vel are connected and provide data to node recorder. Node controller move_pub_Leader and node gazebo are connected and in two way communication to node minilab3. On the other hand, if there is any broken chained link, using this graph, we can detect and locate the problem.

4.5 MiniLab as Platform for Cooperative Control of Multi-Agent Systems

In this section, we will present the procedure for the implementation of the wireless configuration among robots described in Figure 4.25 and the decentralized communication architecture described in Figure 4.29. First, we need to configure address reservation and verify the reservation from the PC workstation. To have a proper configuration of the network, we need to modify the */etc/hosts* file for each robot and PC. Afterward we can start `multimaster_fkie` package for our topology. Then, we can implement our cooperative control protocol on this ROS network configuration.

4.5.1 Multi-Robots Wireless Configuration

Let we consider Figure 4.25. This is an example of possible hardware configuration for a wireless decentralized communication architecture between multiple robots. Note that in Figure 4.25, the multi-agent system consists of master and two slaves which are connected to the master wireless network and one monitoring workstation which is also connected to the master.

Router Address Reservation

We need to specify a dedicated IP address for all robots and workstation in the ROS Network, such that all robots and workstation will always receive the same IP address each time when it connects

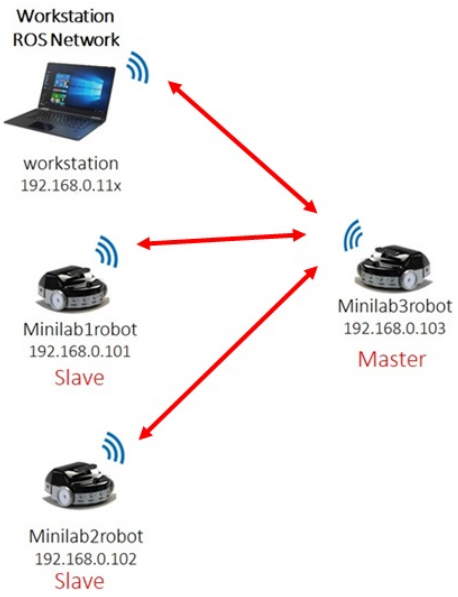

Figure 4.25: Network topology for the illustrative example.

to the DHCP (Dynamic Host Configuration Protocol Server) server. Since each MiniLab Enova robot requires a permanent IP address, we need to configure the address reservation of the router.

First, we open the web browser and in the address bar, we type in: http://192.168.0.254. Then, we type the username and password in the login page. Then, we should click on DHCP−>Address Reservation on the left side and click Add New button. The MAC and IP address should be given and the status should be selected as enabled. This configuration is shown in Figure 4.26.

Note that the MAC address is the MAC address of the device where we want to reserve the IP address. For our case, we need to know the MAC address of each router in the robot and PC workstation. The IP address of the robots are reserved with 192.168.0.2xx and for the workstation 192.168.0.11x

Master-slave wireless configuration

To verify the reservation of the IP address for the PC workstation, we have just to connect to the wifi of the leader. Then, we can check from connection information of the PC workstation as shown in Figure 4.21(b).

Host name and IP address binding

For each robot and workstation, it is necessary to modify the */etc/hosts* file using text editor. Figure 4.27 shows the contents of this file for the workstation for the example presented in Figure 4.25. Figure

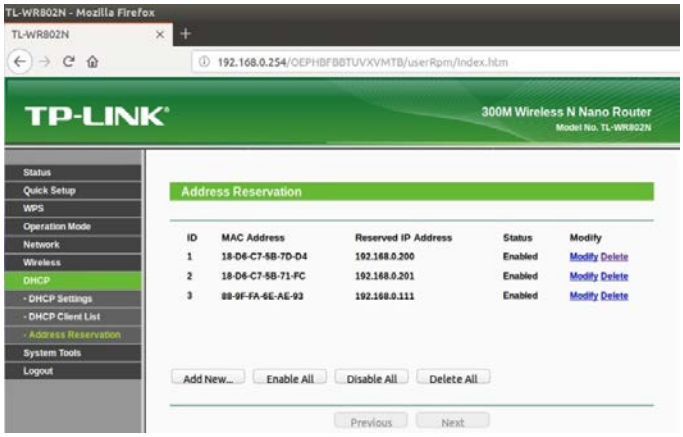

Figure 4.26: TP-Link address reservation.

4.28 shows the contents of this file for each robot for the example presented in Figure 4.1.

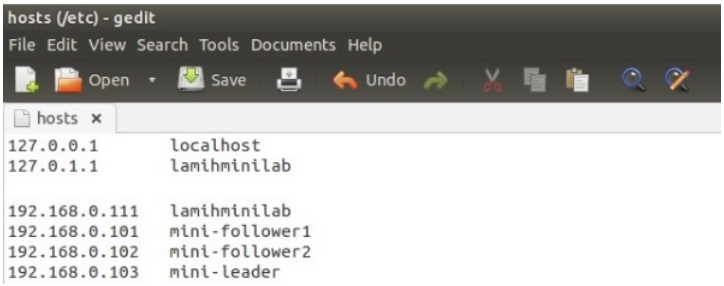

Figure 4.27: Contents of the */etc/hosts* file for the workstation for the example presented in Fig. 4.1.

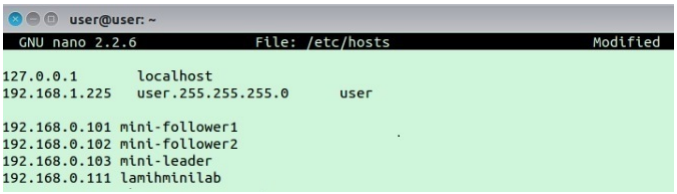

Figure 4.28: Contents of the /etc/hosts file for each robot for the example presented in Fig. 4.1.

To verify the appropriate configuration of the network, before launching any ROS nodes, it is interesting to ping all other robots from the workstation, using both the host name and the IP address. If all the pings return a reply, the network has been properly configured. Using the current console, the following command should be executed, where hostname or IP address must be the IP address or host name of each robot and the workstation.:

`$export ROS_MASTER_URI=http://<host_ip>:11311`

`$ROS_MASTER_URI` command is required to inform the nodes where they able to locate the master.

For all robots and the workstation, we have to verify if the multicast feature (group communication) is temporary enabled using the following command:

```
$sudo sh -c "echo 0 /proc/sys/net/ipv4/icmp_echo_ignore_broadcasts"
```

If this command returns 0, the multicast feature is enabled. However, when all robots and workstation restart, this configuration will be lost. Now, the ROS wireless network for multiple robots has been configured. The next step is to discover and synchronize each robot and the workstation to obtain a decentralized communication architecture.

4.5.2 Decentralized communication architecture

In multi-agent systems, multiple robots need to exchange information. Using ROS, there is two possible solutions which can create a single large ROS network managed by a single roscore node or create a configuration to allow information to be exchanged between ROS sub-systems.

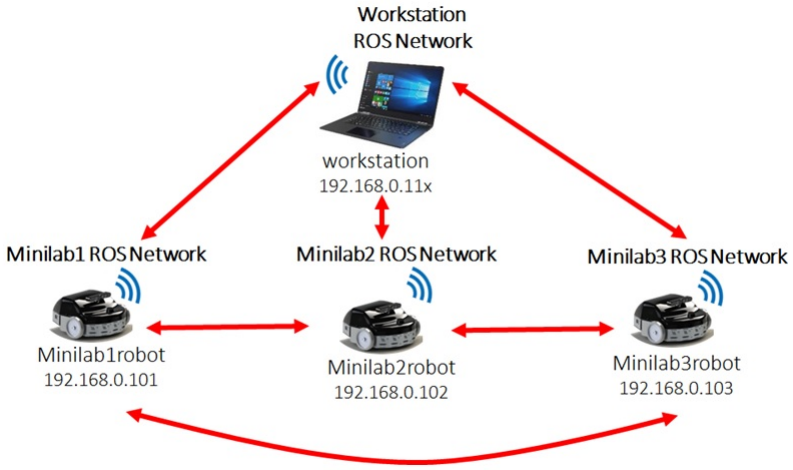

Figure 4.29: MiniLab robot runs its own master managing local communication.

Figure 4.29 illustrates the configuration of 3 robots to allow information to be exchanged between ROS sub-systems. With this distributed approach, every robot executes its own master. Local inter-process communication is handled by the local master while global communication between robots is handled by a special communication package. Robots may communicate directly forming an ad hoc wireless network and do not rely on a central controller.

Multimaster fkie

ROS multi-master system is built from two or more ROS networks, each one with its own roscore node. For this purpose, we need a package called `multimaster_fkie` [**?**]. This package can be easily installed as shown below:

```
$sudo apt-get install ros-indigo-multimaster-fkie
```

This package offers a set of nodes to establish and manage a multi-master network. This requires no

or minimal configuration. The changes are automatically detected and synchronized. The `multimaster_fkie` allows two substantial nodes: the `master_discovery` and the `master_sync` nodes to run simultaneously. The main features of `master_discovery` is to send multicast messages periodically to the ROS network to make the other `roscore` environments aware of its presence. It also detects the changes in the local network and informs all `roscore` about these changes. The other nodes called `master_sync` enable us to select which hosts, topics and services which should be synchronized or ignored between different `roscore`. It also helps to register and update information of topics and services to the local `roscore`.

Figure 4.30 presents an illustration of ROS multi-master system. For our experimental setup, we have four master ROS (workstation, Minilab 1, Minilab 2 and Minilab 3). Each ROS Master will be detected and discovered by any other master in the network.

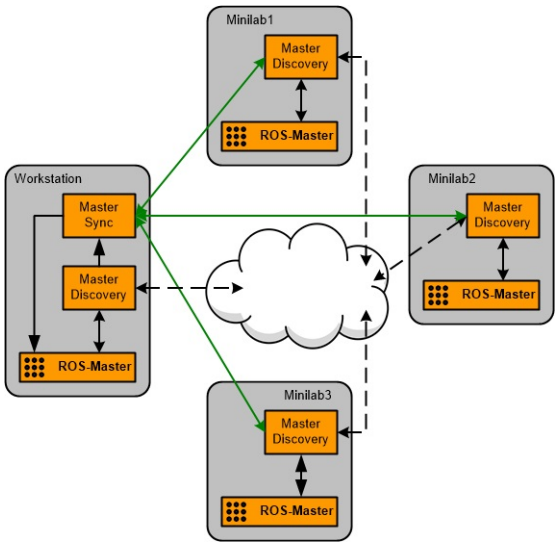

Figure 4.30: Multimaster fkie for multiple-minilab robots.

Multi-master Configuration

Now, we can launch the `multimaster_fkie` nodes and take a first look at how it works. First of all, it is needed to launch a local roscore on each computer, i.e.

```
$roscore
```

Then, the master_discovery node should be launched in each computer, passing as an argument the mcast_group parameter to specify the multicast address to be used, i.e.

```
$rosrun master_discovery_fkie master_discovery_mcast_group:=224.0.0.1
```

Afterwards, the master_sync node should be launched in each computer. Without any additional parameter, all topics and services on all computers will be synchronized with all others, i.e.

```
$rosrun master_sync_fkie master_sync
```

When both nodes are running on all robots and workstation, the following command will list all the available ROS masters on the common network:

```
$rosservice call /master_discovery/list_masters
```

Figure 4.31 shows the information reported by this command for the example presented in Figure 4.1.

```
lamih-minilab@lamihminilab:~$ rosservice call /master_discovery/list_masters
masters:
  -
    name: 192.168.0.101
    uri: http://192.168.0.101:11311/
    timestamp: 1527161324.16
    timestamp_local: 1527161324.16
    online: True
    discoverer_name: /master_discovery
    monitoruri: http://192.168.0.101:11611
  -
    name: 192.168.0.103
    uri: http://192.168.0.103:11311/
    timestamp: 1527161442.47
    timestamp_local: 1527161434.65
    online: True
    discoverer_name: /leader/master_discovery
    monitoruri: http://192.168.0.103:11611
  -
    name: lamihminilab
    uri: http://lamihminilab:11311/
    timestamp: 1527160708.62
    timestamp_local: 1527160708.62
    online: True
    discoverer_name: /master_discovery
    monitoruri: http://localhost:11611
  -
    name: 192.168.0.102
    uri: http://192.168.0.102:11311/
    timestamp: 1527190608.74
    timestamp_local: 1527190607.67
    online: True
    discoverer_name: /master_discovery
    monitoruri: http://192.168.0.102:11611
lamih-minilab@lamihminilab:~$
```

Figure 4.31: *rosservice call* command result.

4.5.3 Leader-Follower Node Communication

This subsection deals with node communication in terms of multi-robot configuration. "Node" is the ROS term for an executable that is connected to the ROS network. Here, we define a publisher node which will continually broadcast a message and a subscriber node which will continually receive a message.

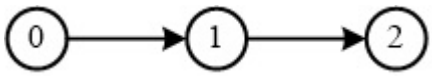

Figure 4.32: Communication topology.

Both publisher and subscriber nodes are configured according to the communication topology. For example, in our case as shown in Figure 4.32, we will define the leader "minilab 3" as a publisher of his position and velocity to follower "minilab 1". Furthermore, the follower "minilab 1" is also configured as a subscriber of the leader "minilab 3". At the same time, follower "minilab 1" also sets as a publisher to follower "minilab 2" and follower "minilab 2" is configured as a subscriber of follower "minilab 1".

The example code of publisher and subscriber are shown below. The first one is the leader's code and the second one is the follower's code.

```
1
2   int main(int argc, char **argv)
3   {
4       ...
5
6       ROS_INFO("start");
7
8       ros::init(argc, argv, "move_fix_Leader");
9       ros::NodeHandle n;
10      ros::Subscriber sub_odometry = n.subscribe("/minilab3/odom", 10,
    odomCallbackLeader);
11      ros::Publisher movement_pub = n.advertise<geometry_msgs::Twist>("/minilab3/
    cmd_vel",10);
12      //for sensors the value after , should be higher to get a more accurate result
    (queued)
13      pub_pose2d = n.advertise<geometry_msgs::Pose2D>("/minilab3/pose2d", 10);
14
15      ros::Rate rate(1000); //the larger the value, the "smoother"
16
17      ...
18  }
```

Listing 4.1: Leader 's program.

and

```
1
2   int main(int argc, char **argv)
3   {
4       ...
5
6       ROS_INFO("start");
7
8       ros::init(argc, argv, "move_fix_agent1x");
9       ros::NodeHandle n;
10
11      ros::Subscriber sub_odometryAgent1 = n.subscribe("/minilab1/odom", 10,
    odomCallbackagent1);
12      ros::Publisher movement_pubAgent1 = n.advertise<geometry_msgs::Twist>("/
    minilab1/cmd_vel",10);
13      pub_pose2dAgent1 = n.advertise<geometry_msgs::Pose2D>("/minilab1/pose2d", 10);
14
15      ros::Rate rate(100); //the larger the value, the "smoother"
16
17      ros::Subscriber sub_odometry = n.subscribe("/minilab3/odom", 10,
    odomCallbackLeader);
18      pub_pose2d = n.advertise<geometry_msgs::Pose2D>("/minilab3/pose2d", 10);
```

```
19
20          ...
21      }
```

Listing 4.2: Follower 's program.

NodeHandle is the main access point to communications with the ROS system. The first constructed NodeHandle will fully initialize this node, and the last destructed NodeHandle will close down the node.

The advertise() function is how we tell ROS that we want to publish on a given topic name. This invokes a call to the ROS master node, which keeps a registry of who is publishing and who is subscribing. After this advertise() call is made, the master node will notify anyone who is trying to subscribe to this topic name, and they will in turn negotiate a peer-to-peer connection with this node. advertise() returns a Publisher object which allows us to publish messages on that topic through a call to publish(). Once all copies of the returned Publisher object are destroyed, the topic will be automatically unadvertised. The second parameter to advertise() is the size of the message queue used for publishing messages. If messages are published more quickly than we can send them, the number here specifies how many messages to buffer up before throwing some away.

4.6 Conclusion

The multi-agent system framework was presented using Robot Operating System (ROS). Due to the requirements of the proposed consensus algorithms, we first introduce the robot hardware specifications, communication network configuration and minimum amount of workstation we can use for the coordination of multi-robots using ROS and multi Minilab robots.

Using a wireless master-slave scheme, it is possible that multiple robots communicate through a wireless network with only one workstation for monitoring and control. This configuration is a low cost configuration. For decentralized architectures, `multimaster_fkie` is a solution to the multi-master ROS problem. Node calling algorithm has allowed to create leader-follower topology in this ROS multi-agent system network. This algorithm has used a publisher and a subscriber to broadcast and/or receive messages continually from each other.

In next chapter, a group of Minilab are used to test the decentralized leader-follower consensus algorithms.

Chapter 5

Experimental results on Consensus for a Group of Minilab Robots

5.1 Introduction

In this chapter, using our experimental setup described in the previous chapter, we apply the schemes designed in Chapter 2 for two applications, e.g. fixed-time trajectory tracking and leader-follower consensus. First, we study the fixed-time trajectory tracking control algorithms for one agent with single-integrator dynamics. Then, we analyze the results for the leader-follower consensus algorithms. The same is done for double-integrator dynamics. At last, since nonholonomic dynamics can better describe the motion of mobile robots in a real world, we implement the proposed scheme to achieve fixed-time consensus tracking for a multi-agent system with unicycle-type dynamics.

The fixed-time methodology used in this chapter guarantees that a settling time bound can be prescribed without depending on the initial states of the agents. More specifically, for the consensus problem, a distributed protocol based on fixed-time stability techniques is implemented for each follower to accomplish the consensus tracking in a desired time. We provide experiment to demonstrate the effectiveness of the proposed controllers for fixed-time trajectory tracking and consensus. Using Gazebo ROS simulation and Minilab Enova robotic platform, the experimental results show the effectiveness and robustness of the proposed algorithms.

The experiments for all the following subsections (i.e. simple integrator, double integrator, chained-form dynamics) are done using the same fixed topologies. Figure 5.1 shows the communication topology for the leader-follower MAS scenario in ROS-Gazebo. A MAS with $N = 6$ followers labeled by $1-6$ and one leader labeled by 0 is considered. One can see that the communication topology is fixed and connected. It is characterized by the following Laplacian L and the matrix B which describes

links between the leader and the followers given as follows

$$L = \begin{bmatrix} 2 & -1 & -1 & 0 & 0 & 0 \\ -1 & 1 & 0 & 0 & 0 & 0 \\ -1 & 0 & 2 & -1 & 0 & 0 \\ 0 & 0 & -1 & 1 & 0 & 0 \\ 0 & 0 & 0 & 0 & 1 & -1 \\ 0 & 0 & 0 & 0 & -1 & 1 \end{bmatrix}, \qquad B = \begin{bmatrix} 1 & 0 & 0 & 0 & 0 & 0 \\ 0 & 0 & 0 & 0 & 0 & 0 \\ 0 & 0 & 0 & 0 & 0 & 0 \\ 0 & 0 & 0 & 0 & 0 & 0 \\ 0 & 0 & 0 & 0 & 1 & 0 \\ 0 & 0 & 0 & 0 & 0 & 0 \end{bmatrix}$$

From matrix B, it is clear that agents 2, 3, 4 and 6 do not have direct link with agent 0. Assumption 1 is satisfied.

For the implementation using the available multiple minilab robots, since we have only three robots, the topology, shown in Figure 5.2 corresponds to node 0 as leader, $1-2$ as followers.

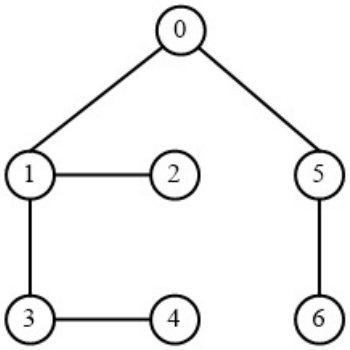

Figure 5.1: Topology of MAS using ROS for six agents.

Figure 5.2: Topology of MAS using using our Minilab Enova robot platform.

The remainder of the chapter is organized as follows. Section 5.2 considers the fixed-time trajectory tracking and leader-follower consensus problems for agents with single-integrator dynamics. The same problems are studied for double-integrator dynamics in Section 5.3. In Section 5.4, experimental

results are provided to verify the effectiveness of the proposed methods for nonholonomic systems. Section 5.5 concludes this chapter.

5.2 Fixed-Time tracking for agents with Single-Integrator dynamics

In this section, we show some experimental results using Gazebo-ROS and Minilab robot platform for tracking and consensus with Single-Integrator Dynamics to verify the theoretical analysis.

5.2.1 Fixed-Time trajectory Tracking for Single-Integrator Dynamics

For the trajectory tracking application, the Minilab robots are modeled as a single-integrator system:

$$\dot{x}(t) \quad = \quad u(t) \tag{5.1}$$

where $x \in \mathbb{R}$ (resp. $u \in \mathbb{R}$) is the state (resp. control input) of the single-integrator system. In this experiment, the state can be described as the robot position $x(t)$ and the control input $u(t)$ as the linear velocity of the robot.

The dynamics of the desired trajectory is generated using the following system:

$$\dot{x}_d(t) \quad = \quad u_d(t) \tag{5.2}$$

where $x_d \in \mathbb{R}$ (resp. $u_d \in \mathbb{R}$) is the state (resp. control input) of the desired trajectory. The control objective is that system (5.1) follows the desired trajectory (5.2) in a fixed-time.

As described in Chapter 2, the fixed-time tracking problem is solved using the following controller:

$$u = -(\alpha + a)\lfloor e \rceil^2 - \beta \operatorname{sign}(e) \tag{5.3}$$

where $e = x - x_d$, α, β and a are positive constants. The settling time is explicitly defined as

$$T = \frac{\pi}{\sqrt{\alpha\beta}} \tag{5.4}$$

The corresponding algorithm is given in Algorithm 1. At each sampling time instant t_k, we calculate the desired position and determine the error position between the desired trajectory and the actual robot position. After calculating the controller u, we implement the corresponding linear velocity input of the robot.

Step Linear Velocity Input for the desired trajectory

The control parameters are selected as: $\alpha = \beta = 0.5$ for protocol (5.3). The initial state of the robot is $x = -2$. Based on the control parameters, the settling time is $T = 6.28s$. The desired trajectory is generated by (5.2) with $x_d(0) = 0$, $u_d(t) = 0.2$. Since $a \geq d + u_d$, we set $a = 1$. The control objective is that system (5.1) tracks the desired trajectory x_d.

Algorithm 1 Fixed-time Tracking controller for Single Integrator dynamics

Input: $x_d(t_k), x(t_k)$

Parameters: α, β, a

Output: $v(t), t_k \leq t < t_{k+1}$

1: **if** $t = t_k$ **then**
2: Compute $e(t_k) = x(t_k) - x_d(t_k)$
3: Compute $u = -(\alpha + a)\lfloor e \rceil^2 - \beta \operatorname{sign}(e)$
4: Implement the linear velocity $v(t)$
5: **end if**

$x(t_k)$ is the x position of the Minilab robot at instant t_k, $x_d(t_k)$ is the x desired position at instant t_k

Using Theorem 1, the tracking controller (5.3) guarantees the stabilization of the tracking errors to the origin in a finite-time bounded by $T = 6.28s$. Figure 5.3.a. shows that the actual state trajectory x accurately tracks the desired state x_d before T in spite of the presence of disturbances and uncertainties inherent to the experimental setup. Hence, the origin of the closed-loop system is globally finite-time stable. Furthermore, since T does not depend on the initial states, the proposed protocol is a fixed-time controller.

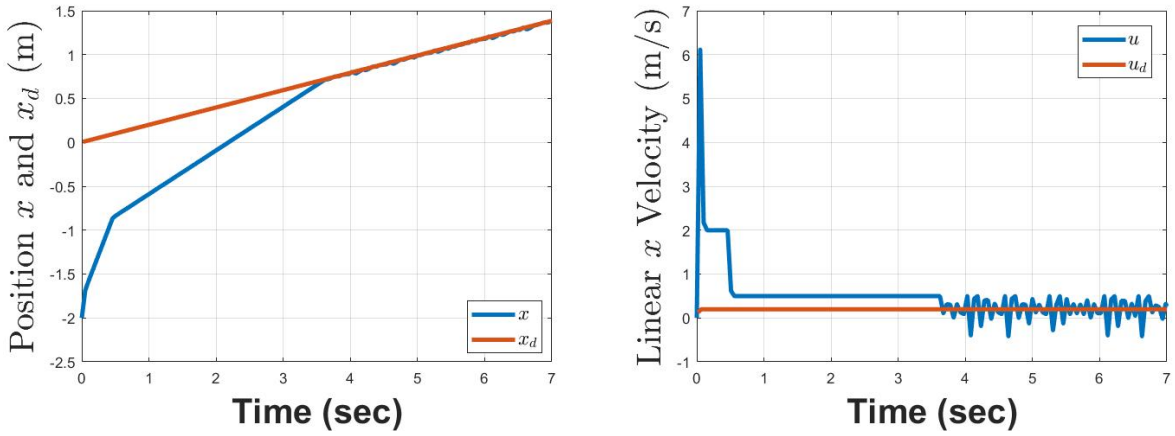

(a) (b)

Figure 5.3: Experimental results for Algorithm 1: Time response of actual state trajectory x and desired state trajectory x_d with constant linear desired velocity.

The tracking errors are depicted in Figure 5.3. One can see that the tracking errors between the actual trajectory and the desired trajectory converge to zero at $T = 3.5s$. Using the proposed controller, the tracking controller is achieved in a prescribed time before $T = 6.28s$. The control inputs for linear x velocity are shown in Figure 5.3.b. One can note that the magnitude of control inputs may be large during the transients to achieve a fast convergence of the sliding surface e. The control

parameters should be adjusted to obtain a good compromise between magnitude of the control input and the settling time.

Sinusoidal Linear Velocity Input for the desired trajectory

The control parameters are selected as: $\alpha = \beta = 1$ and $a = 1$ for protocol (5.3). The initial state of the robot is $x = -1.5$. Based on the control parameters, the settling time is $T = 3.14s$. The desired trajectory is generated by (5.2) with $x_d(0) = 0$, $u_d(t) = 0.2sin(2\pi t)$. The control objective is that system (5.1) tracks the desired trajectory x_d.

Figure 5.4 shows that the tracking controller (5.3) guarantees the stabilization of the tracking errors to the origin in a finite-time bounded by $T = 3.14s$. From Figure 5.4.b., one can see that the actual state trajectory x accurately tracks the desired state x_d before $2.5s$.

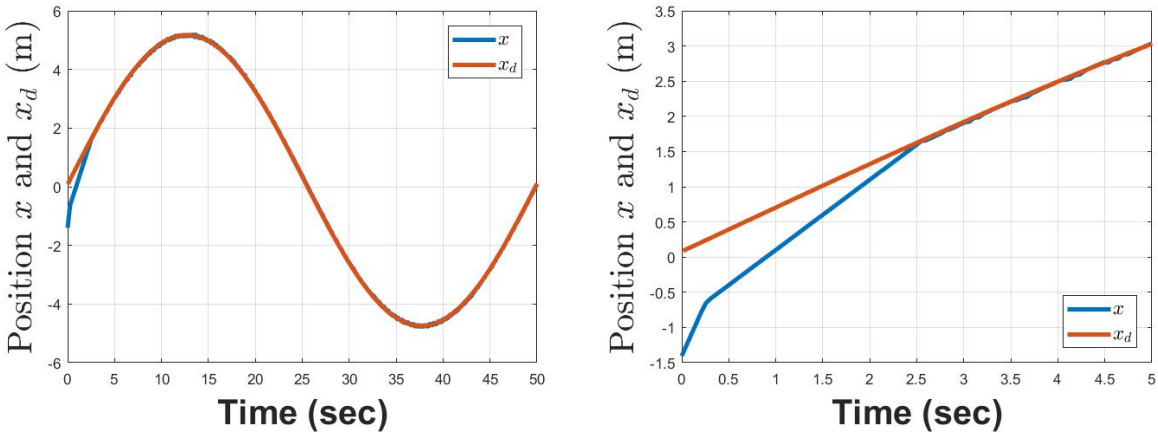

(a)

(b)

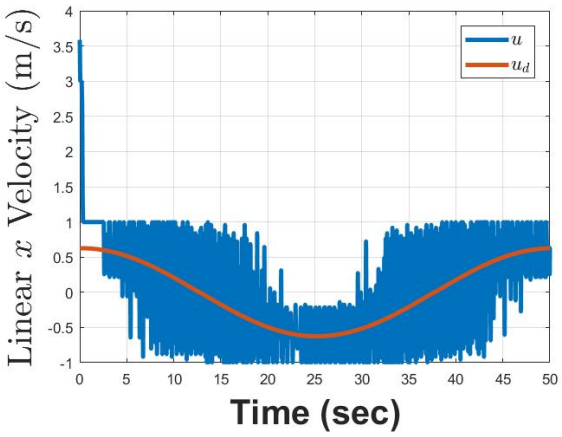

(c)

Figure 5.4: Experimental results for Algorithm 1: Time response of actual state trajectory x and desired state trajectory x_d with sinusoidal linear desired velocity.

5.2.2 Fixed-Time Consensus for MAS with Single-Integrator Dynamics

For the consensus tracking application, the Minilab robots are modeled as system (5.1). The dynamics of the leader is generated by (5.2). The control objective is that system (5.1) follows the leader (5.2) in a fixed-time using only local exchanged information. The communication topology is given by Figure 5.1.

The initial position of the robots is given by the following vector $x(0) = [3, 2, 1, -1, -2, -3]^T$. Recall that T_o is time needed for an agent to estimate the leader state (prescribed time observation). It should be noted that the estimation in (2.10) depends on the gains of observer. The settling time is explicitly defined as $T = T_o + \frac{\pi}{\sqrt{\alpha\beta}}$.

The corresponding fixed-time algorithm for MAS with single integrator dynamics is given in Algorithm 2. At each sampling time instant t_k, based on local exchanged information, each agent i estimates the leader position $\hat{x}_i$ and compute the tracking error between the leader, itself and neighboring agents. After calculating the controller u, we implement the corresponding linear velocity input of the robot.

Algorithm 2 Fixed-time consensus for MAS with Single Integrator dynamics

For each agent i,

Input: $x_0(t_k)$ (if $b_i = 1$), $x_i(t_k)$, $x_j(t_k)$ (for all j such that $a_{ij} \neq 0$)

Parameters: ρ, σ, α, β, a_i

Output: $v_i(t), t_k \leq t < t_{k+1}$

1: **if** $t = t_k$ **then**
2: When $t < T_o$, $v_i(t) = 0$
3: Agent i samples its current states $x_i(t)$, its estimate of the leader $\hat{x}_i(t)$ and broadcasts it to its neighbors
4: Compute the estimation error $\tilde{x}_i = \hat{x}_i - x_0$
5: Update the distributed observer (2.7) (convergence in time T_o)
6: When $t \geq T_o$, compute the tracking error $e_i = x_i - \hat{x}_i$
7: Compute $u = -(\alpha + a_i)\lfloor e_i \rceil^2 - \beta \operatorname{sign}(e_i)$
8: Implement the linear velocity
9: **end if**

$x_i(t_k)$ is the x position of Minilab robot i at instant t_k, $x_0(t_k)$ is x leader position at instant t_k

The performances of the proposed observer-based leader-follower consensus controller for single integrator MAS are studied through the following experimental results.

Step Linear Velocity Input for the leader trajectory

The control parameters are selected as: $\alpha = \beta = 1$ for protocol (2.17). The initial state of the robots is $x(0) = [3, 2, 1, -1, -2, -3]^T$. The desired trajectory of the leader is generated by (2.5) with $x_0(0) = 0$, $u_0(t) = 0.2$. Since $a_i \geq d_i + u_0$, we set $a_i = 1$. The control objective is that each system (2.6) tracks the leader x_0 using only local information.

Using Theorem 1, the distributed observer (2.7) guarantees the stabilization of the estimation errors (2.8) to the origin in a finite-time bounded by $T_o = 5s$. The distributed observers accurately reconstruct the leader state for each agent before T_o. Using Theorem 2, the tracking controller guarantees the stabilization of the tracking errors to the origin in a finite-time bounded by $T = 15s$. Figure 5.5.a. shows that the actual state trajectory x accurately tracks the leader state x_0 before T in spite of the presence of disturbances and uncertainties inherent to the experimental setup. One can conclude that using the proposed controller, the leader-follower consensus is achieved in a prescribed time. The control inputs for each agent are shown in Figure 5.5.b. One can note that the magnitude of control inputs may be large during the transients to achieve a fast convergence of the sliding surface given by the different steps of the consensus protocol. Hence, the control parameters should be adjusted to obtain a good compromise between magnitude of the control input and the settling time. The origin of the closed-loop system is globally finite-time stable contrary to existing controllers which only provide semi-global finite-time stability property. Furthermore, since T does not depend on the initial states of agents, the proposed protocol is distributed.

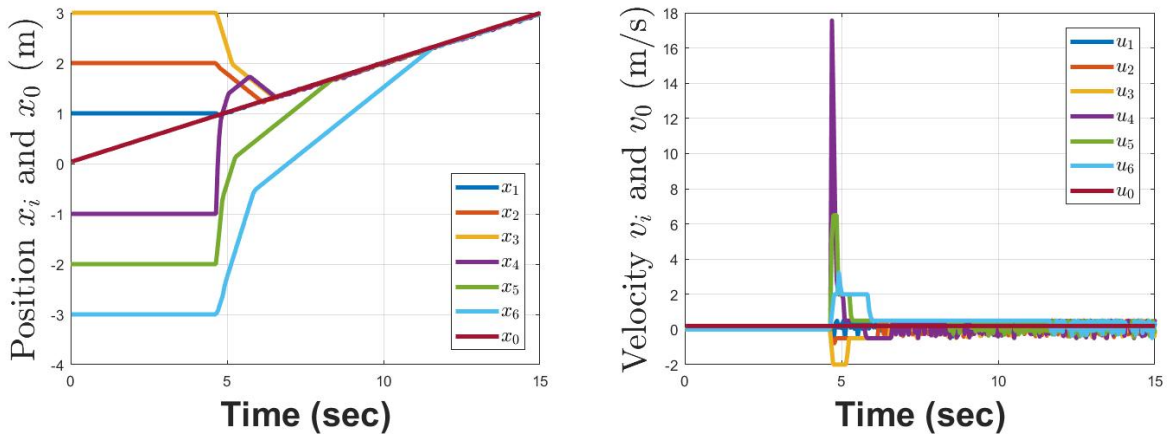

(a) (b)

Figure 5.5: Experimental results for Algorithm 2: Time response of the actual state trajectory of the followers and of the leader with a step linear leader trajectory.

Sinusoidal Linear Velocity Input for the leader trajectory

The control parameters are selected as: $\alpha = \beta = 1.5$, $a_i = 1$, $\epsilon = 0.52$ for protocol (2.17). The initial state of the robots is $x(0) = [3, 2, 1, -1, -2, -3]^T$. The desired trajectory of the leader is generated by (2.5) with $x_0(0) = 0$, $u_0(t) = 0.2sin(2\pi t)$. Based on the control parameters, the settling time is $T = 10.71s$ ($T_o = 6s$). The control objective is that each system (2.6) tracks the leader x_0 using only local information.

The fixed-time consensus tracking performance of the MAS with single-integrator dynamics when the leader input has a sinusoidal linear velocity is shown in Figure 5.6. Using Theorem 2, the robust controller 2.17 solves the fixed-time trajectory tracking problem with an estimation of the settling time less than T. Figure 5.6(a) shows that the tracking controller guarantees the stabilization of the tracking errors to the origin in a finite-time bounded by Ts (a zoom is given in Figure 5.6(b)). From Figure 5.7, one can see that the corresponding control inputs.

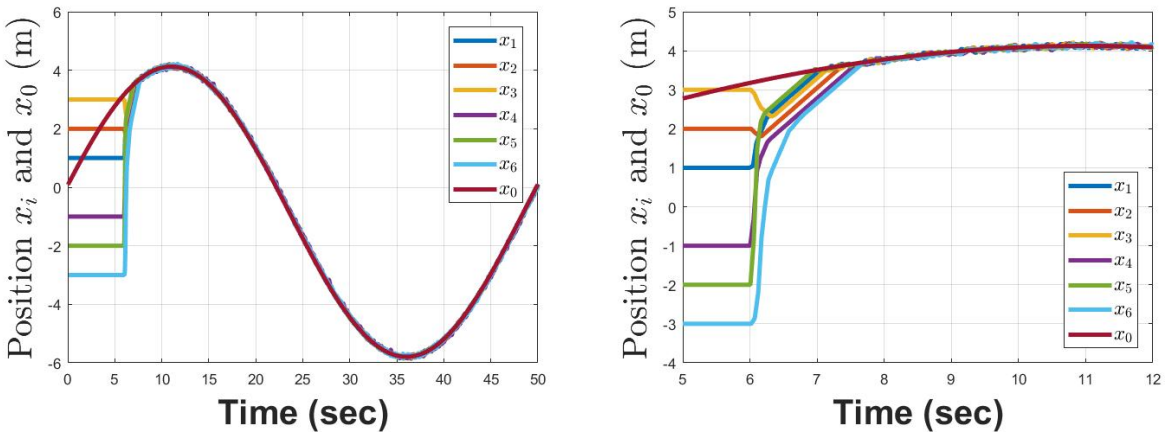

(a) (b)

Figure 5.6: Experimental results for Algorithm 2: Time response of the actual state trajectory of the followers and of the leader with a sinusoidal linear leader trajectory.

5.3 Fixed-Time Tracking for agents with Double-Integrator Dynamics

In this section, we show some experimental results using Gazebo-ROS and Minilab robot platform for tracking and consensus with double-integrator dynamics to verify the theoretical analysis.

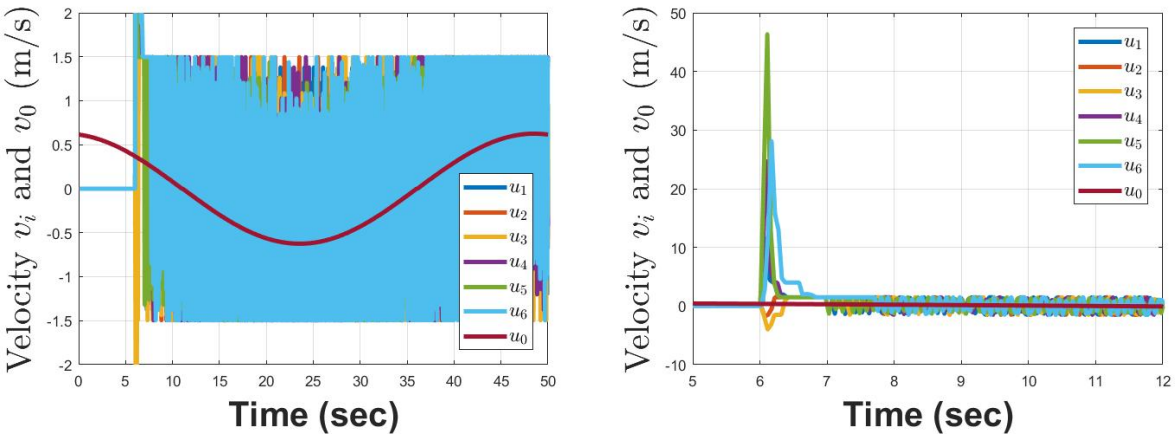

(a) (b)

Figure 5.7: Experimental results for Algorithm 2: Control input for each agent and the leader.

5.3.1 Fixed-Time trajectory Tracking for Double-Integrator Dynamics

For the trajectory tracking application, the Minilab robots are modeled as a double-integrator system:

$$\begin{aligned} \dot{x}_1(t) &= x_2(t) \\ \dot{x}_2(t) &= u_(t) \end{aligned} \tag{5.5}$$

where $x = [x_1, x_2]^T \in \mathbb{R}^2$ (resp. $u \in \mathbb{R}$) is the state (resp. control input) of the double-integrator system. In this experiment, the state can be described as the robot position $x_1(t)$ and the linear velocity $x_2(t)$ with the control input $u(t)$ as the linear acceleration of the robot.

The dynamics of the desired trajectory is generated using the following system:

$$\begin{aligned} \dot{x}_{1,d}(t) &= x_{2,d}(t) \\ \dot{x}_{2,d}(t) &= u_d(t) \end{aligned} \tag{5.6}$$

where $x_d = [x_{1,d}, x_{2,d}]^T \in \mathbb{R}^2$ (resp. $u_d \in \mathbb{R}$) is the state (resp. control input) of the desired trajectory. The control objective is that system (5.5) follows the desired trajectory (5.6) in a fixed-time.

Let us define the tracking errors as

$$e(t) = x(t) - x_d(t) \tag{5.7}$$

As described in Chapter 2, the fixed-time tracking problem is solved using the following controller:

$$u = u_d + \varphi(e) \tag{5.8}$$

with

$$\begin{aligned} \varphi(e) &= -\frac{\alpha_1 + 3\beta_1 e_1^2 + 2d_{max}}{2} sign\big(s_1(e_1, e_2)\big) \\ &\quad -\lfloor \alpha_2 s(e_1, e_2) + \beta_2 \lfloor s(e_1, e_2) \rceil^3 \rceil^{\frac{1}{2}} \end{aligned} \tag{5.9}$$

and

$$s(e_1, e_2) = e_2 + \lfloor \lfloor e_2 \rceil^2 + \alpha e_1 + \beta_1 \lfloor e_1 \rceil^3 \rceil^{\frac{1}{2}} \tag{5.10}$$

where α_1, α_2, β_1, β_2 and a are positive constants. The settling time is explicitly defined as

$$T = \frac{2}{\sqrt{\alpha}_2} + \frac{2}{\sqrt{\beta}_2} + \frac{2\sqrt{2}}{\sqrt{\alpha}_1} + \frac{2\sqrt{2}}{\sqrt{\beta}_1} \tag{5.11}$$

The corresponding algorithm is given in Algorithm 3. At each sampling time instant t_k, the robot calculates the desired position and velocity. Then, it determines the error position between the desired trajectory and the actual robot position and velocity. After calculating the controller u, we implement the corresponding input of the robot.

Algorithm 3 Fixed-time Tracking for Double-Integrator dynamics

Input: $x_{1,d}(t_k), x_{2,d}(t_k), x_1(t_k), x_2(t_k)$

Parameter: α_1, β_1, α_2, β_2, a

Output: $v(t), t_k \leq t < t_{k+1}$

1: **if** $t = t_k$ **then**
2: Compute $e(t_k) = x(t_k) - x_d(t_k)$
3: Compute $\varphi(e)$, $u = u_d + \varphi(e)$
4: Implement the linear velocity $v(t)$
5: **end if**

$x(t_k)$ is x position of the Minilab robot at instant t_k, $x_d(t_k)$ is x desired position at instant t_k

Step Linear Acceleration Input for the desired trajectory

The initial state of the robot is $x = [x_1 = -1.5, x_2 = 0]^T \in \mathbb{R}^2$. Based on the control parameters, the settling time is $T = 3.05s$. The desired trajectory is generated by (5.6) with $x_d(0) = 0$, $u_d(t) = 0.2$. Since $a \geq d + u_d$, we set $a = 1$. The control objective is that system (5.5) follows the desired trajectory x_d.

Using Theorem 4, the tracking controller (5.8) guarantees the stabilization of the tracking errors to the origin in a finite-time bounded by $T = 3.05s$. Figure 5.8.a. shows that the actual state trajectory x accurately tracks the desired state x_d at $1.2s$ for the first state and from Figure 5.8.b. for the second state at $1.25s$. Hence, the origin of the closed-loop system is globally finite-time stable. Furthermore, since T does not depend on the initial states, the proposed protocol is a fixed-time controller. The control inputs for linear x acceleration are shown in Figure 5.8.c.

Sinusoidal Linear acceleration Input for the desired trajectory

The initial state of the robot is $x = [x_1 = -1.5, x_2 = 0]^T \in \mathbb{R}^2$. Based on the control parameters, the settling time is $T = 2.67s$. The desired trajectory is generated by (5.6) with $x_d(0) = 0$, $u_d(t) =$

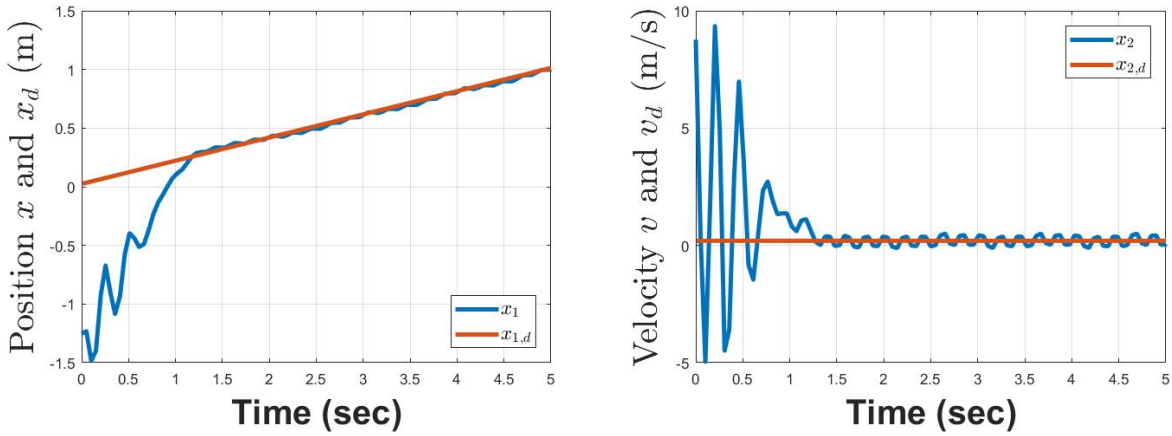

(a)

(b)

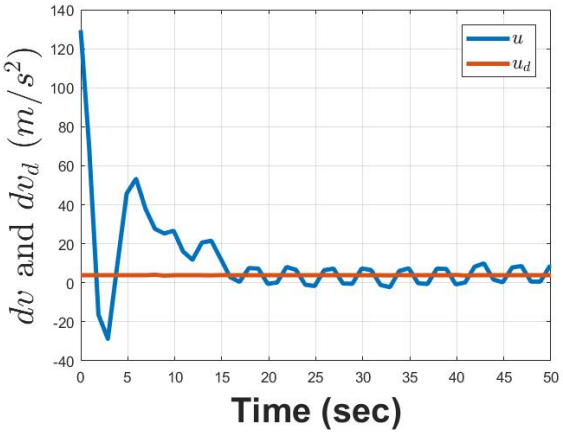

(c)

Figure 5.8: Experimental results for Algorithm 3: Time response of actual state trajectory x and desired state trajectory x_d with constant linear desired control input.

$0.2sin(2\pi t)$. The control objective is that system (5.5) follows the desired trajectory x_d.

Figure 5.9 shows that the tracking controller (5.8) guarantees the stabilization of the tracking errors to the origin in a finite-time bounded by $T = 2.67s$ for all the state. Figure 5.9 shows the actual and desired state position trajectories (convergence at $1.25s$). Figure 5.10.a. shows the actual and desired velocities (convergence at $1.3s$). The control inputs are shown in Figure 5.10.b.

5.3.2 Fixed-Time Consensus for MAS with Double-Integrator Dynamics

Similarly as previously, the communication topology is given by Figure 5.1. It is fixed and connected where the agent 2, 3, 4 and 6 do not have direct link with agent 0. Assumption 1 is satisfied. For the consensus tracking application, the Minilab robots are modeled as system (5.5). The dynamics of the leader is generated by (5.6). The control objective is that system (5.5) follows the leader (5.6) in a

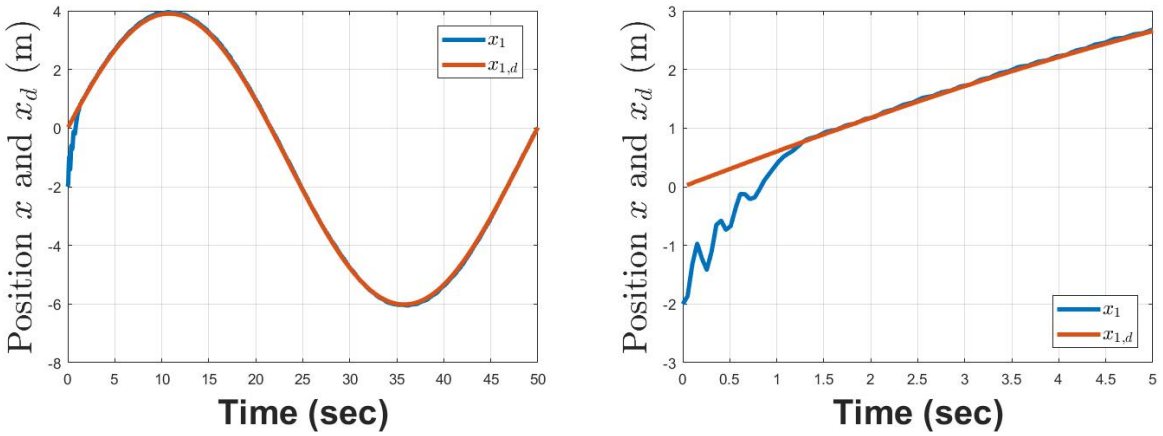

(a) (b)

Figure 5.9: Experimental results for Algorithm 3: Time response of actual position trajectory x_1 and desired position trajectory $x_{1,d}$ with sinusoidal linear desired control input.

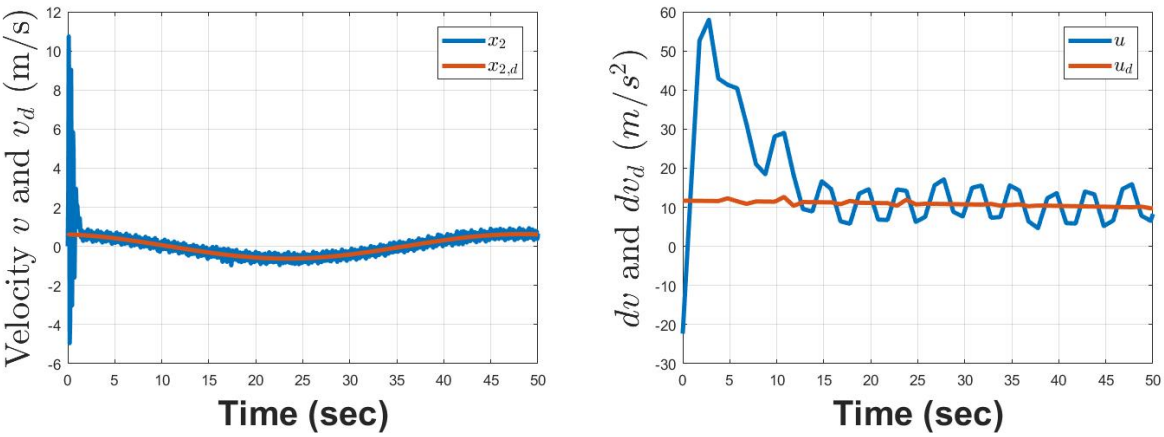

(a) (b)

Figure 5.10: Experimental results of Algorithm 3: Time response of actual velocity trajectory x_2 and desired velocity trajectory $x_{2,d}$ and the corresponding control inputs.

fixed-time using only local exchanged information.

The initial position of the robots is given by the following vector $x(0) = [3, 2, 1, -1, -2, -3]^T$. Recall that T_o is time needed for an agent to estimate the leader state (prescribed time observation). It should be noted that the estimation in (2.26) depends on the gains of observer. The settling time is explicitly defined as $T = T_o + \frac{2}{\sqrt{\alpha_2}} + \frac{2}{\sqrt{\beta_2}} + \frac{2\sqrt{2}}{\sqrt{\alpha_1}} + \frac{2\sqrt{2}}{\sqrt{\beta_1}}$.

The corresponding fixed-time algorithm for MAS with double integrator dynamics is given in Algorithm 4. At each sampling time instant t_k, based on local exchanged information, each agent i estimates the leader position $\hat{x}_i$ and compute the tracking error between the leader, itself and

neighboring agents. After calculating the controller u, we implement the corresponding linear velocity input of the robot.

Algorithm 4 Fixed-time consensus for MAS with Double Integrator dynamics

For each agent i, **Input:** $x_{1,0}(t_k)$, $x_{2,0}(t_k)$ (if $b_i = 1$), $x_{1,i}(t_k)$, $x_{2,i}(t_k)$, $x_{1,j}(t_k)$, $x_{2,j}(t_k)$ (for all j such that $a_{ij} \neq 0$)

Parameter: ρ_1 and σ_1, ρ_2 and σ_2, α_1, β_1, α_2, β_2, a

Output: $v_i(t), t_k \leq t < t_{k+1}$

1: **if** $t = t_k$ **then**
2: When $t < T_o$, $v_i(t) = 0$
3: Agent i samples its current states $x_i(t)$, its estimate of the leader $\hat{x}_i(t)$ and broadcasts it to its neighbors
4: Compute the estimation error $\tilde{x}_i = \hat{x}_i - x_0$
5: Update the distributed observer (2.23) (convergence in time T_o)
6: When $t \geq T_o$, compute the tracking error $e_i = x_i - \hat{x}_i$
7: Compute u according to Equation (2.35)
8: Implement the linear velocity
9: **end if**

$x_{1,i}(t_k)$ is x position of Minilab robot i and $x_{1,0}(t_k)$ is x leader position at instant t_k. $x_{2,i}(t_k)$ is x linear velocity of Minilab robot i and $x_{2,0}(t_k)$ is x leader velocity at instant t_k.

The performances of the proposed observer-based leader-follower consensus controller for double integrator MAS are studied through the following experimental results.

Step Linear Input for the leader trajectory

The control parameter are selected as: $\alpha_1 = \alpha_2 = \beta_1 = \beta_2 = 10$ for protocols 2.35. The initial position of the robots is $[3, 2, 1, -1, -2, -3]^T$ while the initial velocity is 0. The desired trajectory is generated by (5.6) with $x_{1,0}(0) = 0$, $x_{2,0}(t) = 0.2$. Hence, we set $a = 1$. The control objective is that each system (5.5) tracks the leader x_0 using only local information.

Using Theorem 3, the distributed observer (2.23) guarantees the stabilization of the estimation errors to the origin in a finite-time bounded by $T_o = 1s$. The distributed observers accurately reconstruct the leader state for each agent before T_o. Using Theorem 4, the tracking controller guarantees the stabilization of the estimation errors to the origin in a finite-time bounded by $T = 6.55s$. Figure 5.11 shows that the actual state trajectory accurately tracks the leader state before T in spite of the presence of disturbances and uncertainties inherent to the experimental setup. One can conclude that using the proposed controller, the leader-follower consensus is achieved in a prescribed time. The

origin of the closed-loop system is globally finite-time stable contrary to existing controllers which only provide semi-global finite-time stability property. Furthermore, since T does not depend on the initial states of agents, the proposed protocol is distributed.

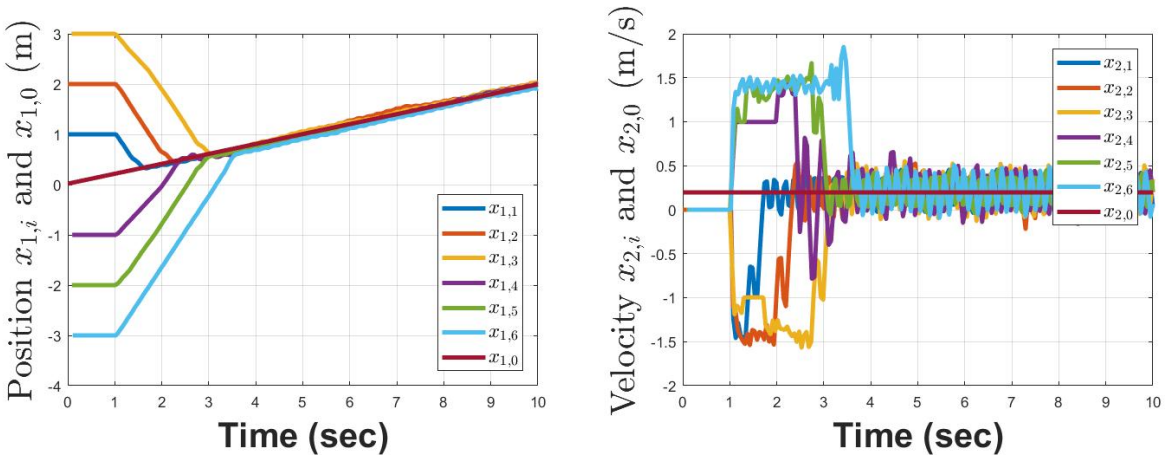

(a) (b)

Figure 5.11: Experimental results for Algorithm 4: Time response of the actual state trajectory of the followers and of the leader with a step linear leader trajectory.

Sinusoidal Linear Input for the leader trajectory

The control parameters are selected as: $\alpha_1 = \alpha_2 = \beta_1 = \beta_2 = 2$ and $a = 1$ for protocol 2.35. The initial position of the robots is $[3, 2, 1, -1, -2, -3]^T$ while the initial velocity is 0. The desired trajectory of the leader is generated by (5.6) with $u_0(t) = 0.2\sin(2\pi t)$. Based on the control parameters, the settling time is $T = 15s$ ($T_o = 5s$). The control objective is that each system (5.5) tracks the leader x_0 using only local information.

The fixed-time consensus tracking performance of the MAS with double-integrator dynamics when the leader input has a sinusoidal linear input is shown in Figure 5.12. Using Theorem 4, the robust controller (2.35) solves the fixed-time trajectory tracking problem with an estimation of the settling time less than T. Figure 5.12.(a) shows that the tracking controller guarantees the stabilization of the tracking errors in position to the origin in a finite-time bounded by T. Figure 5.12.(b) shows the tracking errors in velocity.

5.4 Fixed-Time Tracking for agents with Unicycle-type Dynamics

In this section, we show some experimental results using Gazebo-ROS and Minilab robot platform for tracking and consensus with unicycle-type dynamics to verify the theoretical analysis.

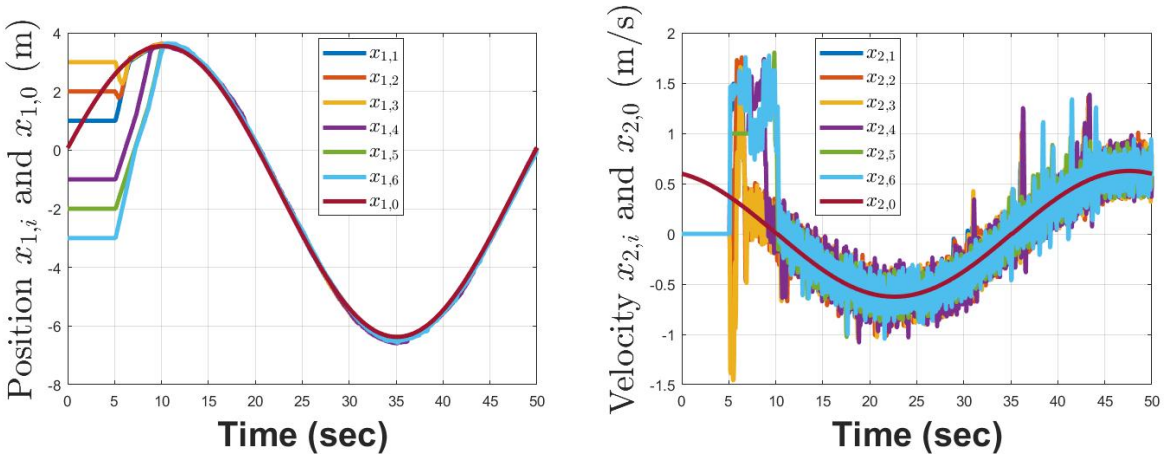

(a) (b)

Figure 5.12: Experimental results for Algorithm 4: Time response of the actual state trajectory of the followers and of the leader with a sinusoidal leader trajectory.

5.4.1 Fixed-Time Trajectory Tracking for Unicycle-type Dynamics

The algorithm for trajectory tracking is given in Algorithm 5. At each sampling time instant t_k, the robot calculates the desired position and velocity. Then, it determines the error position between the desired trajectory and its actual position. After calculating the controller u, we implement the corresponding linear and angular velocity input of the robot.

Algorithm 5 Fixed-time Tracking for Unicycle-type Dynamics

Input: $x_1(t_k), x_2(t_k), x_3(t_k), x_4(t_k), x_{1,d}(t_k), x_{2,d}(t_k), x_{3,d}(t_k), x_{4,d}(t_k)$

Parameters: α_1, β_1, α_2, β_2, a

Output: $v_{linear\ x}(t), v_{angular}(t), t_k \leq t < t_{k+1}$

1: **if** $t = t_k$ **then**
2: Compute the tracking errors $e(t) = x(t) - x_d(t)$
3: Compute s_1, φ_1, u_1
4: Compute s_2, φ_2, u_2
5: Implement the linear velocity
6: Implement the angular velocity
7: **end if**

First, the desired trajectory is illustrated in Figure 5.13. It is composed of a line and a circle (see the curve in blue color). The control parameter are selected as: $\alpha_1 = \beta_1 = 20, \alpha_2 = \beta_2 = 10$, $a = b = 1$ for controller (2.54). The initial state of the robot is $x(0) = -2$, $y(0) = -2$, $\theta(0) = 0$. Based on the control parameters, the settling time is $T = 2.6s$. Figure 5.13 shows the time response of x and y position of the robot. The robot successfully tracks the desired trajectory with an offset $0.25m$ (which

has been added for collision avoidance consideration).

Using Theorem 5, the tracking controller (2.54) guarantees the stabilization of the tracking errors to the origin in a finite-time bounded by $T = 2.6s$. Figure 5.14 shows the actual and desired trajectories in x (both in position and velocity). It is shown that the actual position x accurately tracks the desired state x_d before T (i.e. $0.8s$) in spite of the presence of disturbances and uncertainties inherent to the experimental setup.

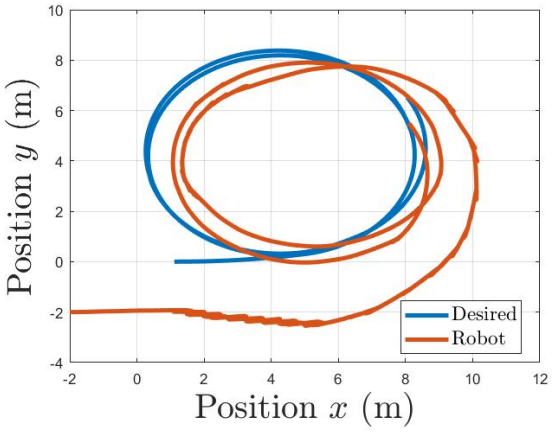

Figure 5.13: Actual and desired trajectory of the robot in the plane

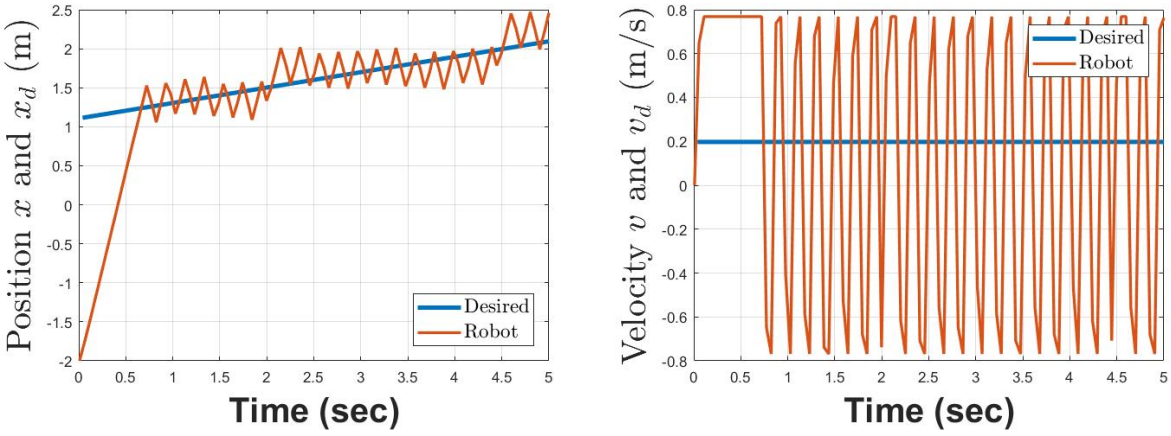

(a) (b)

Figure 5.14: Time evolution of the x position and x velocity

Figure 5.15 shows the actual and desired trajectories in θ (both in position and velocity). It is shown that the actual position θ accurately tracks the desired state θ_d before T (i.e. $0.8s$) in spite of the presence of disturbances and uncertainties inherent to the experimental setup. Hence, the origin of the closed-loop system is globally finite-time stable. Furthermore, since T does not depend on the

initial position and linear velocity, the proposed protocol is fixed-time.

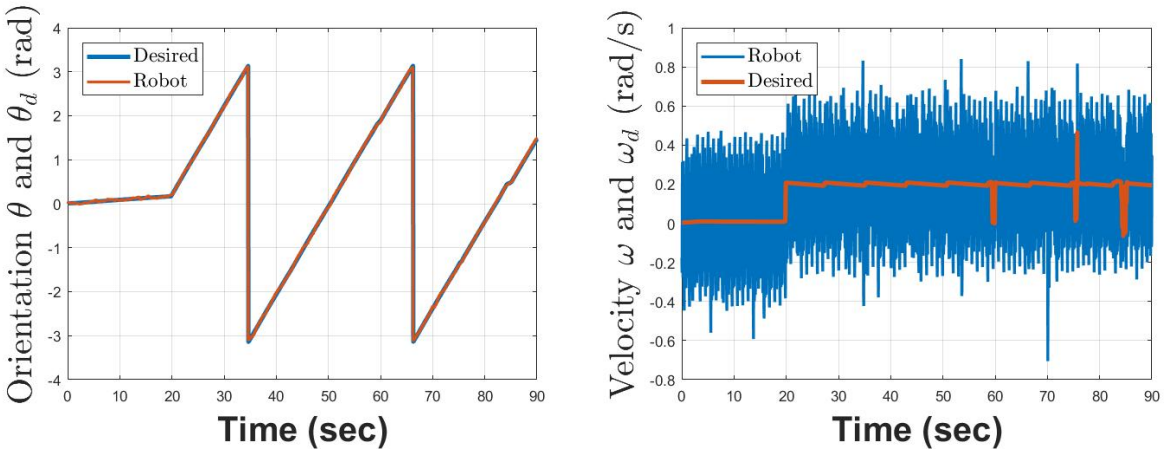

(a) (b)

Figure 5.15: Time evolution of the θ position and angular velocity

5.4.2 Fixed-Time Consensus for MAS with Unicycle-type Dynamics

The communication topology is given in Figure 5.2. Assumption 1 is satisfied. For the consensus tracking application, the Minilab robots are modeled as system (2.49). The dynamics of the leader is generated by (2.61). The control objective is that systems (2.49) follow the leader in a fixed-time using only local exchanged information.

The initial $x-y$ position of the robots is given by the following vector $(-1,-1)$ and $(1,1)$ for robot 1 and 2 respectively. Recall that T_o is time needed for agents to estimate the leader state (in a prescribed time). It should be note that the estimation in (2.26) depends on the gains of observer. The settling time is explicitly defined as $T = T_o + \frac{2}{\sqrt{\alpha_2}} + \frac{2}{\sqrt{\beta_2}} + \frac{2\sqrt{2}}{\sqrt{\alpha_1}} + \frac{2\sqrt{2}}{\sqrt{\beta_1}}$.

The corresponding fixed-time algorithm for MAS with unicycle-type is given in Algorithm 6. At each sampling time instant t_k, based on local exchanged information, each agent i estimates the leader position $\hat{x}_i$ and compute the tracking error between the leader, itself and neighboring agents. After calculating the controller u, we implement the corresponding linear and angular velocity input of the robot.

Algorithm 6 Fixed-time consensus algorithm for MAS with Unicycle-type dynamics

For each agent i, **Input:** $x_{1,0}(t_k), x_{2,0}(t_k), x_{3,0}(t_k), x_{4,0}(t_k)$ (if $b_i = 1$), $x_{1,i}(t_k), x_{2,i}(t_k), x_{3,i}(t_k), x_{4,i}(t_k)$, $x_{1,j}(t_k), x_{2,j}(t_k), x_{3,j}(t_k), x_{4,j}(t_k)$ (for all j such that $a_{ij} \neq 0$)

Parameter: ρ_1 and σ_1, ρ_2 and σ_2, α_1, β_1, α_2, β_2, a

Output: $v_{linear,i}(t), v_{angular,i}(t), t_k \leq t < t_{k+1}$

1: **if** $t = t_k$ **then**
2: Agent i samples its current states, its estimate of the leader and broadcasts it to its neighbors
3: Compute the estimation error $\tilde{x}_i = \hat{x}_i - x_0$
4: Update the distributed observer (convergence in time T_o)
5: When $t \geq T_o$, compute the tracking error
6: Compute the control inputs
7: Implement the linear and angular velocities
8: **end if**

The performances of the proposed observer-based leader-follower consensus controller for unicycle-type are studied through experimental results. The control parameter are selected as: $\alpha_1 = \beta_1 = 12, \alpha_2 = \beta_2 = 12$ for protocols (2.85). The desired trajectory is generated by (2.61) with initial desired position (0,0), $u_{linear\ d}(t) = 0.2$ and $u_{angular\ d}(t) = 0.8$. Hence, since $a \geq d_1 + u_{1,d}$ and $b \geq d_2 + u_{2,d}$, we set $a = b = 1$. The control objective is that system (2.62) tracks the leader x_0 and y_0 using only local information. Based on the control parameters, the settling time is $T = 6.78s$.

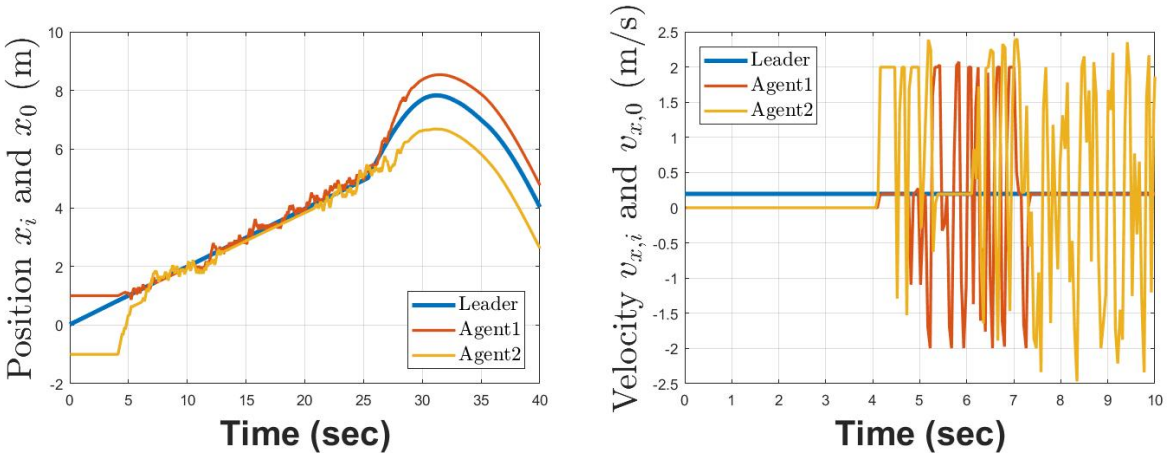

(a) (b)

Figure 5.16: Time response of the tracking for x position and v_x linear velocity

Using Theorem 6, the distributed observer (2.66) guarantees the stabilization of the estimation errors (2.67) to the origin in a finite-time bounded by $T_o = 4s$. Figure 5.16 shows the distributed observers accurately reconstruct the leader state for each agent before T_o. Using Theorem 7, the

tracking controller guarantees the stabilization of the estimation errors (2.67) to the origin in a finite-time bounded by $T = 6s$.

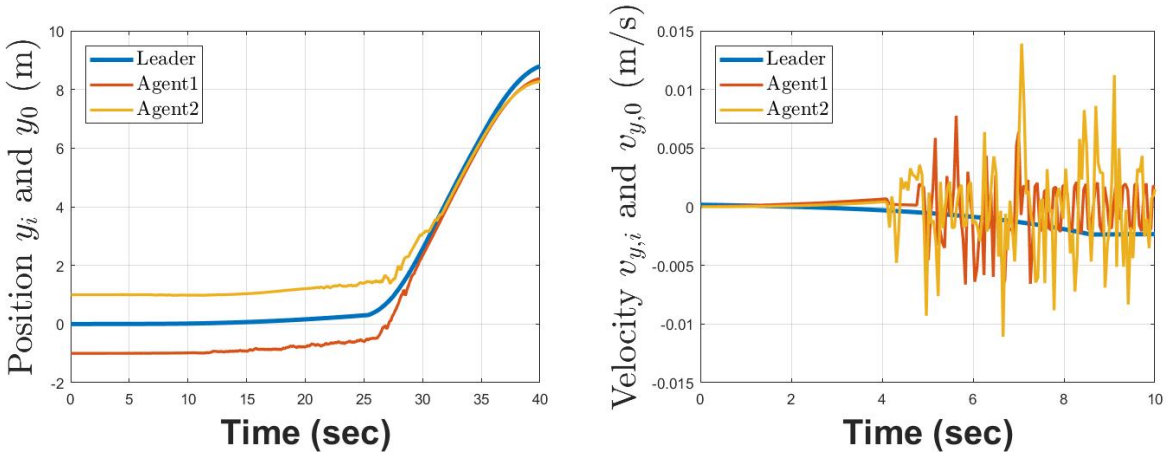

(a) (b)

Figure 5.17: Time response of the tracking for y position and v_y linear velocity

Figures 5.18 (a) and (b) show that the real orientation θ_i and angular velocity ω_i have converged to their respective desired trajectories θ_d and ω_d.

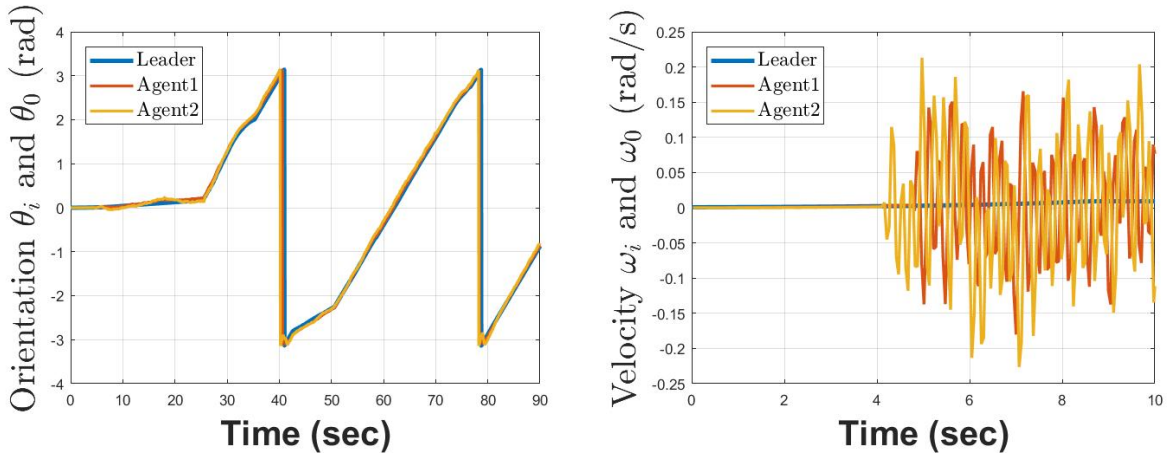

(a) (b)

Figure 5.18: Time response of the tracking for θ position and ω angular velocity

Unlike the previous sections, the results presented herein have proven the consensus to be harder to achieve due to multiple hardware constraints. In fact, the maximum sampling rate in the Minilab robots are limited to 10 Hz maximum, and collisions often occurred while agents tried to achieve their convergence.

5.5 Conclusion

In this chapter, the fixed-time consensus tracking problem for a group of Minilab robots is investigated. Both of tracking and consensus algorithms for single-integrator, double-integrator, and unicycle-type systems was developed respectively. The observer gains are properly chosen and sufficient conditions are established in terms of the graph connectivity to ensure consensus. The effectiveness is validated by experimental results.

However, when it came to real robot experimentations, hardware constraints imposed limitations on the proposed scheme, and therefor, convergence was harder to attain in optimal conditions. The robots' sampling rates restrict the performances of our proposed controller and prevent it from working properly. The collisions have often occurred while robots tried to achieve their convergence. The real robot experiments also depend on the performance of the workstation. The latter is responsible for the control as well as monitoring the experiments. An increasing amount of robots would require better workstation performances.

General conclusion and perspectives

The work of this thesis has been focussed on the study of the navigation scheme for MAS, while taking into account some practical constraints. We were mainly interested in designing cooperative controllers for each agent, in a fully decentralized way, while considering the robot model and temporal constraints. The temporal constraints have been investigated in two directions: consensus problem in a fixed-time framework and consensus problem in a discrete-time framework.

General conclusion

The main results of this thesis are summarized as follows:

- In the first chapter, we have presented the basic concepts of algebraic graph theory for describing the communication topology among the agents. Furthermore, we have given a brief general overview on MAS and consensus control problem in cooperative control both in continuous-time and discrete-time. Convergence rates motivated us to investigate how a fast controller can be designed.

- In the second chapter, it was considered fixed-time leader-follower consensus tracking problem for MAS. Over a fixed topology, distributed observers and decentralized controllers have been designed for each agent to solve the leader-follower consensus problem in a fixed time. Distributed observers have been proposed for each agent to estimate the leader state in a fixed-time. A switching controller has been proposed to solve the consensus problem. An upper bound of the settling time, which only depends on the controller parameters has been estimated regardless of the initial conditions. First, the study of fixed-time leader-follower consensus has been addressed for linear MAS (i.e. single-integrator and double-integrator dynamics). Subsequently, the fixed-time consensus tracking problem has been investigated for multiple unicycle-type mobile robots under matched perturbations.

- In chapter 3, we have proposed a distributed model predictive control protocol for consensus of MAS with discrete-time linear dynamics under time-varying directed topologies. The control protocol is designed by combining graph theory with a predictive control algorithm to take into account the switches on the communication topology. Our proposed controller has been designed using the difference between two consecutive inputs. The controller has also integrator properties to eliminate the steady-state errors. The convergence time of the closed-loop system depends on the prediction horizon parameters. First, the study of distributed model predictive control consensus protocol has focussed on MAS with single-integrator dynamics. Some comparative studies have shown the advantage of the proposed scheme compared to existing ones. Then, the extension to MAS with double-integrator dynamics have been successfully done.

- In chapter 4, we have discussed about the implementation of the proposed control schemes for MAS. Due to the requirements of the proposed consensus algorithms, we have first introduced the robot hardware specifications, communication network configuration and minimum amount of workstations we can use for the coordination of multi-robots using Robot Operating System (ROS) and multiple Minilab robots. Multiple robots communicate through a wireless network with only one workstation for monitoring and control using a wireless master-slave scheme. This configuration is a low cost configuration.

  In this ROS MAS network, decentralized architectures were solved using multi-master ROS. The package of `multimaster_fkie` is shown as a solution for a decentralized implementation. Node calling algorithm has allowed to create the leader-follower topology. This algorithm has used a publisher and a subscriber to broadcast and/or receive messages continually from each other.

- In chapter 5, we have experimentally implemented and validated the fixed-time consensus tracking controller on a group of Minilab robots using ROS with a wireless network. The sampling rate of the minilab robot is only 10 Hz. Both tracking and consensus algorithms for single-integrator, double-integrator, and unicycle-type systems were successfully implemented. The effectiveness of the theoretical results was validated by experimental results.

Perspectives

Despite the results that have been proposed in this thesis, there are still several aspects that could be further investigated in future works. Some of related topics for future research are highlighted as follows.

- In chapter 2, we have dealt with the fixed-time leader-follower consensus problem for MAS with linear dynamics and multiple unicycle-type mobile robots under matched perturbations. It will be possible to investigate the fixed-time leader-follower consensus control problem for MAS with

chained-form dynamics in consideration of unmatched perturbations and noise measurement.

We have also dealt with fixed topology and undirected graph. Hence, it would be an interesting direction if the communication network is switching and include a collection of directed graphs. Obviously, new controllers and Lyapunov functions should be designed to deal with general switching directed graphs.

We have investigated the fixed-time leader-follower consensus problem for MAS with single-integrator, double-integrator and unicycle-type mobile robot dynamics separately. However, in a leader-following architecture, it is possible that leaders have different dynamics from the followers. In fact, in the group of leaders or followers, the dynamics could also be different to build a complex network. Hence, it will be interesting to investigate the fixed-time leader-follower consensus problem for MAS with heterogeneous dynamics.

The fixed-time leader-follower consensus developed in this thesis is achieved and guarantees that the settling time is estimated regardless of the initial condition of the agents. However, this estimate is sometimes too large. To improve this estimate, the concept of predefined-time stability could be interesting to obtain the least upper bound of the settling time.

- In chapter 3, we have studied a distributed model predictive control protocol consensus for MASs with discrete-time linear dynamics under time-varying directed topologies. The proposed controller has only focused on the leaderless case. We plan to extend the results to the leader-follower consensus problem. Another interesting concern for the future work of Chapter 3 can be design of distributed model predictive control protocol consensus for MASs with unicycle-type dynamics. A proof of stability should also be investigated.

- The works presented in Chapters 4 and 5 have focused on the implementation of consensus protocols for a group of multiple Minilab robots. This work for the coordination between robots only use the odometry sensors of each minilab robot. Hence, it may be interesting to develop a visual based motion for future works.

  Due to the method of `multimaster_fkie`, the obtained results depend on the specification of the Master Workstation. It will be interesting to have good specifications for the Master Workstation. Another physical limitation is the sampling rate which significantly influences the performances of the proposed controllers. Interesting extensions of this work can also be pursued to consider physical hardware specifications of the agents and workstation.

It should be noted that in our experiments, the results of fixed-time leader-following consensus are obtained without considering the collision avoidance. Collision between agents and obstacle avoidance are not discussed in this thesis, which motivates us to conduct a more in-depth study to investigate consensus while avoiding collisions.

List of Figures

List of Tables

Bibliography

[1] Roger A Horn and Charles R Johnson. Matrix analysis cambridge university press. *New York*, 37, 1985.

[2] Russell Merris. Laplacian matrices of graphs: a survey. *Linear algebra and its applications*, 197:143–176, 1994.

[3] Yoonsoo Kim and Mehran Mesbahi. On maximizing the second smallest eigenvalue of a state-dependent graph laplacian. *IEEE transactions on Automatic Control*, 51(1):116–120, 2006.

[4] Sonia MartíNez and Francesco Bullo. Optimal sensor placement and motion coordination for target tracking. *Automatica*, 42(4):661–668, 2006.

[5] Yongcan Cao and Wei Ren. Distributed coordinated tracking with reduced interaction via a variable structure approach. *IEEE Transactions on Automatic Control*, 57(1):33–48, 2012.

[6] X Luo, D Liu, X Guan, and S Li. Flocking in target pursuit for multi-agent systems with partial informed agents. *IET control theory & applications*, 6(4):560–569, 2012.

[7] Zhan Li, Hugh HT Liu, Bo Zhu, and Huijun Gao. Robust second-order consensus tracking of multiple 3-dof laboratory helicopters via output feedback. *IEEE/ASME Transactions on Mechatronics*, 20(5):2538–2549, 2015.

[8] Yang Tang, Xing Xing, Hamid Reza Karimi, Ljupco Kocarev, and Jürgen Kurths. Tracking control of networked multi-agent systems under new characterizations of impulses and its applications in robotic systems. *IEEE Transactions on Industrial Electronics*, 63(2):1299–1307, 2016.

[9] Dongbing Gu and Zongyao Wang. Leader–follower flocking: algorithms and experiments. *IEEE Transactions on Control Systems Technology*, 17(5):1211–1219, 2009.

[10] Jingyuan Zhan and Xiang Li. Flocking of multi-agent systems via model predictive control based on position-only measurements. *IEEE Transactions on Industrial Informatics*, 9(1):377–385, 2013.

[11] Wei Li and Mark W Spong. Analysis of flocking of cooperative multiple inertial agents via a geometric decomposition technique. *IEEE Transactions on Systems, Man, and Cybernetics: Systems*, 44(12):1611–1623, 2014.

[12] Yongnan Jia and Long Wang. Leader–follower flocking of multiple robotic fish. *IEEE/ASME Transactions on Mechatronics*, 20(3):1372–1383, 2015.

[13] Swagatam Das, Udit Halder, and Dipankar Maity. Chaotic dynamics in social foraging swarms—an analysis. *IEEE Transactions on Systems, Man, and Cybernetics, Part B (Cybernetics)*, 42(4):1288–1293, 2012.

[14] Andrea Gasparri, Giuseppe Oriolo, Attilio Priolo, and Giovanni Ulivi. A swarm aggregation algorithm based on local interaction for multi-robot systems with actuator saturations. In *Intelligent Robots and Systems (IROS), 2012 IEEE/RSJ International Conference on*, pages 539–544. IEEE, 2012.

[15] Jorge Cortés, Sonia Martínez, and Francesco Bullo. Robust rendezvous for mobile autonomous agents via proximity graphs in arbitrary dimensions. *IEEE Transactions on Automatic Control*, 51(8):1289–1298, 2006.

[16] Jie Lin, A Stephen Morse, and Brian DO Anderson. The multi-agent rendezvous problem. part 2: The asynchronous case. *SIAM Journal on Control and Optimization*, 46(6):2120–2147, 2007.

[17] Jorge Cortes, Sonia Martinez, Timur Karatas, and Francesco Bullo. Coverage control for mobile sensing networks. *IEEE Transactions on robotics and Automation*, 20(2):243–255, 2004.

[18] Islam I Hussein and Dusan M Stipanovic. Effective coverage control for mobile sensor networks with guaranteed collision avoidance. *IEEE Transactions on Control Systems Technology*, 15(4):642–657, 2007.

[19] Xinmiao Sun and Christos G Cassandras. Optimal dynamic formation control of multi-agent systems in constrained environments. *Automatica*, 73:169–179, 2016.

[20] Sara Susca, Francesco Bullo, and Sonia Martinez. Monitoring environmental boundaries with a robotic sensor network. *IEEE Transactions on Control Systems Technology*, 16(2):288–296, 2008.

[21] Matthew Dunbabin and Lino Marques. Robots for environmental monitoring: Significant advancements and applications. *IEEE Robotics & Automation Magazine*, 19(1):24–39, 2012.

[22] Michael Defoort, Thierry Floquet, Annemarie Kokosy, and Wilfrid Perruquetti. Sliding-mode formation control for cooperative autonomous mobile robots. *IEEE Transactions on Industrial Electronics*, 55(11):3944–3953, 2008.

[23] Khac Duc Do. Bounded assignment formation control of second-order dynamic agents. *IEEE/ASME Transactions on Mechatronics*, 19(2):477–489, 2014.

[24] Zhiyun Lin, Lili Wang, Zhimin Han, and Minyue Fu. Distributed formation control of multi-agent systems using complex laplacian. *IEEE Transactions on Automatic Control*, 59(7):1765–1777, 2014.

[25] Lara Brinón-Arranz, Alexandre Seuret, and Carlos Canudas-de Wit. Cooperative control design for time-varying formations of multi-agent systems. *IEEE Transactions on Automatic Control*, 59(8):2283–2288, 2014.

[26] Kwang-Kyo Oh, Myoung-Chul Park, and Hyo-Sung Ahn. A survey of multi-agent formation control. *Automatica*, 53:424–440, 2015.

[27] J Alexander Fax and Richard M Murray. Information flow and cooperative control of vehicle formations. *IEEE transactions on automatic control*, 49(9):1465–1476, 2004.

[28] Ali Jadbabaie, Jie Lin, and A Stephen Morse. Coordination of groups of mobile autonomous agents using nearest neighbor rules. *IEEE Transactions on automatic control*, 48(6):988–1001, 2003.

[29] Zhiyun Lin, Mireille Broucke, and Bruce Francis. Local control strategies for groups of mobile autonomous agents. *IEEE Transactions on automatic control*, 49(4):622–629, 2004.

[30] Reza Olfati-Saber and Richard M Murray. Consensus problems in networks of agents with switching topology and time-delays. *IEEE Transactions on automatic control*, 49(9):1520–1533, 2004.

[31] Wei Ren and Randal W Beard. Consensus seeking in multiagent systems under dynamically changing interaction topologies. *IEEE Transactions on automatic control*, 50(5):655–661, 2005.

[32] Jian Wu and Yang Shi. Average consensus in multi-agent systems with time-varying delays and packet losses. In *2012 American Control Conference (ACC)*, pages 1579–1584. IEEE, 2012.

[33] Hamed Rezaee and Farzaneh Abdollahi. Consensus problem over high-order multiagent systems with uncertain nonlinearities under deterministic and stochastic topologies. *IEEE transactions on cybernetics*, 47(8):2079–2088, 2017.

[34] Wenhui Liu, Feiqi Deng, Jiarong Liang, and Haijun Liu. Distributed average consensus in multi-agent networks with limited bandwidth and time-delays. *IEEE/CAA Journal of Automatica Sinica*, 1(2):193–203, 2014.

[35] Christoforos N Hadjicostis and Themistoklis Charalambous. Average consensus in the presence of delays in directed graph topologies. *IEEE Transactions on Automatic Control*, 59(3):763–768, 2014.

[36] Yuan Gong Sun, Long Wang, and Guangming Xie. Average consensus in networks of dynamic agents with switching topologies and multiple time-varying delays. *Systems & Control Letters*, 57(2):175–183, 2008.

[37] Wei Ren, Randal W Beard, and Ella M Atkins. Information consensus in multivehicle cooperative control. *IEEE Control Systems*, 27(2):71–82, 2007.

[38] Wei Ren and Randal W Beard. Consensus algorithms for double-integrator dynamics. *Distributed Consensus in Multi-vehicle Cooperative Control: Theory and Applications*, pages 77–104, 2008.

[39] Haibo Du, Shihua Li, and Peng Shi. Robust consensus algorithm for second-order multi-agent systems with external disturbances. *International Journal of Control*, 85(12):1913–1928, 2012.

[40] Wenwu Yu, Guanrong Chen, Wei Ren, Jürgen Kurths, and Wei Xing Zheng. Distributed higher order consensus protocols in multiagent dynamical systems. *IEEE Transactions on Circuits and Systems I: Regular Papers*, 58(8):1924–1932, 2011.

[41] Bin Zhou and Zongli Lin. Consensus of high-order multi-agent systems with large input and communication delays. *Automatica*, 50(2):452–464, 2014.

[42] Jiangping Hu and Gang Feng. Distributed tracking control of leader–follower multi-agent systems under noisy measurement. *Automatica*, 46(8):1382–1387, 2010.

[43] Wanli Guo, Jinhu Lü, Shihua Chen, and Xinghuo Yu. Second-order tracking control for leader–follower multi-agent flocking in directed graphs with switching topology. *Systems & Control Letters*, 60(12):1051–1058, 2011.

[44] Guoqiang Hu. Robust consensus tracking of a class of second-order multi-agent dynamic systems. *Systems & Control Letters*, 61(1):134–142, 2012.

[45] Wangli He, Guanrong Chen, Qing-Long Han, and Feng Qian. Network-based leader-following consensus of nonlinear multi-agent systems via distributed impulsive control. *Information Sciences*, 380:145–158, 2017.

[46] Zhiyun Lin, Wei Ding, Gangfeng Yan, Changbin Yu, and Alessandro Giua. Leader–follower formation via complex laplacian. *Automatica*, 49(6):1900–1906, 2013.

[47] Giuseppe Notarstefano, Magnus Egerstedt, and M Haque. Containment in leader–follower networks with switching communication topologies. *Automatica*, 47(5):1035–1040, 2011.

[48] Jiahu Qin, Wei Xing Zheng, Huijun Gao, Qichao Ma, and Weiming Fu. Containment control for second-order multiagent systems communicating over heterogeneous networks. *IEEE transactions on neural networks and learning systems*, 28(9):2143–2155, 2017.

[49] Peng Yang, Randy A Freeman, Geoffrey J Gordon, Kevin M Lynch, Siddhartha S Srinivasa, and Rahul Sukthankar. Decentralized estimation and control of graph connectivity for mobile sensor networks. *Automatica*, 46(2):390–396, 2010.

[50] Wilfrid Perruquetti and Jean-Pierre Barbot. *Sliding mode control in engineering*. CRC Press, 2002.

[51] AF Filippov. *Differential Equations with Discontinuous Righthand Sides: Control Systems*, volume 18. Springer Science & Business Media, 1988.

[52] Sanjay P Bhat and Dennis S Bernstein. Geometric homogeneity with applications to finite-time stability. *Mathematics of Control, Signals and Systems*, 17(2):101–127, 2005.

[53] Long Wang and Feng Xiao. Finite-time consensus problems for networks of dynamic agents. *IEEE Transactions on Automatic Control*, 55(4):950–955, 2010.

[54] Suiyang Khoo, Lihua Xie, and Zhihong Man. Robust finite-time consensus tracking algorithm for multirobot systems. *IEEE/ASME transactions on mechatronics*, 14(2):219–228, 2009.

[55] Yu Zhao, Zhisheng Duan, Guanghui Wen, and Yanjiao Zhang. Distributed finite-time tracking control for multi-agent systems: an observer-based approach. *Systems & Control Letters*, 62(1):22–28, 2013.

[56] Yu Zhao, Zhisheng Duan, Guanghui Wen, and Guanrong Chen. Distributed finite-time tracking for a multi-agent system under a leader with bounded unknown acceleration. *Systems & Control Letters*, 81:8–13, 2015.

[57] Saleh Mobayen. Finite-time tracking control of chained-form nonholonomic systems with external disturbances based on recursive terminal sliding mode method. *Nonlinear Dynamics*, 80(1-2):669–683, 2015.

[58] Andrey Polyakov. Nonlinear feedback design for fixed-time stabilization of linear control systems. *IEEE Transactions on Automatic Control*, 57(8):2106–2110, 2012.

[59] Sergey Parsegov, Andrey Polyakov, and Pavel Shcherbakov. Nonlinear fixed-time control protocol for uniform allocation of agents on a segment. In *Decision and Control (CDC), 2012 IEEE 51st Annual Conference on*, pages 7732–7737. IEEE, 2012.

[60] Emmanuel Cruz-Zavala, Jaime A Moreno, and Leonid Fridman. Uniform second-order sliding mode observer for mechanical systems. In *Variable Structure Systems (VSS), 2010 11th International Workshop on*, pages 14–19. IEEE, 2010.

[61] SE Parsegov, AE Polyakov, and PS Shcherbakov. Fixed-time consensus algorithm for multi-agent systems with integrator dynamics. *IFAC Proceedings Volumes*, 46(27):110–115, 2013.

[62] Andrey Polyakov and Leonid Fridman. Stability notions and lyapunov functions for sliding mode control systems. *Journal of the Franklin Institute*, 351(4):1831–1865, 2014.

[63] Junkang Ni, Ling Liu, Chongxin Liu, Xiaoyu Hu, and Shilei Li. Fast fixed-time nonsingular terminal sliding mode control and its application to chaos suppression in power system. *IEEE Transactions on Circuits and Systems II: Express Briefs*, 64(2):151–155, 2017.

[64] Zongyu Zuo and Lin Tie. A new class of finite-time nonlinear consensus protocols for multi-agent systems. *International Journal of Control*, 87(2):363–370, 2014.

[65] Zongyu Zuo and Lin Tie. Distributed robust finite-time nonlinear consensus protocols for multi-agent systems. *International Journal of Systems Science*, 47(6):1366–1375, 2016.

[66] Michael Defoort, Andrey Polyakov, Guillaume Demesure, Mohamed Djemai, and Kalyana Veluvolu. Leader-follower fixed-time consensus for multi-agent systems with unknown non-linear inherent dynamics. *IET Control Theory & Applications*, 9(14):2165–2170, 2015.

[67] Huifen Hong, Wenwu Yu, Guanghui Wen, and Xinghuo Yu. Distributed robust fixed-time consensus for nonlinear and disturbed multiagent systems. *IEEE Transactions on Systems, Man, and Cybernetics: Systems*, 47(7):1464–1473, 2017.

[68] Xue Lin and Yuanshi Zheng. Finite-time consensus of switched multiagent systems. *IEEE Transactions on Systems, Man, and Cybernetics: Systems*, 47(7):1535–1545, 2017.

[69] Zongyu Zuo. Nonsingular fixed-time consensus tracking for second-order multi-agent networks. *Automatica*, 54:305–309, 2015.

[70] Junjie Fu and Jinzhi Wang. Fixed-time coordinated tracking for second-order multi-agent systems with bounded input uncertainties. *Systems & Control Letters*, 93:1–12, 2016.

[71] Junkang Ni, Ling Liu, Chongxin Liu, Xiaoyu Hu, and Tianshi Shen. Fixed-time dynamic surface high-order sliding mode control for chaotic oscillation in power system. *Nonlinear Dynamics*, 86(1):401–420, 2016.

[72] Zongyu Zuo, Bailing Tian, Michael Defoort, and Zhengtao Ding. Fixed-time consensus tracking for multiagent systems with high-order integrator dynamics. *IEEE Transactions on Automatic Control*, 63(2):563–570, 2018.

[73] Deyuan Meng and Zongyu Zuo. Signed-average consensus for networks of agents: a nonlinear fixed-time convergence protocol. *Nonlinear Dynamics*, 85(1):155–165, 2016.

[74] Deyuan Meng and Yingmin Jia. Robust consensus algorithms for multiscale coordination control of multivehicle systems with disturbances. *IEEE Transactions on industrial electronics*, 63(2):1107–1119, 2016.

[75] Michael Defoort, Guillaume Demesure, Zongyu Zuo, Andrey Polyakov, and Mohamed Djemai. Fixed-time stabilisation and consensus of non-holonomic systems. *IET Control Theory & Applications*, 10(18):2497–2505, 2016.

[76] Feng Xiao and Long Wang. Consensus protocols for discrete-time multi-agent systems with time-varying delays. *Automatica*, 44(10):2577–2582, 2008.

[77] L Wang and F Xiao. Dynamic behavior of discrete-time multi-agent systems with general communication structure. *Physical A*, 370(2):364–380, 2006.

[78] Mauro Franceschelli, Alessandro Giua, and Carla Seatzu. A gossip-based algorithm for discrete consensus over heterogeneous networks. *IEEE Transactions on Automatic Control*, 55(5):1244–1249, 2010.

[79] Chong Tan and Guo-Ping Liu. Consensus of discrete-time linear networked multi-agent systems with communication delays. *IEEE Transactions on Automatic Control*, 58(11):2962–2968, 2013.

[80] Shaobao Li, Gang Feng, Xiaoyuan Luo, and Xinping Guan. Output consensus of heterogeneous linear discrete-time multiagent systems with structural uncertainties. *IEEE transactions on cybernetics*, 45(12):2868–2879, 2015.

[81] Jian Wu and Yang Shi. Consensus in multi-agent systems with random delays governed by a markov chain. *Systems & Control Letters*, 60(10):863–870, 2011.

[82] Bingxian Mu, Huxiong Li, Jie Ding, and Yang Shi. Consensus in second-order multiple flying vehicles with random delays governed by a markov chain. *Journal of the Franklin Institute*, 352(9):3628–3644, 2015.

[83] Hassan K Khalil. Noninear systems. *Prentice-Hall, New Jersey*, 2(5):5–1, 1996.

[84] Mircea Lazar, WPMH Heemels, Alberto Bemporad, and Siep Weiland. On the stability and robustness of non-smooth nonlinear model predictive control. In *Workshop on Assessment and Future Directions of NMPC*, pages 327–334. Freudenstadt-Lauterbad Germany, 2005.

[85] John Tsitsiklis, Dimitri Bertsekas, and Michael Athans. Distributed asynchronous deterministic and stochastic gradient optimization algorithms. *IEEE transactions on automatic control*, 31(9):803–812, 1986.

[86] Luc Moreau. Stability of multiagent systems with time-dependent communication links. *IEEE Transactions on automatic control*, 50(2):169–182, 2005.

[87] J Richalet, A Rault, JL Testud, and J Papon. Model algorithmic control of industrial processes. *IFAC Proceedings Volumes*, 10(16):103–120, 1977.

[88] Charles R Cutler and Brian L Ramaker. Dynamic matrix control?? a computer control algorithm. In *joint automatic control conference*, number 17, page 72, 1980.

[89] S Joe Qin and Thomas A Badgwell. A survey of industrial model predictive control technology. *Control engineering practice*, 11(7):733–764, 2003.

[90] Zhaomeng Cheng, Ming-Can Fan, and Hai-Tao Zhang. Distributed mpc based consensus for single-integrator multi-agent systems. *ISA transactions*, 58:112–120, 2015.

[91] David Q Mayne, James B Rawlings, Christopher V Rao, and Pierre OM Scokaert. Constrained model predictive control: Stability and optimality. *Automatica*, 36(6):789–814, 2000.

[92] Giancarlo Ferrari-Trecate, Luca Galbusera, Marco Pietro Enrico Marciandi, and Riccardo Scattolini. Model predictive control schemes for consensus in multi-agent systems with single-and double-integrator dynamics. *IEEE Transactions on Automatic Control*, 54(11):2560–2572, 2009.

[93] H-T Zhang, Michael ZhiQiang Chen, and Tao Zhou. Improve consensus via decentralized predictive mechanisms. *EPL (Europhysics Letters)*, 86(4):40011, 2009.

[94] Tomas Menard, Emmanuel Moulay, and Wilfrid Perruquetti. Fixed-time observer with simple gains for uncertain systems. *Automatica*, 81:438–446, 2017.

[95] Michael Defoort, Jorge Palos, Annemarie Kokosy, Thierry Floquet, and Wilfrid Perruquetti. Performance-based reactive navigation for non-holonomic mobile robots. *Robotica*, 27(2):281–290, 2009.

[96] ROS. Line spacing in latex documents. `http://wiki.ros.org/multimaster_fkie`. Accessed April, 2018.